APPENDIX 2

UPRC Stratos Final Topical Report – Phase II

Greater Green River Basin Production Improvement Project

Topical Report - Phase 2: Drilling, Testing, and Completion of the UPRC Stratos Federal #1

Prepared by: B. Blakeney DeJarnett and D. Calogero

January 1997

Work Performed Under Contract No. DE-AC21-95MC31063

For
U. S. Department of Energy
Office of Fossil Energy
Morgantown Energy Technology Center
Morgantown, West Virginia

By
Union Pacific Resources Company
P. O. Box 7
Fort Worth, TX 76101-0007

DISCLAIMER

This report was prepared as an account of work sponsored by an agency of the United States Government Neither the United States Government nor any of agency thereof, nor any of their employees, makes any warranty, express or implied, or assumes any legal liability or responsibility for the accuracy, completeness, or usefulness of any information, apparatus, product, or process disclosed, or represents that its use would not infringe privately owned rights Reference herein to any specific commercial product, process, or service by trade name, trademark, manufacturer, or otherwise does not necessarily constitute of imply its endorsement, recommendation, or favoring by the United States Government or any agency thereof The views and opinions of authors expressed herein do not necessarily state or reflect those of the United States Government or any agency thereof

This report has been reproduced directly from the best available copy

TABLE OF CONTENTS

1 Introduction
- 1 1 Objectives of Phase II
- 1 2 Drilling prognosis for the UPRC Stratos Federal #1-24

2 Drilling History
- 2 1 Location and drilling
- 2 2 Directional drilling
- 2 3 Coring
- 2 4 Total depth and logging

3 Reservoir characterization
- 3 1 Sedimentological interpretation of the Second Frontier
  - 3 11 Core description
  - 3 12 Comparison between Stratos and Blue Rim wells
- 3 2 Petrographic analyses and diagenetic history of the Second Frontier
  - 3 21 Thin section analysis
  - 3 22 Scanning electron microscopy and X-Ray Diffraction
- 3 3 Core analysis - porosity and permeability
  - 3 31 Routine unstressed porosity and permeability
  - 3 32 Stressed (in situ) permeability analyses
  - 3 33 Effect of increasing water saturation on permeability
- 3 4 Fracture characterization and analysis of in-situ stresses
  - 3 41 Characterization of macrofractures in core
  - 3 42 Preliminary analysis of microfractures
  - 3 43 Core-based methods for estimating in situ stress conditions
  - 3 44 Wellbore breakout analysis
- 3 5 Well log analysis

4 Completion and testing of the Stratos Federal #1-24

5 Future plans and recommendations

Appendices

Appendix A Core photographs of the UPRC Stratos Federal #1-24

Appendix B SEM photomicrographs of the Second Frontier sandstones, UPRC Stratos Federal #1-24

Appendix C	UPRC - Stratos Federal #1 - Special Core Analysis Study - Hycal Energy Laboratories
Appendix D	Core-based methods for in situ stress determination applied to core from UPRC Stratos well DSCA and DWVA - Sandia National Laboratories
	Core-based methods for in situ stress determination applied to core from UPRC Stratos well Velocity anisotropy study - Sandia National Laboratories
Appendix E	Preliminary analysis of three samples from UPRC Stratos Federal well, Frontier Formation Natural Fracture Analysis Project, Bureau of Economic Geology
Appendix F	Logging/formation evaluation - Schlumberger
Appendix G	Cased hole stress test, breakdown treatment and pressure buildup evaluation and analyses - Integrated Petroleum Technologies, Inc

LIST OF FIGURES

Figure 1-1 Index map of major oil and gas fields in the Greater Green River Basin, Wyoming with respect to the Stratos Federal #1-24 in Sweetwater County

Figure 1-2 Structure map on top of Frontier Formation, Green River Basin, Wyoming Contour interval = 500 ft

Figure 1-3 Regional isopach map of net feet of pay in the Second Frontier fluvial interval at the Stratos location (shown as star) Contour interval = 5 ft

Figure 1-4 Local isopach map of net feet of pay in the Second Frontier fluvial interval at the Stratos location (shown as star) Contour interval = 5 ft

Figure 1-5 Regional isopach map of net feet of pay in the Second Frontier marine interval at the Stratos location (shown as star) Contour interval = 10 ft

Figure 1-6 Local isopach map of net feet of pay in the Second Frontier marine interval at the Stratos location (shown as star) Contour interval = 10 ft

Figure 2-1 Plot of depth versus drilling time for the UPRC Stratos Federal #1-24

Figure 2-2 Mudlogger's Report

Figure 2-3 Wellbore Trajectory Diagram - Vertical View

Figure 2-4 Wellbore Trajectory Diagram - Surface View

Figure 2-5 Wellbore Diagram

Figure 3-1 Schematic vertical profile of the Second Frontier Formation, Green River Basin, WY

Figure 3-2 Core description

Figure 3-3 Dip azimuth plot for fluvial bedding planes

Figure 3-4 Location map for the UPRC Stratos #1-24

Figure 3-5 Stratigraphic cross-section for the Stratos #1-24 and the two Blue Rim wells

Figure 3-6 Comparison of total permeability-feet between the Stratos #1-24 and the Blue Rim #1-30 (Second Frontier sandstone only)

Figure 3-7 Comparison of total porosity-feet between the Stratos #1-24 and the Blue Rim #1-30 (Second Frontier sandstone only)

Figure 3-8 Comparison of post-breakdown flow rates between the Stratos and two Blue Rim wells

Figure 3-9 Summary plot of the comparison of total permeability-feet and porosity-feet between the Stratos #1-24 and the Blue Rim #1-30 (Second Frontier sandstone only)

Figure 3-10 Petrographic composition of the Second Frontier sandstones based on point count analysis (300 points per sample)

Figure 3-11 Ternary diagram for the petrographic classification of the Second Frontier sandstones

Figure 3-12 Effect of confining pressure on permeability of the Frontier sandstones

Figure 3-13 Representative scanned CL images

Figure 3-14 Rose diagram showing the strike of measured microfractures from 16027 feet (Note that the area of thin section studied is less than 1% of total thin section)

Figure 3-15 Relationship of wellbore breakout orientation, maximum horizontal stress, natural fracture orientation, and other features

Figure 3-16 Plot of four-arm caliper data for the Frontier Formation (and part of the Baxter Shale) in the Stratos Federal #1-24

LIST OF TABLES

Table 2-1 Well Log Inventory

Table 3-1 Core-derived, routine unstressed porosity and permeability for the UPRC Stratos Federal #1-24

Table 3-2 Core-derived stressed permeabilities for the UPRC Stratos Federal #1-24

Table 3-3 Core-derived, routine unstressed porosity and permeability for the ERG Blue Rim #1-30

Table 3-4 Results of point count analysis for the Second Frontier sandstones in the UPRC Stratos #1-24

Table 3-5 GR Petrology Consultants, Inc 's petrographic analysis of three samples from the Second Frontier

Table 3-6 X-Ray diffraction analyses

Table 3-7 Full diameter fracture permeability measurements - Hycal Laboratories

Table 3-8 Incremental phase trap evaluation tests - Hycal Laboratories

Table 3-9 Samples used in Sandia's core-based in situ stress tests

Table 3-10 Microfracture categories and their interpreted origin

Table 3-11 Microfracture data quality index for assessing reliability of macrofracture strike determination

Table 3-12 Summary of four-arm caliper data for the Frontier Formation, Stratos Federal #1-24

APPENDICES - LIST OF FIGURES AND TABLES

Appendix A Core photographs of the UPRC Stratos Federal #1-24

Appendix B SEM photomicrographs of Second Frontier sandstones, UPRC Stratos Federal #1-24

Appendix C UPRC - Stratos Federal #1 - Special Core Analysis Study - Hycal Energy Laboratories

Figure 1 Core #6B - Fracture Fluid Leakoff with Halliburton Frac Gel 2 Permeability Summary

Figure 2 Core #7A - Fracture Fluid Leakoff with BJ Titan Borate HT 4500 Permeability Summary

Figure 3 Core #31A - Fracture Fluid Leakoff with BJ Titan Borate HT 4500 Permeability Summary

Figure 4 Core #31B - Fracture Fluid Leakoff with Halliburton Frac Gel 2 Permeability Summary

Figure 5 Core #6A - Incremental Phase Trap Relative Permeability Test Permeability Summary - Threshold Pressure Regains

Figure 5A Core #6A - Incremental Phase Trap Relative Permeability Test Permeability vs Water Saturation

Figure 6 Core #37 - Incremental Phase Trap Relative Permeability Test Permeability Summary - Threshold Pressure Regains

Figure 6A Core #37 - Incremental Phase Trap Relative Permeability Test Permeability vs Water Saturation

Figure 7 Core #9 - Water-Gas Relative Permeability Test Cumulative Production vs Cumulative Injection

Figure 8 Core #9 - Water-Gas Relative Permeability Test Pressure vs Cumulative Injection

Figure 9 Core #9 - Water-Gas Relative Permeability Test Relative Permeability vs Water Saturation (Cartesian)

Figure 10 Core #9 - Water-Gas Relative Permeability Test

Relative Permeability vs Water Saturation (Semi-Log)

Figure 11 Core #48B - Water-Gas Relative Permeability Test
Cumulative Production vs Cumulative Injection

Figure 12 Core #48B - Water-Gas Relative Permeability Test
Pressure vs Cumulative Injection

Figure 13 Core #48B - Water-Gas Relative Permeability Test
Relative Permeability vs Water Saturation (Cartesian)

Figure 14 Core #48B - Water-Gas Relative Permeability Test
Relative Permeability vs Water Saturation (Semi-Log)

Figure 15 Core #12 - Fracture Permeability vs Overburden and Fluid Saturation Test
Permeability Summary - Threshold Pressure Regains

Figure 16 Core #32 - Fracture Permeability vs Overburden and Fluid Saturation Test
Permeability Summary - Threshold Pressure Regains

Table 1 Routine Porosity and Gas Permeability

Table 2 Core #6B - Fracture Fluid Leakoff with Halliburton Frac Gel 2
Core and Test Parameters

Table 3 Core #6B - Fracture Fluid Leakoff with Halliburton Frac Gel 2
Permeability Summary

Table 4 Core #6B - Fracture Fluid Leakoff with Halliburton Frac Gel 2
Leakoff Summary

Table 5 Core #7A - Fracture Fluid Leakoff with BJ Halliburton Borate HT 4500
Core and Test Parameters

Table 6 Core #7A - Fracture Fluid Leakoff with BJ Titan Borate HT 4500
Permeability Summary

Table 7 Core #7A - Fracture Fluid Leakoff with BJ Titan Borate HT 4500
Leakoff Summary

Table 8 Core #31A - Fracture Fluid Leakoff with BJ Titan Borate HT 4500
Core and Test Parameters

Table 9 Core #31A - Fracture Fluid Leakoff with BJ Titan Borate HT 4500

Permeability Summary

Table 10 Core #31A - Fracture Fluid Leakoff with BJ Titan Borate HT 4500 Leakoff Summary

Table 11 Core #31B - Fracture Fluid Leakoff with Halliburton Frac Gel 2 Core and Test Parameters

Table 12 Core #31B - Fracture Fluid Leakoff with Halliburton Frac Gel 2 Permeability Summary

Table 13 Core #31B - Fracture Fluid Leakoff with Halliburton Frac Gel 2 Leakoff Summary

Table 14 Core #6A - Incremental Phase Trap Relative Permeability Test Core and Test Parameters

Table 15 Core #6A - Incremental Phase Trap Relative Permeability Test Permeability Summary - Threshold Pressure Regains

Table 16 Core #37 - Incremental Phase Trap Relative Permeability Test Core and Test Parameters

Table 17 Core #37 - Incremental Phase Trap Relative Permeability Test Permeability Summary - Threshold Pressure Regains

Table 18 Core #9 - Water-Gas Relative Permeability Test Core and Test Parameters

Table 19 Core #9 - Water-Gas Relative Permeability Test Saturation and Permeability Summary

Table 20 Core #9 - Water-Gas Relative Permeability Test Experimental Pressure and Production History

Table 21 Core #9 - Water-Gas Relative Permeability Data

Table 22 Core #48B - Water-Gas Relative Permeability Test Core and Test Parameters

Table 23 Core #48B - Water-Gas Relative Permeability Test Saturation and Permeability Summary

Table 24 Core #48B - Water-Gas Relative Permeability Test Experimental Pressure and Production History

Table 25 Core #48B - Water-Gas Relative Permeability Data

Table 26 Core #12 - Fracture Permeability vs Overburden and Fluid Saturation Test Core and Test Parameters

Table 27 Core #12 - Fracture Permeability vs Overburden and Fluid Saturation Test Permeability Summary - Threshold Pressure Regains

Table 28 Core #32 - Fracture Permeability vs Overburden and Fluid Saturation Test Core and Test Parameters

Table 29 Core #32 - Fracture Permeability vs Overburden and Fluid Saturation Test Permeability Summary - Threshold Pressure Regains

Table 30 Results of Geomechanical Testing

Appendix A Results of Mercury Injection Capillary Pressure Measurements

Appendix B Petrographic Analysis Summary

Appendix C Technical Papers

1 "Recent Improvements In Experimental Laboratory Techniques In The Analysis Of Unsteady-State Relative Permeability Data"
2 SPE 35577 "Low Permeability Gas Reservoirs Problems, Opportunities and Solutions for Drilling, Completion, Stimulation and Production"
3 CIM96-80 "Remediation of Water and Hydrocarbon Phase Trapping Problems in Low Permeability Gas Reservoirs"
4 "Reductions in the Productivity of Oil and Low Permeability Gas Reservoirs due to Aqueous Phase Trapping

Appendix D Preliminary analysis of three samples from UPRC Stratos Federal well, Frontier Formation Natural fracture analysis project Bureau of Economic Gepology, The University of Texas at Austin, July, 1996

Appendix E Core-based methods for in situ stress determination applied to core from UPRC Stratos well DSCA and DWVA Sandia National Laboratories, July, 1996

Figure 1 View of DSCA and DWVA sample, showing 3 strain gage rosettes and 4of 6 P transducers

Figure 2 V_P as a function of depth for all samples At each depth, the maximum and minimum velocity in the horizontal plane is shown (+ and x, respectively) as well as the velocity along the axis of the

sample (o) Velocities for the unpressurized sample are shown as heavy symbols, while the matching light symbols indicate V_P at the peak presure of 190 Mpa

Figure 3 V_P as a function on depth for all samples, normalized to the value at the peak pressure of 190 Mpa At each depth, the maximum and velocity ratio in the horizontal plane is shown (+ and x, respectively) as well as te velocity ratio along the axis of the sample (o)

Figure 4 For sample at a depth of 16025 6 feet, a Compressional wave velocity, V_P, in the horizontal plane, unpressurized b, c, d V_P in the vertical direction and parallel to the initial minimum and maximum horizontal velocity directions, respectively as a function of confining pressure

Figure 5 For sample at a depth of 16026 2 feet, a Compressional wave velocity, V_P, in the horizontal plane, unpressurized b, c, d V_P in the vertical direction and parallel to the initial minimum and maximum horizontal velocity directions, respectively as a function of confining pressure

Figure 6 For sample at a depth of 16038 4 feet, a Compressional wave velocity, V_P, in the horizontal plane, unpressurized b, c, d V_P in the vertical direction and parallel to the initial minimum and maximum horizontal velocity directions, respectively as a function of confining pressure

Figure 7 For sample at a depth of 16050 1 feet, a Compressional wave velocity, V_P, in the horizontal plane, unpressurized b, c, d V_P in the vertical direction and parallel to the initial minimum and maximum horizontal velocity directions, respectively as a function of confining pressure

Figure 8 For sample at a depth of 16051 3 feet, a Compressional wave velocity, V_P, in the horizontal plane, unpressurized b, c, d V_P in the vertical direction and parallel to the initial minimum and maximum horizontal velocity directions, respectively as a function of confining pressure

Figure 9 For sample at a depth of 16051 9 feet, a Compressional wave velocity, V_P, in the horizontal plane, unpressurized b, c, d V_P in the vertical direction and parallel to the initial minimum and maximum horizontal velocity directions, respectively as a function of confining pressure

Figure 10 Crack strains for all samples Strains are $\varepsilon_{ij}\eta_i\eta_j$ for η_i in the Z direction (ε_z plotted as "o") and the maximum and minimum for n_i in the horizontal plane ($\varepsilon_{H,max}$ and $\varepsilon_{H,min}$, plotted as "x" and "+") At 16025 6 feet, $\varepsilon_Z = 0$ 6 is not shown as it would have compressed the scale too much

Figure 11 Principal strains as a function of pressure for a sample from a depth of 16025 6 feet a Crack strains, b elastic strains Values of strain and orientation at the peak pressure are indicated on the figure

Figure 12 Orientation of principal crack strains for a sample from a depth of 16025 6 feet, a projected into the E-W, N-S plane b projected into the N-S U-D plane The maximum, intermediate, and minimum compressive crack strains are indicated by (+,o) resepctively, and the orientation at the peak pressure is circled On a , the heavy and thin lines indicate the maximum and minimum horizontal stress orientations as inferred from the velocity measurements

Figure 13 a Principal strains as a function of pressure for a sample from a depth of 16026.2 feet a Crack strains, b elastic strains Values of strain and orientation at the peak pressure are indicated on the figure

Figure 14 Orientation of principal crack strains for a sample from a depth of 16026 2 feet, a projected into the E-W, N-S plane b projected into the N-S U-D plane The maximum, intermediate, and minimum compressive crack strains are indicated by (+,o) resepctively, and the orientation at the peak pressure is circled On a , the heavy and thin lines indicate the maximum and minimum horizontal stress orientations as inferred from the velocity measurements

Figure 15 a Principal strains as a function of pressure for a sample from a depth of 16038 4 feet a Crack strains, b elastic strains Values of strain and orientation at the peak pressure are indicated on the figure

Figure 16 Orientation of principal crack strains for a sample from a depth of 16038 4 feet, a projected into the E-W, N-S plane b projected into the N-S U-D plane The maximum, intermediate, and minimum compressive crack strains are indicated by (+,o) resepctively, and the orientation at the peak pressure is circled On

a , the heavy and thin lines indicate the maximum and minimum horizontal stress orientations as inferred from the velocity measurements

Figure 17 a Principal strains as a function of pressure for a sample from a depth of 16050 1 feet a Crack strains, b elastic strains Values of strain and orientation at the peak pressure are indicated on the figure

Figure 18 Orientation of principal crack strains for a sample from a depth of 16050 1 feet, a projected into the E-W, N-S plane b projected into the N-S U-D plane The maximum, intermediate, and minimum compressive crack strains are indicated by (+,o) resepctively, and the orientation at the peak pressure is circled On a , the heavy and thin lines indicate the maximum and minimum horizontal stress orientations as inferred from the velocity measurements

Figure 19 a Principal strains as a function of pressure for a sample from a depth of 16051 3 feet a Crack strains, b elastic strains Values of strain and orientation at the peak pressure are indicated on the figure

Figure 20 Orientation of principal crack strains for a sample from a depth of 16051 3 feet, a projected into the E-W, N-S plane b projected into the N-S U-D plane The maximum, intermediate, and minimum compressive crack strains are indicated by (+,o) resepctively, and the orientation at the peak pressure is circled On a , the heavy and thin lines indicate the maximum and minimum horizontal stress orientations as inferred from the velocity measurements

Figure 21 a Principal strains as a function of pressure for a sample from a depth of 16051 9 feet a Crack strains, b elastic strains Values of strain and orientation at the peak pressure are indicated on the figure

Figure 22 Orientation of principal crack strains for a sample from a depth of 16051 9 feet, a projected into the E-W, N-S plane b projected into the N-S U-D plane The maximum, intermediate, and minimum compressive crack strains are indicated by (+,o) resepctively, and the orientation at the peak pressure is circled On a , the heavy and thin lines indicate the maximum and minimum horizontal stress orientations as inferred from the velocity measurements

Figure 23 Crack strain for a sample from a depth of 16025 6 feet, projected into the E-W, N-S plane The heavy line indictes the maximum horizontal stress orientations as inferred from the shear wave birefringence (crossed polars) measurements

Figure 24 Crack strain for a sample from a depth of 16026 2 feet, projected into the E-W, N-S plane The heavy line indictes the maximum horizontal stress orientations as inferred from the shear wave birefringence (crossed polars) and V_P measurements, respectively

Figure 25 Crack strain for a sample from a depth of 16038 4 feet, projected into the E-W, N-S plane The heavy line indictes the maximum horizontal stress orientations as inferred from the shear wave birefringence (crossed polars) and V_P measurements, respectively

Figure 26 Crack strain for a sample from a depth of 16050 1 feet, projected into the E-W, N-S plane The heavy line indictes the maximum horizontal stress orientations as inferred from the shear wave birefringence (crossed polars) and V_P measurements, respectively

Figure 27 Crack strain for a sample from a depth of 16051 3 feet, projected into the E-W, N-S plane The heavy line indictes the maximum horizontal stress orientations as inferred from the shear wave birefringence (crossed polars) and V_P measurements, respectively

Figure 28 Crack strain for a sample from a depth of 16051 9 feet, projected into the E-W, N-S plane The heavy line indictes the maximum horizontal stress orientations as inferred from the shear wave birefringence (crossed polars) and V_P measurements, respectively

Figure 29 Orientation of σ_H, the maximum horizontal stress, as inferred from the maximum horizontal crack strain (o), shear wave birefringence (X), and V_P (+) measurements, respectively

Figure 30 Crack strain ratios for all samples The ratio of macimum horizontal crack strain to vertical crack strain ($\varepsilon_H/\varepsilon_Z$) is plotted as a +, while the ration for minimum horizontal crack strain ($\varepsilon_h/\varepsilon_Z$) is plotted using an o

Figure 31 V_P as a function of corresponding crack strain for all samples $V_{P,Z}$ as a function of vertical crack strain is plotted using "o", $V_{P,H}$ as a function of maximum horizontal crack strain is plotted using "x" and $V_{P,h}$ as a funtion of minimum crack stratin is shown using "+"

Figure 32 The velocity ratios $V_{P,Z}/V_{P,h}$ (plotted with "+") and $V_{P,Z}/V_{P,H}$ (plotted with "x") where $V_{P,Z}$ is the vertical velocity and the maximum and minimum horizontal velocities are $V_{P,h}$ and $V_{P,H}$ The convention is that "h" and "H", denote the minimum and maximum horizontal stress directions, respectively and thus the direction of maximum and minimum velocity

Table 1 Sample ID's, depths, and master scribe orientation for the UPRC cores Note that the orientations are relative to true north

Table 2 Summary of test results for six samples from UPRC Stratos well

Table 3 Crack strain ratios for all samples, computed using the maximum and minimum horizontal strains (ε_H and ε_h) divided by the vertical strain (ε_Z)

Table 4 Velocity ratios for all samples, computed using the vertical velocity ($V_{P,Z}$) divided by the maximum and minimum horizontal velocities ($V_{P,h}$ and $V_{P,H}$) The convention is that "H" and "h" denote the maximum and minimum horizontal stress directions, respectively and thus the direction of minimum and maximum velocity

Table 5 Vertical and horizontal stresses from crack closure pressures estimated from straight line fits to the low and high pressure portions of the corresponding velocity-pressure plots, for the vertical velocity ($V_{P,Z}$) and the minimum and maximum horizontal velocities ($V_{P,H}$ and $V_{P,h}$) The convention is that "H" and "h" denote the maximum and minimum horizontal stress directions, respectively and thus the direction of minimum and maximum velocity

Core-based methods for in-situ stress determination applied to core from UPRC Stratos well velocity anisotropy study Sandia National Laboratories, June, 1996

Figure 1 For sample at a depth of 16038 4 feet, a compressional wave velocity, V_P, in the horizontal plane and along the azis, b shear wave velocity, V_{SV} in the horizontal plane, polarized parallel to vertical, sample axis, c amplitude of signal for fast wave propagated along the vertical axis between cross-polarized shear transducers All quantities are as a function of θ, the angle from true North Solid lines connect data, dotted lines are the simplex fit to the data See text for meaning of ϕ

Figure 2 Signals received when a shear wave was propagated at various polarization angles (y axis) and received by a transducer with parallel polarization The offset was chosen such that the fast shear wave arrived at 0 Signals were taken at 15° intervals Note the disappearance of the fast wave at about 8°

Figure 3 Signals received when a shear wave was propagated at various polarization angles (y axis) and received by a transducer with perpendicular polarization The offset was chosen such that the fast shear wave arrived at 0 Signals were taken at 15° intervals Note the polarity inversion between 8 and 23°*irc* and again between 98° and 113°, indicating exact alignment of the polarization with the fast and slow axis

Figure 4 For sample at a depth of 16025 6 feet, a compressional wave velocity, V_P, in the horizontal plane and along the azis, b shear wave velocity, V_{SV} in the horizontal plane, polarized parallel to vertical, sample axis, c amplitude of signal for fast wave propagated along the vertical axis between cross-polarized shear transducers All quantities are as a function of θ, the angle from true North Solid lines connect data, dotted lines are the simplex fit to the data See text for meaning of ϕ

Figure 5 For sample at a depth of 16026 2 feet, a compressional wave velocity, V_P, in the horizontal plane and along the azis, b shear wave velocity, V_{SV} in the horizontal plane, polarized parallel to vertical, sample axis, c amplitude of signal for fast wave propagated along the vertical axis between cross-polarized shear transducers All quantities are as a function of θ, the angle from true North Solid lines connect data, dotted lines are the simplex fit to the data See text for meaning of ϕ

Figure 6 For sample at a depth of 16050 6 feet, a compressional wave velocity, V_P, in the horizontal plane and along the azis, b shear wave velocity, V_{SV} in the horizontal plane, polarized parallel to vertical, sample axis, c amplitude of signal for fast wave propagated along the vertical axis between cross-polarized shear transducers All quantities are as a function of θ, the angle from true North Solid lines connect data, dotted lines are the simplex fit to the data See text for meaning of ϕ

Figure 7 For sample at a depth of 16051 8 feet, a compressional wave velocity, V_P, in the horizontal plane and along the azis, b shear wave velocity, V_{SV} in the horizontal plane, polarized parallel to vertical, sample axis, c amplitude of signal for fast wave

propagated along the vertical axis between cross-polarized shear transducers All quantities are as a function of θ, the angle from true North Solid lines connect data, dotted lines are the simplex fit to the data See text for meaning of ϕ

Figure 8 For sample at a depth of 16052 3 feet, a compressional wave velocity, V_P, in the horizontal plane and along the azis, b shear wave velocity, V_{SV} in the horizontal plane, polarized parallel to vertical, sample axis, c amplitude of signal for fast wave propagated along the vertical axis between cross-polarized shear transducers All quantities are as a function of θ, the angle from true North Solid lines connect data, dotted lines are the simplex fit to the data See text for meaning of ϕ

Figure 9 V_P as a function of depth for all samples At each depth, the maximum and minimum velocity in the horizontal plane is shown (+ and o respectively) as well as the velocity along the axis of the sample (*)

Figure 10 V_{SH} and V_{SV} as a function of depth for all samples At each depth, the maximum and minimum veleocity in the horiaontal plane is shown +,* and o,x respectively)

Figure 11 A comparison of the velocity of the fast and slow shear waves ($V_{SA,\ fast}$ and $V_{SA,\ slow}$) along the axes of the samples with the maximum and minimum velocity of the vertically polarized shear wave propagating in the horizontal plane (VSV) By the symmetry these should be the same and with the exception of the sample at 16025 6 feet, the agreement is excellent, indicating proper picking of the arrival times and phases

Figure 12 Phase angles for the minimum of the compressional velocity in the horizontal plane (+,V_P) and the polarization reversal of the signals between crossed polarization transducers (x) as a function of depth This angle is the predicted orientation of the maximum horizontal in situ stress

Figure 13 Phase angles for the minimum of the compressional and vertically polarized shear waves in the horizontal plane (+, V_P and 0, V_{SV}), the polarization reversals of the signals between crossed polarization transducers (x), and the zero amplitude for parallel polarization transducers (*) as a function of depth This angle is the predicted orientation of the maximum horizontal in situ stress

Figure 14 View of DSCA and DWVA sample, showing 3 strain gage rosettes and 4 of 6 P transducers

Table 1 Sample ID's, depths and master scribe orientation for the UPRC cores Note that the orientations are relative to true north

Table 2 Estimates of the orientation of the maximum in situ horizontal stress by four methods Question marks indicate quantities that could not be determined Note that the orientations are relative to true north

Appendix F Logging/formation evaluation - Schlumberger

Figure 1 Porosity and lithology determination from Formation Density Log and CNL Compensated Neutron Log (Schlumberger Chart Book 1984, Chart CP-1c)

Figure 2 Matrix identification plot (Schlumberger Chart Book - 1984, Chart CP-21)

Figure 3 Formation Evaluation Summary using the Dual Laterlog-Density and Neutron

Figure 4 Core comparisons with Porosity and Water Saturations using Rw = 0 10 and m = 2

Figure 5 Porosity and Revised Water Saturations with Rw = 0 07 and m = 1 8

Figure 6 ARI Response in Fracture with FMI **(Not From This Well)**

Figure 7 ARI response in the upper Frontier section

Figure 8 FMI in the upper Frontier

Figure 9 FMI in the lower Frontier

Figure 10 ARI in the lower Frontier

Figure 11 Borehole ovality from FMI caliper

Figure 12a UBI Example of Hole being pushed in by strong tectonic force **(Not From This Well)**

Figure 12b UBI Borehole slip example **(Not From This Well)**

Figure 13 Mineral identification from Litho-Density Log and Natural Gamma Ray Spectrometry Log (Schlumberger Chart Book - 1984, Chart CP-18)

Figure 14 Mineral identification from Natural Gamma Ray Spectrometry (potassium) (Schlumberger Chart Book - 1984, Chart CP-19)

Figure 15 APS with LDT CNL and Flushing Estimates

Figure 16 Station CMR at 16550 ft

Figure 17 Porosity analysis with CMR

Figure 18 CMR T2 Distribution

Figure 19 Benchmark Estimates

Figure 20a Mechanical Properties Upper Frontier

Figure 20b Mechanical Properties Lower Frontier

Figure 21 Example of BCR in Fractures **(Not From This Well)**

Figure 22 BCR from Stratos Federal #1

Figure 23 Anisotropy fast shear and stress direction from BCR

Appendix G Cased hole stress test, breakdown treatment and pressure buildup evaluation and analyses - Integrated Petroleum Technologies, Inc

Figure 1 CHST 16150'-16152' PI/SI #1 Treatment data

Figure 2 CHST 16150'-16152' PI/SI #1 BHP versus square root of time

Figure 3 CHST 16150'-16152' PI/SI #1 Log-log plot of delta pressure vs delta time

Figure 4 CHST 16150'-16152' PI/SI #2 Treatment data

Figure 5 CHST 16150'-16152' PI/SI #2 BHP versus square root of time

Figure 6 CHST 16150'-16152' PI/SI #2 Log-log plot of delta pressure vs delta time

Figure 7 CHST 16150'-16152' PI/SI #3 Treatment data

Figure 8 CHST 16150'-16152' PI/SI #3 BHP versus square root of time

Figure 9 CHST 16150'-16152' PI/SI #3 Log-log plot of delta pressure vs delta time

Figure 10 CHST 15900'-15902' PI/SI #1 Treatment data

Figure 11 CHST 15900'-15902' PI/SI #1 BHP versus square root of time

Figure 12 CHST 15900'-15902' PI/SI #1 Log-log plot of delta pressure vs delta time

Figure 13 CHST 15900'-15902' PI/SI #2 BHP versus square root of time

Figure 14 CHST 15900'-15902' PI/SI #2 Log-log plot of delta pressure vs delta time

Figure 15 CHST 15900'-15902' PI/SI #3 BHP versus square root of time

Figure 16 CHST 15900'-15902' PI/SI #3 Log-log plot of delta pressure vs delta time

Figure 17 Breakdown treatment data

Figure 18 Net pressure history match of the breakdown treatment data

Figure 19 Breakdown BHP versus square root of time

Figure 20 Breakdown Log-log plot of delta pressure vs delta time

Figure 21 Cartesian Plot of Pressure build-up and temperature data

Figure 22 Log-log plot of the delta pseudo-pressure vs delta time of the build-up data

Figure 23 Horner plot of pressure build-up data

Table 1 Predicted fracture dimensions

Table 2 Stress and leakoff parameters

Table 3 Assumed reservoir and fluid properties

Appendix A Technical Paper SPE 29599 "An Evolving Approach In The Analysis of Stress Test Pressure Decline Data"

BBD 2/10/97 (mod 01/12/2000)

Phase II - Topical Report
UPRC/DOE Greater Green River Production Improvement Project: Drilling, Testing, and Completion of the UPRC Stratos Federal #1

Abstract

The objectives of phase II of the UPRC/DOE Greater Green River Basin Production Improvement Project were to drill, complete, and test a vertical wellbore in the Second Frontier Formation. Information gained from the vertical well was to be used to further characterize the geology of the site, reservoir quality, natural fractures, stress directions, and gas productivity in support of subsequent phases of the project. The UPRC Stratos Federal #1 (SE 1/4 of Sec. 24-T22N-R107W, Sweetwater Co , WY) was drilled through the Second Frontier to a total depth of 16,250 ft. Eight gross feet and four net feet (porosity>6% and water saturation<60%) of fluvial channel sandstones and approximately forty gross feet and 19 net feet (porosity>6% and water saturation<60%) of marine sandstones were encountered in the well Core porosities ranged from 3.3 to 7.3% in the fluvial sandstones and from 3 5% to 11 4% in the marine sandstones. The unstressed horizontal permeabilities to air ranged from <0.01 millidarcies to 0 25 millidarcies in the fluvial sandstones and from < 01 to 0.1 millidarcies in the marine sandstones Special core analyses revealed that permeabilities decreased on the order of one magnitude after the application of confining pressures up to 4000 psi. Permeabilities also decreased an additional one order of magnitude as water saturations (Sw) were increased to 40%.

Petrographic analysis indicates that porosity in the reservoir is a combination of primary intergranular porosity and secondary porosity created by the dissolution of feldspar and chert grains The fluvial sandstones can be classified as sublitharenites to litharenites, with extensive silica cementation occluding much of the porosity The lower shoreface marine sandstones are primarily sublitharenites, however, these lower shoreface sandstones contain much more feldspar and generally less chert than the fluvial sandstones. The best porosity and permeability in the marine section occurs not in the cleanest lower shoreface sandstone, but in a slightly muddy, thoroughly bioturbated lower shoreface sandstone. The presence of the detrital mud within the bioturbated sandstone has precluded the extensive precipitation of quartz overgrowths and therefore preserved a greater amount of primary intergranular porosity Some of the lithic grains have been partially to completely

altered to clay, resulting in the creation of relatively isolated microporous grains Both calcite and dolomite cements (ferroan and non-ferroan) are present in some of the marine sandstone samples, with values ranging from 1 to 8%

Macroscopic natural fractures are relatively isolated in the core Three relatively short, calcite-filled fractures are oriented east-northeast to west-southwest while three longer fractures filled with dark gouge are oriented northeast - southwest One partially open fracture is also oriented northeast - southwest. One ASR (anelastic strain recovery) sample performed by Terra Tek yielded a maximum horizontal strain azimuth of N64.7°E, roughly consistent with the fractures encountered in the core Sandia National Laboratories performed velocity and strain anisotropy measurements on six Frontier core samples, and these analyses yielded an orientation for maximum horizontal *in situ* stress of approximately N10°E at 16,025 ft and 16,038 ft. The stress apparently rotates to approximately N35°E at 16,051 ft.

Quartz-filled microfractures are abundant in the Second Frontier sandstones Several thin sections are currently being analyzed by scientists at the Bureau of Economic Geology at the University of Texas using photomultiplier-based electron beam-induced luminescence (scanned CL) imaging to determine the orientation(s) of the microfractures and their timing relative to other diagenetic events

Wellbore breakout data from the four-arm caliper tool yield an essentially north-south direction for maximum horizontal stress through the fluvial sediments of the Second Frontier, but show an essentially round borehole through the marine sediments, yielding no information about maximum horizontal stress through that interval Formation MicroScanner (FMS) logs show a lack of significant natural fracturing in the reservoir near the vertical wellbore.

The Second Frontier sandstones were perforated from 16,000 to 16,060 ft with 4 JSPF. The perforated interval includes both the fluvial and marine sandstones. Initial gas production after a 50 barrel 3% KCl water breakdown was approximately 20 MCFD with a flowing tubing pressure of 38 psi, a much lower rate than predicted after comparison to two offset wells with similar reservoir characteristics An acid job with a retarded HCl/acetic blend was performed in November, 1997 in order to clean up existing near-wellbore damage and to potentially improve productivity by removing carbonate cement from the matrix as well as from calcite-cemented microfractures However, post-

acidization rates remained relatively unchanged, at less that 50 MCFD. The well is currently shut-in, pending further evaluation

Phase II - Topical Report
UPRC/DOE Greater Green River Production Improvement Project
Drilling, Testing, and Completion of the UPRC Stratos Federal #1

1. Introduction

1.1 Objectives of Phase II

The objectives of phase II of the UPRC/DOE Greater Green River Basin Production Improvement Project include the drilling, testing and completion of a vertical wellbore in the Cretaceous Second Frontier Formation (Fig 1-1). The information gained from this wellbore is to be used to further characterize the geology of the site, reservoir quality, natural fractures, in situ stress regime, and gas productivity in support of subsequent phases of the project.

1.2 Drilling prognosis for the Stratos Federal #1

The UPRC Stratos Federal #1 was proposed as a step-out from the Energy Reserves Group Blue Rim Federal 1-30 and 1-31 wells (Secs. 30 and 31, T22N-R106W, Sweetwater County, Wyoming) which tested 1.3 MMCFD and 1 8 MMCFD respectively from the Second Frontier sandstones after fracture stimulation Pre-fracture stimulation rates (post breakdown) from the same wells were 378 and 817 MCFD respectively The Frontier Formation in the Stratos Federal #1-24 (SE 1/4 of Sec 24-T22N-R107W) was interpreted to be structurally flat to the Frontier in the ERG Blue Rim #1-30 well, and the anticipated top of the Frontier Formation was 15,984 ft (-9,280 ft subsea) (Fig 1-2) The ERG Blue Rim Federal 1-30 and the ERG Blue Rim Federal 1-31 contained 31 feet and 22 feet of net sand respectively (log responses with greater than 6% porosity and water saturations less than 60%), and comparable amounts of sandstone were expected in the UPRC Stratos Federal #1 (Figures 1-3 and 1-4).

2. Drilling History

2.1 Location and drilling

This project involved the drilling and completion of a 16,250 ft Second Frontier gas well located at 1321' FSL and 1321' FEL in the SE/4 of Section 24, T22N-R107W in

Sweetwater County, Wyoming UPR owns the mineral rights to this location while the BLM owns the surface rights

The Stratos Federal Unit #1 (API# 49-037-23539) was spudded using a 26" bit at 12.30 AM 7/31/95 and 20" surface casing was set and cemented at a depth of 499 ft (Fig 2-1) A 17.5" hole was then drilled to 5023 ft and 13-3/8" surface casing was set at 5020 ft Mud weight averaged 8 4 pounds Drilling resumed using a 12-1/4" bit to a depth of 10,822 ft with a minimal amount of downtime At this point, however, a cracked drill collar resulted in the loss of the drill collars and the bottom hole assembly and required a 2 5 day successful fishing job.

2.2 Directional drilling

In order to facilitate the fracture characterization portion of this project, the wellbore was deviated, thereby increasing the probability of intersecting one or more vertical fractures during drilling. At a depth of 13,872 ft, a MWD tool was included with the drill string to begin closely monitoring the angle of deviation Previous periodic mechanical surveys showed a maximum deviation of 1-1/4° at 6337 ft A mud motor was added to the bottom hole assembly at 14,703 ft The bit was steered until 15,835 ft MD when all three of the nose cones from the bit were lost. Only two were recovered and the directional drilling continued to a depth of 15,990 ft MD (15,984 ft TVD) which was the core point for the Second Frontier Prior to the directional drilling, the mud weight averaged 9 0 pounds Thereafter, the mud weight ranged from 9 7 pounds to 11 9 pounds during directional drilling, coring, and logging operations (Fig 2-2). Maximum deviation from vertical was 12°, resulting in the core point being 106.15' N23° E5° from the surface location (Figs. 2-3 and 2-4).

2.3 Coring

Oriented cores were taken through the fluvial and marine sections of the Second Frontier to aid in the understanding of the reservoir and in designing the completion of the well. The core analyses included routine gamma ray, detailed lithology, unsteady state permeability, fracture identification, and porosity and grain density measurements Special core analyses included capillary pressure, specific water and gas permeabilities, steady state permeability, and stress analysis. After conditioning the hole and orienting the core barrel, the coring of the Frontier commenced with a 8.75" core bit, yielding a 4" diameter oriented core from 15,990-16,015 ft MD. The barrel jammed, but a total of 25 ft of core was recovered (100% recovery) Core #2, 16,015-16,039 ft MD, also had a jammed core

barrel Recovery was 24 8 ft (100% recovery - 16,015-20 ft MD shale, 16,020-29 ft MD sand, 16,029-39 ft MD sand and shale). Core #3 went from 16,039-16,100 ft MD and retrieved 60 ft of core (100% recovery - 16,040-16,070 ft MD sand, 16,070-16,084 ft MD shaley sand, 16,084-16,098 ft MD silty shale, 16,098-16,100 ft MD shale) Total cored interval was 15,990-16,100 5 ft MD or 110 5 ft (Fig 3-2)

2.4 Total depth and logging

After washing and reaming the hole, drilling of the 12-1/4" hole continued to a final TD of 16,250 ft MD at 12:30 PM on 10/12/95 (73 days). After coring, the wellbore was no longer directionally drilled and no deviation surveys were taken between 16,100 ft and TD The final bottom hole location was 1412' FSL and 1273' FEL, Sec 24, T22N-R107W. At TD, the wellbore was conditioned for open hole logging. The open hole logs were obtained in four runs (Table 2-1). The maximum bottom hole temperature from the logs was 250°F, but further testing indicated that 285°F is more indicative of reservoir temperature When the combineable magnetic resonance tool (CMR - Run 3) was run back down to 16,036 ft for a station, it became stuck and required an additional trip in and out of the hole to successfully fish the tool Upon the completion of all the open hole logging runs, the hole was circulated and readied for casing A total of 396 joints of 9-7/8" casing were run and cemented. After drilling out, a Cement Bond Log was run whereby the top of the good cement was determined to be at 15,278 ft MD Velocity shots were also taken at regular intervals from 16,150 ft MD to 500 ft Depths measured by the electric logs proved to be +22 ft to the driller's depth The rig was released at 9 00 AM 10/26/95 (87 days) (Fig 2-5).

3. Reservoir Characterization

3.1 Sedimentological interpretation of the Second Frontier

As mentioned in the previous section, the Frontier Formation was cored from 15,990 to 16,100.5 ft, recovering 110 5 feet of core. Color copies of the core photographs are included as Appendix A. The cored interval contains both fluvial and marine sandstones typically found in the Second Bench of the Second Frontier sandstone (Fig 3-1), as well as the sequence boundary that separates the two facies (See figure 3-2a for a complete core description.) Core #1 is from 15,990 ft to 16,039 ft and consists of coastal plain fluvial mudstones and stacked active channel fill sandstones The channel sandstones are eight feet thick, and ten feet of coastal plain fluvial mudstones separate the channel

sandstones from the underlying sequence boundary and marine sandstones The sequence boundary that separates the coastal plain fluvial sediments from the lower shoreface marine sediments is not preserved in the core In fact, the break between cores #3 and #4 coincides with the contact between fluvial and lower shoreface marine sediments.

Coastal plain fluvial deposits - The coastal plain fluvial sediments of the Second Frontier are composed of both mudstones and sandstones (15,990 ft to 16,039 ft). The mudstones are typically dark gray to black, organic-rich, and silty with thin silt and very fine-grained sandstone interbeds. The mudstones are locally rooted and occasionally contain wood clasts The fluvial sandstones are fine to medium-grained and exhibit sharp and locally scoured bases. Internally, the sandstones contain small scale trough cross-stratification with abundant mudstone chips and carbonaceous laminations Bedding plane orientations were measured by TerraTek for the fluvial interval between 16,021 and 16,029 ft Their dip azimuth plot indicates that bedding generally dips to the east, although some beds dip to the northeast and southeast (Fig. 3-3) This indicates that transport within the fluvial channels was generally to the east.

Marine deposits - The marine deposits of the Second Frontier (16,039 ft to base of core) consist of the following lithofacies· burrowed to bioturbated mudstones and siltstones; muddy, bioturbated very fine-grained sandstones; relatively clean very fine-grained, bioturbated sandstones; clean, massive to hummocky cross-stratified, very fine-grained sandstones, and massive fine-grained sandstones that contain some shell debris and are occasionally graded. The base of the core is composed of several incomplete coarsening-upward cycles of burrowed to bioturbated mudstones and muddy siltstones These sediments are interpreted to represent deposition in an offshore transition environment. These units grade gradually upward into a muddy sandstone that coarsens upwards and gradually becomes cleaner toward the top of the unit, it is thoroughly bioturbated by *Ophiomorpha, Planolites, Teichichnus,* and occasionally *Asterosoma.* This sandstone is interpreted to represent deposition by storms in a lower shoreface environment This unit is capped by a two-foot thick, sharp-based, fine-grained massive sandstone that contains shell debris and graded bedding Directly on top of the fine-grained sandstone is a two-foot thick, very-fine-grained sandstone that is highly contorted by soft-sediment deformation Capping the contorted unit is another one to two-foot thick fine-grained massive sandstone The two thin massively bedded sandstone bodies are interpreted to represent slurry deposits. The contorted sandstone between the two massive beds was probably deposited by storms in a lower shoreface environment, and was subsequently

disturbed shortly after deposition to produce the contorted bedding. A thin, one-foot thick, shaley sandstone that is thoroughly bioturbated lies directly on top of the uppermost fine-grained massive sandstone unit This thin shaley sand is interpreted as a transgressive event It is capped by a sharp-based, very fine-grained, hummocky cross-stratified sandstone that is interpreted as a lower shoreface sandstone The sandstone is occasionally burrowed by *Ophiomorpha*, and becomes more massive near the top of the unit This sandstone is abruptly overlain by coastal plain fluvial mudstone, and the contact between the two units is interpreted as a major sequence-bounding unconformity, or a sequence boundary.

Comparison of the Stratos Federal #1-24 and the Blue Rim wells - The UPRC Stratos Federal #1-24 was drilled only 4100 feet to the northwest of the ERG Blue Rim # 1-30 (Fig 3-4), yet the two wells exhibit some important variations in reservoir quality within the Second Frontier sandstones. The stratigraphic relationship between the Stratos Federal # 1-24 and the two Blue Rim wells is shown on figure 3-5, and core descriptions of the Stratos #1 and the Blue Rim #1-30 are included as figures 3-2a and 3-2b, respectively. The cross-section shows that the Blue Rim #1-30 contains approximately 14 feet of fluvial sandstone while the Stratos Federal #1-24 contains 8 feet of fluvial sandstone However, the most important distinction is that all of the fluvial sandstone in the Blue Rim #1-30 exhibits porosity greater than 6% while the fluvial sandstone in the Stratos Federal #1-24 contains only four feet of porosity greater than 6 % The Stratos Federal #1-24 marine sandstones are cleaner than the muddier, more bioturbated Blue Rim marine sandstones, and apparently the Blue Rim wells are located on a more distal part of the Second Frontier marine shelf. Unfortunately, the cleaner marine sandstones appear to contain more quartz cementation than the muddier lower shoreface sandstones, and therefore exhibit lower porosities overall. The Blue Rim #1-30 contains over 20 feet of marine sandstone with electric log porosities of 6-10%. However, routine core analysis indicates that there are only 10 feet of sandstone with porosities 6% or greater in the marine sandstones of the Blue Rim well (Table 3-3) Routine core analysis shows that the Stratos Federal #1-24 contains 35 feet of marine sandstone with greater than 6% porosity (Table 3-1) In summary, the Blue Rim well contains 10 more feet of fluvial sandstone with porosities of 6% or greater while the Stratos well contains 25 more feet of marine sandstone with porosities of 6% or greater.

As previously discussed, core-derived porosity and permeability measurements for the Frontier Formation in the UPRC Stratos Federal #1-24 and the ERG Blue Rim Federal

#1-30 are presented in tables 3-1 and 3-3 A comparison of total permeability-feet (permeability value multiplied by number of feet) and porosity-feet (porosity value multiplied by number of feet) between the Stratos Federal #1-24 and the Blue Rim #1-30 shows that the Stratos Federal # 1-24 actually exhibits higher values in both categories (Figs. 3-6 and 3-7) However, the ERG Blue Rim Federal #1-30 had an initial production rate of 378 MCFD after breakdown as compared to the initial production rate of 20 MCFD for the Stratos Federal #1 (Fig 3-8).

The Stratos Federal #1-24 appears to contain a somewhat similar distribution and amount of porosity in the Second Frontier as the other Blue Rim well (the ERG Blue Rim Federal #1-31) Note however, that the porosity information is based solely on the comparison of electric logs because the ERG Blue Rim Federal #1-31 was not cored The Blue Rim #1-31 contains six feet of fluvial sandstone with 6% or greater porosity (as compared to four feet in the Stratos), and the Blue Rim #1-31 contains eighteen feet of marine sandstone with 6% or greater porosity as compared to 35 feet in the Stratos well There is also a zone in the Blue Rim #1-31 located between the fluvial and marine sandstones that could be interpreted as either fluvial or marine from the electric logs (It has been interpreted to be fluvial on the stratigraphic cross-section - Figure 3-5) This zone contains an additional five feet of 6% or greater porosity. The Blue Rim #1-31 well had an initial production after breakdown of 817 MCFD as compared to the Stratos initial production rates of 20 MCFD.

A possible explanation for the discrepancy in flow rates between the three wells is that the fluvial sandstone is a better reservoir than the marine; therefore, the reason that the Stratos well did not perform well is because the Stratos contains less fluvial sandstone than the two Blue Rim wells However, it is not apparent from the core analyses nor from petrographic analyses why the fluvial sandstone would be a better reservoir. The porosities and permeabilities in the better marine sandstones are comparable to those of the fluvial sandstones, and the petrographic work indicates similar diagenetic histories for the two sandstones. The answer may involve a subtle distinction in the distribution and/or size of pore throats which would require additional detailed mercury injection capillary pressure analyses to be performed for both lithofacies in both wells.

The anomaly between the apparently comparable reservoir qualities yet vastly different production rates between the Stratos and the Blue Rim wells could also suggest, as predicted, that natural fractures play a critical role in gas productivity, and that for some

reason, the Stratos well is not well connected to the natural fracture system that has enhanced the performance of the Blue Rim wells.

Another possible explanation for the low rates in the Stratos well is that some of the perforations in the Stratos well are not open, and that there is not good communication between the formation and the wellbore The latter has been proposed by Integrated Petroleum Technologies, Inc. after their analysis of some of the post-breakdown, pressure buildup data However, the acetic/hydrochloric acid treatment that was performed on the Stratos well indicated that all of the perforation tunnels were open

Another possible explanation for the difference in production rates between the Blue Rim wells and the Stratos well is that a lower sandstone bench of the Frontier (the Fourth Frontier) that was not penetrated in the Stratos well contributed significantly to the production of the Blue Rim wells This lower zone is approximately fifty feet below the base of the Second Frontier sandstone and is six to eight feet thick Based on log correlations it is interpreted as a marine shoreface sandstone in the lower Frontier This lower sandstone bench was perforated, acidized, and fracture stimulated along with the Second Frontier zone in both of the Blue Rim wells

The Blue Rim #1-30 tested 1 316 MMCFD from perforations in the Second Frontier and the Fourth Frontier After numerous mechanical problems, the well was plugged and abandoned. The Blue Rim #31-1 had an initial production of 1 797 MMCFD after hydraulic fracture treatment of both the Second Frontier and Fourth Frontier sands It was subsequently shut-in for approximately four years until it was tested at 1 5 to 3.7 MMCFD on a six-day flow test The well was then temporarily abandoned for approximately three years until it was placed on production after begin hooked to a surface pipeline. The Fourth Frontier perforations were apparently plugged by equipment lost in the hole during the previous flow test, and therefore did not contribute to any subsequent production of the well

Technical evaluation of the Fourth Frontier sandstone indicated that it was probably not the main contributor to the production in the Blue Rim wells, therefore the decision was made not to drill to the depths needed to encounter the sandstone. However, since this zone was not penetrated in the Stratos well, the possibility remains that some of the gas production in the Blue Rim wells is coming from this lower sandstone.

3.2 Petrographic analysis and diagenetic history of the Frontier Formation

3.21 Thin section analysis

The petrographic study conducted at Union Pacific Resources of the Second Frontier sandstones in the UPRC Stratos Federal #1-24 was based primarily on detailed analysis of sixteen thin sections and twelve scanning electron microscope samples. Point counts (300 points) were made for all of the thin sections, and the results are shown in Table 3-4 The composition of the Second Frontier sandstone samples is graphically shown in figure 3-10 With porosity, cement and clays excluded, the fluvial sandstones contain 64% to 81% monocrystalline quartz, and can be classified as sublitharenites to litharenites (Fig 3-10) Sedimentary chert is the most common type of rock fragment in the fluvial sandstones (11.3 to 20.6% of the total rock) With porosity, cements and clays excluded, the majority of the lower shoreface marine sandstones are also primarily sublitharenites (75% to 93% monocrystalline quartz), however, the lower shoreface sandstones contain much more feldspar (2 3% to 6.3% of the total rock) and generally less chert (2% to 16.6% of the total rock) than the fluvial sandstones. Hycal Energy Research Laboratories also performed petrographic analyses on three additional thin sections (Table 3-5), and their point count analyses of the samples result in the same lithologic classification of the sandstones as the more extensive study performed at Union Pacific Resources.

Porosity is a combination of primary intergranular porosity and secondary porosity created by the partial dissolution of lithic grains such as feldspars and cherts. The primary porosity that is preserved is typically clay-filled Porosity has been reduced by compaction as well as by extensive quartz overgrowths which appear to have precipitated periodically throughout the diagenetic history of the sandstone. Analysis of the thin sections indicates that dissolution of most of the cherts and feldspars occurred after a relatively early episode of quartz cementation, however, a later episode of quartz cementation can also be inferred from the scattered presence of quartz overgrowths growing into secondary pores created by the earlier dissolution of a lithic grain Ferroan calcite and ferroan dolomite cement are also present, but typically occur as partial to complete replacements of feldspar grains Determination of the timing of the carbonate cements is difficult, however, it appears that much of the carbonate cement precipitated at approximately the same time as the lithic grains were dissolved Many of the lithic grains have also been partially to completely altered to clay. This alteration results in the creation of microporosity inherent in the framework of the authigenic clays

3.22 Scanning election microscopy (SEM Analysis) and X-Ray Diffraction Analysis

Twelve samples were analyzed with the scanning electron microscope (SEM) in order to determine the type and distribution of clays within the reservoir Photomicrographs of each of these samples can be seen in Appendix B X-Ray diffraction analysis was performed on three sandstone samples (Table 3-6) Both the SEM and the X-Ray diffraction analyses indicate that the most common types of clays present in the Second Frontier are illite (4% to 7%), kaolinite (1% to 3.3%), mixed-layer clay (1%) and chlorite (trace). The illite is abundant in most of the samples, and occurs in both pore-bridging and pore-lining forms Smaller amounts of chlorite are commonly mixed in with the illite The extensive quartz cementation is also evident in the SEM photomicrographs

3.3 Core analysis - porosity and permeability

3.31 Unstressed porosity and permeability measurements

Terra Tek performed routine porosity and permeability measurements as well as stressed (in situ) permeability measurements for the Second Frontier in the Stratos Federal #1-24 The results for the routine analyses are presented in table 3-1, and the stressed permeability values are presented in table 3-2. Routine porosities in the fluvial sandstone range from 3.3% to 7 3%, and unstressed horizontal permeabilities range from <0 01 md to 0 25 md Routine porosities and permeabilities in the marine sandstone vary widely The cleanest sandstone, massive to hummocky cross-stratified in character (16,040 ft to 16,062 ft in the core), exhibits low porosities and very low permeabilities Porosity ranges from 3 5% to 9.5%, and horizontal permeabilities range from <0.01 md. up to 0 03 md , with the majority of the samples exhibiting permeabilities of <0 01 md The best porosity and permeability in the marine section occurs within the relatively clean, but bioturbated lower shoreface sandstones (16,066 ft to 16,083 ft). Porosities in this interval range from 8.2% to 11 4 %, and unstressed horizontal permeabilities range from 0 02 to 0 1 md

3.32 Stressed (in situ) permeability analyses

Terra Tek performed six stressed permeability analyses on the Frontier from the Stratos Federal #1, and the results are presented in table 3-2. Permeabilities were measured at 300 psi (net effective stress) and 4000 psi (net effective stress) Figure 3-12 shows that permeability values decrease on the order of one magnitude due to confining pressures up to 4000 psi (4000 psi generally approximates the current reservoir stresses which exist in the virgin reservoir at this time) Two additional full diameter core samples were analyzed up to 11,200 psi by Hycal Energy Research Laboratories to determine the effect of

reservoir overburden stress on fracture permeability. Both core samples contained vertical hairline fractures. The results of the analysis are shown in table 3-7 and indicate that fracture permeability is also significantly reduced by an increase in overburden stress An increase from an unstressed condition to approximately 3750 psi caused over 90% reduction in permeability. A complete report of this procedure and other special core analyses performed by Hycal is located in Appendix C. The data from both laboratories indicate that the effect of confining pressure on reservoir permeability is significant in the Frontier sandstones

3.33 Effect of increasing water saturation on permeability

The effect of increasing water saturation on permeability of the Frontier sandstones is similar to the effect of increasing confining pressure. Hycal's Incremental Phase Trap Evaluation Tests show that even relatively small water saturations of 30% in both the fluvial and marine samples caused significant reductions of over 90% in the effective gas permeabilities in comparison to normal dry unstressed routine core permeabilities (Table 3-8) A complete report of the procedure and other analyses performed by Hycal can be found in Appendix C.

3.4 Fracture characterization and analysis of in-situ stresses

The accurate prediction of the orientation of any naturally-occurring or induced fractures present in a reservoir is critical in optimizing the drilling and completion of both vertical and horizontal wells This is especially true for formations such as the deep, overpressured Second Frontier where it is thought that natural fractures are vital factors in enhancing the permeability of otherwise very tight reservoirs. Since the orientations of natural fractures are commonly parallel to the maximum horizontal stress (S_{Hmax}) azimuth, determination of this azimuth has become important in evaluating naturally fractured reservoirs Estimates of S_{Hmax} can be obtained from the analysis of both core and well log data. Description of macrofractures in oriented core, analysis of microfractures, wellbore breakout analysis, anelastic strain recovery, and other core-based methods were all used to determine the direction of S_{Hmax} in the Stratos Federal # 1 The results of each technique are summarized in the following sections

3.41 Characterization of macrofractures in core

Macroscopic natural fractures are relatively isolated in the Frontier cored interval of the Stratos well. The lack of <u>abundant</u> macrofractures in the core is disappointing, but not

surprising. The Second Frontier was also cored in the offsetting ERG Blue Rim #1-30, and only one thin zone of calcite-filled macrofractures was detected in that core (16,123 ft on core description - Fig 3-2b) However, the Blue Rim core was from a vertical wellbore, and the likelihood of encountering any vertical fractures in a vertical wellbore is small. The presence of natural fractures in the Blue Rim #1-30 was inferred because the well had an initial flow rate of approximately 1 3 MMCFD after breakdown from an otherwise tight sandstone

The Stratos wellbore was deviated up to a maximum of 12°, and several thin zones with natural fractures were encountered in the cored interval Three relatively short, calcite-filled fractures from 16,065 ft are oriented east-northeast while three longer fractures filled with dark gouge from the same depth are oriented northeast One partially open fracture from 16,065 ft is also oriented northeast. One ASR (anelastic strain recovery) sample performed by Terra Tek yielded a maximum horizontal strain azimuth of N64 7°E, consistent with the orientations of the macrofractures documented in the core

3.42 Preliminary analysis of microfractures

Microfractures, those natural fractures that are generally not visible to the unaided eye (microns to millimeters in size), can be used to determine the relative timing of fracturing and to infer the orientation of larger macrofractures (Laubach, in press). However, many of these microfractures typically go undetected in even detailed petrographic analyses because the fractures are completely filled with quartz that is in optical continuity with the host-rock quartz. Most of these microfractures are only faintly visible to invisible using conventional optical techniques, however the use of photomultiplier-based electron beam-induced luminescence (scanned CL) imaging has dramatically improved the resolution of these features This is because the cathodoluminescence of detrital quartz grains is different from that of the diagenetic quartz that lines the natural fractures, even though the quartz may be in optical continuity The scanning microscope also allows for much greater magnification of the sample than is possible with standard petrographic microscopes.

Three thin sections from the Stratos core were sent to the Bureau of Economic Geology at the University of Texas at Austin for scanned CL microscopy, and the preliminary results are presented here and in Appendix D. Work is ongoing with this project and should yield some interesting information upon completion. At the time of this report, preliminary study indicates that quartz-lined, opening-mode fractures are widespread in

the three samples The dominant strike of the highest reliability microfractures is west-northwestward (280°) There is also a subsidiary northeast striking component to the data, this northeast trend is clearest in areas that have few of the west-northwest-trending fractures Figure 3-13 (Photos a through d) illustrates some of oriented microfractures Figure 3-14 is a plot of the orientation of the strikes of all the microfractures measured from a thin section of the fluvial sandstone (16027 ft). It is important to note that although there is a strongly preferred orientation in the areas of the thin sections that have been studied, the actual areas that have been analyzed represent less than one percent of each thin section

Steve Laubach and others at the Bureau of Economic Geology (University of Texas at Austin) have categorized microfractures according to their shape and relationship to other microfractures (Laubach, in press). Table 3-10 defines these microfracture categories and their interpreted origin Laubach and others at the BEG have also defined a microfracture data-quality index for assessing the reliability of macrofracture strike determination from the orientation of microfractures (Table 3-11). All microfractures described in the Stratos well are being categorized and coded for reliability for the final interpretation.

3.43 Core-based methods for estimating in situ stress conditions

Introduction - As previously discussed, the determination of in situ stress orientations and magnitudes is a critical component of natural fracture analysis because it is these parameters which presumably control the orientation and aperture of natural fractures in formations at depth. In order to establish the stress regime present in the Frontier in the Stratos Federal #1 wellbore, Union Pacific Resources contacted Sandia National Laboratories to discuss core-based methods for determining in situ stress orientation and magnitude in this well. These discussions led to an effort by both Sandia National Laboratories and Terra Tek to apply Anelastic Strain Recovery (ASR) to core retrieved from the Stratos well Unfortunately, Sandia felt that the ASR results obtained from the Stratos core were essentially null, probably because of the time required to retrieve core from 16,000 ft. Terra Tek felt that they acquired only one valid ASR reading for in situ maximum horizontal compression (N65°E)

Since the ASR results were disappointing, further discussions with Sandia led to the use of other approaches for the determination of in situ stress orientations. These analyses were applicable to "old" core and used measurements of the anisotropy of elastic wave speeds and anisotropic, non-linear strains exhibited by core subjected to hydrostatic stress Stress

magnitudes were estimated using Differential Strain Curve Analysis (DSCA) and Differential Wave Velocity Analysis (DWVA), both of which rely on determining the pressure required to close relaxation cracks A summary of the results will follow; the two detailed reports provided by David Holcomb and Robert Hardy of Sandia National Laboratories are located in Appendix E

Procedure - Six whole core samples were sent from Terra Tek in Salt Lake City, Utah to Sandia National Laboratories in Albuquerque, New Mexico. The samples were trimmed to approximately 10 centimeters (4 inches) in length using a diamond cutoff saw and water coolant. The core samples were then stored in plastic bags with no control on moisture content. Orientation of the master scribe was determined from the orientation survey conducted during the coring Table 3-9 lists orientations, depths at top of each sample, the test identification number used on plots, etc

Methods - The methods involved measuring velocities and amplitudes for several types and amplitudes of elastic waves, including compressional, shear, and cross-polarization shear waves to detect birefringence Velocity and strain measurements (Differential Strain Curve Analysis and Differential Wave Velocity Analysis) were done on the six samples to a maximum pressure of 190 MPa (27,500 psi) The crack strain tensor was also determined The orientation survey done during coring was presumed to be correct since there were no indication of problems It was assumed that the axis of the core was vertical

Results - The following statements summarize the results of the above analyses

- The velocity and strain anisotropy data indicate, with two exceptions, that the in situ stress was oriented as expected, with one principle axis in the vertical and the other two in the horizontal However, the principal stress in the vertical direction was not usually the maximum compressive stress, as is generally the case The maximum horizontal stress (σ_H) was indicated to be at 10° east of north between 16,025 and 16,038 ft. The data indicate that σ_H then rotates to about 35° east of north at 16,050 ft

- All of the data indicate that the maximum horizontal effective stress is close to (and possibly larger than) the vertical effective stress From Differential Wave Velocity Analysis, the effective stress state was (σ_H, σ_h, σ_Z) = (67,53,60) MPa (σ_H =

maximum horizontal stress, σ_h = minimum horizontal stress, σ_Z = vertical stress) The small differences between the stress magnitudes are not conducive to fracturing

- Since the estimated effective stress state for the Frontier was (σ_H,σ_h, σ_Z) = (67,53,60 MPa) where σ_H = maximum horizontal stress, σ_h = minimum horizontal stress, σ_Z = vertical stress, then the stress state is interpreted as extensional ($\sigma_1 \approx \sigma_2 > \sigma_3$). If this is the case in the Frontier, the ductility of the formation would be decreased under extensional conditions, increasing the likelihood of fracturing; however, the strength of the rock could increase under these conditions, making fracturing more difficult.

- The more severe constraints on possible fracture orientations also decrease the amount of fracturing that would be expected

3.44 Wellbore Breakout Analysis from Four-Arm Caliper Data

Wellbore breakout data obtained from oriented 4-arm caliper tools have been widely used to determine the current stress directions in a wellbore, and wellbore breakout analysis have been typically regarded as one of the more reliable methods for estimating in situ stress configurations Wellbore breakouts occur when the stress concentrations near the wellbore exceed the strength of the rock. This results in an elliptical wellbore where the elongations are aligned parallel to the minimum horizontal stress The relationship between wellbore breakout, maximum and minimum horizontal stress, natural fractures, and other features is summarized in figure 3-15 A detailed analysis of the wellbore breakout data from the entire Frontier Formation in the Stratos wellbore has been performed by Union Pacific Resources, and the results are shown in figure 3-16.

The four-arm caliper data from the Stratos well were analyzed in detail from 15,495 to 16,170 ft (Figure 3-16). This interval encompasses the entire Frontier Formation, and the zone of interest, the Second Frontier sandstone, is situated at approximately 15,990 to 16,100 ft For 60 feet above the Second Frontier sandstone, the borehole is essentially round and gives no indication of any breakouts. For 13 feet of fluvial sandstone in the Second Frontier, the direction of breakout is 88 7°, yielding an orientation of North 1 3° West for maximum horizontal stress (S_{Hmax}) The data yields a 275 4° breakout direction for the eleven feet of non-marine mudstone that separates the fluvial sandstone from the marine sandstones, this yields a direction of North 5.4° East for S_{Hmax}. The remainder of the wellbore through the rest of the Second Frontier sandstones (all marine) is essentially round, giving no indication of any breakouts and therefore no indication of S_{Hmax} In

summary, the wellbore breakout data yield an essentially north-south direction for maximum horizontal stress though the fluvial sediments of the Second Frontier, but do not give any indication of S_{Hmax} in the marine sediments

Note that the orientation of S_{Hmax} changes considerably as one moves uphole in the Stratos well. (See figure 3-16) From 15,495 to 15,579 ft (84 feet), the data show either no breakouts or breakouts that trend in a generally northeast direction There is then a 10-foot zone from 15,581 to 15,591 ft that exhibits a 288 8° (west-northwest) breakout direction, followed by an interval from 15,595 to 15,608 ft that shows breakouts trending in a more northwest direction That zone is followed by approximately 385 feet that show either no wellbore breakouts or breakouts that trend in a west-northwest direction

3.5 Well log analysis

Two important factors for improving production in any area are an understanding of the reservoir and the accuracy of the parameters used in planning the completion of a well In deep, ultra-tight reservoirs, the economics of drilling and completing a well are frequently marginal and the completion methods can economically "make or break" further development of a field. If there is no further development of a field due to poor initial development, then there is a loss of production and a waste of natural resources Ways of trimming completion costs include extrapolating data from comparable reservoirs, modeling pre-completion pressure and flow tests and adjusting the size of completion accordingly, and lastly, substituting wireline data for core data An effort has been made in the Stratos well to address this last methodology of improving production in the Frontier formation by obtaining the necessary parameters to efficiently and accurately plan development through the use of modern well logging techniques A full description of this portion of the project is attached as Appendix F A list of all wireline logs run in this well is included as Table 2-1

In planning the logging package for this project, the information sought could be broken down into two groups The standard logging suite of Neutron/Density and Resistivity logs provided the usual porosities, saturations, and lithologies Since the Frontier formation was to be cored and tested extensively as part of the Statement of Work in the DOE contract, the decision was made to examine the correlation between the core tests and a more complex Hi Tech logging suite It was anticipated that the data from these additional logs could provide a comparison of fracture identification, permeability, thin bed identification, and could aid in planning the eventual completion and even help predict

the outcome of that completion. Good comparison between log and core data leads to confidence in future testing and development using only log data and thereby cutting costly coring operations in cases where coring is not feasible

Unfortunately, this well was not an ideal candidate for the more Hi Tech logging suite since the reservoir at this location contained very few natural fractures, very little pronounced bedding, and very few hydrocarbon shows or other characteristics which the logs were designed to identify Core analysis verified the lithology, porosity and fluid saturations as determined by the standard log interpretation. Quantitative log-derived permeability is suspect in the Stratos well due to possible geologic alterations that may have destroyed the porosity-to-permeability relationship, but the CMR, Neutron/Density and APS neutron profile all indicated low permeability and poor fluid invasion The lack of fractures as seen in the core was confirmed by the ARI, FMI and DSI The calipers from these same three logs also pointed to a NE-SW stress direction, although it is not a strong trend The rock mechanics values calculated from the DSI also provided a good Poisson's ratio match to that computed from lithology

To summarize, there is sufficient correlation between log-derived data and core-derived data from the Stratos well that in future Frontier tests, less expensively obtained log data could be reasonably substituted with some confidence for core data Of course, additional comparisons of fractures and bedding between cores and logs would increase the confidence in these interpretations

4.0 Completion and testing of the Stratos Federal #1-24

As part of Phase II of this DOE contract, the vertical wellbore in Stratos was to be thoroughly tested and evaluated Since the objective of the project was to reduce technical risks and the economic uncertainty impeding development of the deep Frontier in the Green River Basin, UPR teamed with GRI (contract 5094-210-3021) to develop testing and completion procedures under the auspices of their "Emerging Resources in the Greater Green River Basin" study The GRI contract included using IPT (Integrated Petroleum Technologies, Denver, Colorado), a company composed of petroleum engineers specializing in completion optimization, to provide an independent evaluation of the testing performed by GRI and its contractors A more detailed description of IPT's testing and evaluation is included in this report as Appendix G.

UPR's contract with the DOE No. DE-AC21-95MC31063 included the following requirements for the testing and evaluation of Stratos based upon the assumption that the physical properties of the Frontier formation at this location would warrant hydraulic fracture stimulation

- Cased-hole Stress Testing
- Pre-Frac Well Testing
- Mini-Frac
- Main "Moxa-Type" Frac

IPT proceeded with the analysis of the Stress Testing and Pre-Frac Well Testing. The results of these tests along with the various core and well log analyses have demonstrated that the Second Frontier in the Stratos #1-24 does not exhibit reservoir properties that would obviously warrant the further expense of hydraulic fracture stimulations. However, complications during testing have led to questions concerning the validity of the testing results (electrical and mechanical difficulties, packer leakage problems, water sitting on formation, etc)

Cased Hole Stress Testing - Cased hole Stress Tests are used to determine closure stress for reservoir rock and its surrounding formations The contrasts in minimum closure stresses between layers of rock determine the fracture height growth and overall fracture geometry as a result of a hydraulic fracture treatment. While modeling what happens during a fracture treatment is difficult at best and subject to great debate, it is generally agreed that accurate determination of minimum closure stress is critical in optimizing any hydraulic fracture treatment

Although four intervals were perforated for Cased hole Stress Tests (the shales bounding the reservoir and the fluvial and marine reservoir intervals) only the shales were tested due to problems with testing An SPE paper detailing IPT's approach to analyzing the data is included with their report as part of Appendix G

There were three PI/SI (pump in / shut in) tests performed in the marine shale below the bottom of the Frontier These tests had increasing ISIP's (initial shut-in pressures) with each successive pump in This is an indication that the fracture geometry, both near the wellbore and/or far-field, is becoming progressively more complex The upper bound for the closure stress of the lower shale is 1.0 psi/ft or 15,800 psi

There were also three PI/SI tests for the shale above the Fluvial Frontier section These tests had repeatable, consistent ISIP's which suggest that the fracture geometry is not as complex as that in the lower marine shale. This shale had an upper bound of the closure stress of 0.9 psi/ft or 14,300 psi

Because no stress tests were performed on the Frontier pay intervals, the closure stress for the Frontier was estimated to have a gradient of 0.85 psi/ft or to be 13,700 psi. These values were used to model the breakdown treatment analysis using FRACPRO® The history match of the breakdown treatment showed a created fracture length of 78 feet with 6 far-field hydraulic fractures being created Unfortunately, the pressure data recording stopped before the reservoir pressure could decline sufficiently to confirm the closure pressures of the bounding shales.

Pre-frac well testing - Following the breakdown with KCl water, there followed an eight day flow period, followed by a two week pressure buildup Analysis of the buildup showed a reservoir pressure of 11,900 psi or a gradient of 0.74 psi/ft and a conductivity (kh) of 0.036 md-ft which translates to a permeability of 0.0012 md with a net pay of 30 ft This permeability is low compared to core analysis and may be explained by several factors Downhole shut off leaks created disturbances in the pressure transient several times during the buildup test The formation had a 4000 ft water column sitting on it throughout the flow period since it was not "cleaned up" or swabbed dry after the breakdown treatment. This water could have been drawn into the formation by capillary pressure and reduced effective permeability This water could also be imbibed reducing the permeability further Another point raised by IPT is that fresh water breakdowns do not necessarily achieve good communication between the wellbore and the formation since they do not significantly affect cement It is possible that not all the perforations have been opened.

IPT concluded that the productivity of the Stratos well could be enhanced by a hydraulic fracture treatment However, using the test data, which is somewhat suspect, they estimate gas rates of only a few hundred MCFPD as a result. Some of the doubts concerning the results of previous tests could be addressed by further testing, i.e acidizing to clean up the perforations. Rate step-down testing to determine the difference between near wellbore tortuosity and perforation fraction would be helpful in a hydraulic fracture design Extending the post-breakdown observation of closure pressures would also help to confirm the results of the Stress Tests

4.1: Wellbore Cleanup and Acid Stimulation

After evaluating the results of the previous well tests and analyzing acid sensitivity and regain permeability tests on the Frontier reservoir, a wellbore cleanup and acid stimulation job was proposed for the Stratos well. The purpose of the procedure was to clean or remove any damage to the near wellbore by: 1) removing any fluids in the wellbore and near-wellbore matrix pores; and 2) acidizing the Frontier Formation By acidizing the Frontier, UPR hoped to: 1) determine if all of the perforation tunnels were active, 2) enhance the aperture of any calcite-filled fractures near the wellbore; and 3) determine if there was any improvement in reservoir quality in zones that contained more carbonate cement

In preparation for the acid stimulation and wellbore cleanup, acid sensitivity test and regain permeability tests were performed on three Frontier Formation samples from the Stratos well. The tests revealed that an HCl/acetic acid blend dramatically improved the permeability in the marine sandstone sample that contained calcite-filled fractures and carbonate cement (Figure 4-1). The permeabilities of the fluvial sandstone sample were reduced by 100% at drawdown pressures of less that 2500 psi, and slightly improved (23% increase) at a higher drawdown pressure of 3500 psi (Figure 4-2). This indicates that significant capillary trapping effects are present and very high reservoir pressures would be necessary to overcome these effects The permeability of the relatively clean, quartzose marine sandstone was significantly decreased (Figure 4-3)

The Stratos well was shut-in from January 22, 1996 until a bottomhole survey was run in early November 1997 in preparation for the wellbore clean-up and acid stimulation job. The well tested 18 MCFD on January 22 at 38#FTP dry flow after 153 hours total flow period The well was last swabbed on January 5, 1996, with five runs down to a 12,000 ft. fluid level The bottomhole survey (November 1997) identified a 3,880 ft fluid level with 12,192 psig reservoir pressure and 280°F reservoir temperature at 16,030 MPP for the Frontier Formation After flowing the well to pit the fluid level dropped to 9,580 ft or a calculated 33 BW recovery, and the well rate was estimated at 50 MCFD

The acid job was performed in mid-November by Schlumberger Dowell, a copy of the procedure is found in figure 4-4. The well was filled with completion fluid heated to 150°F for tubing movement, while running in the hole with 1 25 inch coiled tubing Once

on bottom, 1000 gallons of HCl/acetic acid blend (20 2% HCl equivalent) was spotted and the coiled tubing was pulled out of the hole The acid blend formulation was as follows· Retarded Acid (426 gpt H34 34% HCl + 107 gpt L401 Acetic Acid + 328 gpt water)=20.2% HCl active + 2 gpt F75N (Surfactant) + 300 ppt L62 (Iron Chelant) + 10% 100 gpt U66 (Mutual solvent) + 7 gpt A261 (Inhibitor) + 30 gpt A201 (Inhibitor Aid) The acid was injected at 3 bpm at 6870 psi to 7015 psi; a slight initial breakdown was observed at 6920 psi. The final recorded wellhead pressure was 5820 psi after 30 minutes These data indicated that the perforations were open and the formation was extremely tight

Coiled tubing was then run to 16,075 ft and nitrogen was circulated The wellbore was blown clear of any fluids over a 1-1/2 hour period After the pressure had bled down, the well was continuously flowed at 48/64 choke with 32 psig WHP at 30 MCGD of dry gas for approximately 48 hours All data indicate that the performance of the Stratos well remained unchanged after the procedure

5.0 Future plans and recommendations

The Stratos well is currently shut in, pending further evaluation by UPRC Phase III (the drilling and completion of a horizontal wellbore) is currently being considered at an alternative location in the Green River Basin Since the Stratos well was drilled, several wells have been drilled through the Second Frontier on the east side of the Rock Springs Uplift The Frontier in these wells is also overpressured and has had strong gas shows Cores taken from the wells contain both partially open and cemented natural fractures Geologic and engineering analysis of these well is currently underway to determine an optimum location for the optional Phase III of the current DOE Greater Green River Basin Production Improvement contract.

References Cited

Laubach, S E , in press, Method to detect natural fractures in sandstones American Association of Petroleum Geologists, v 81, no 3

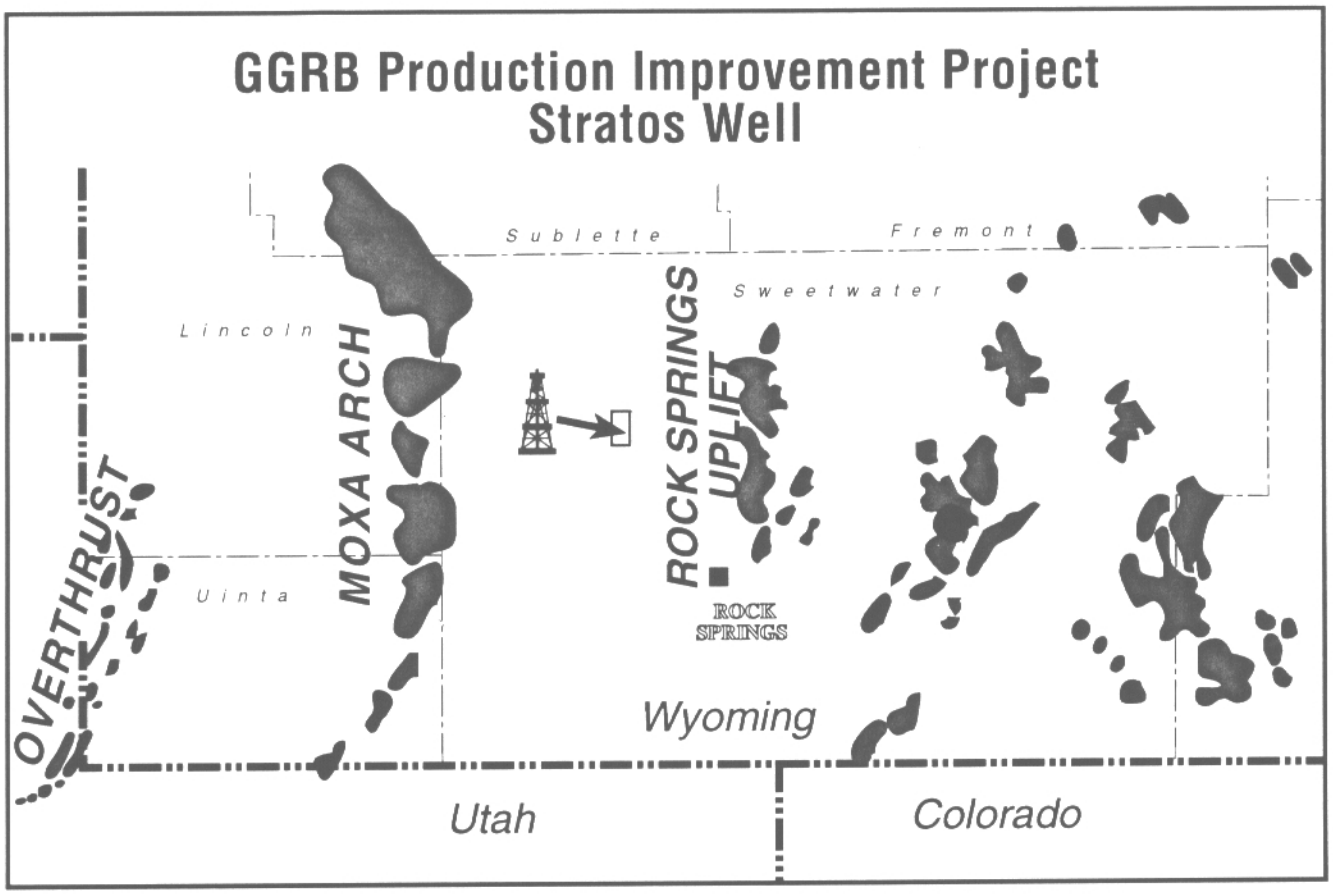

Figure 1-1. Index map of major oil and gas fields in the Greater Green River Basin, Wyoming with respect to the Stratos Federal #1-24 in Sweetwater County.

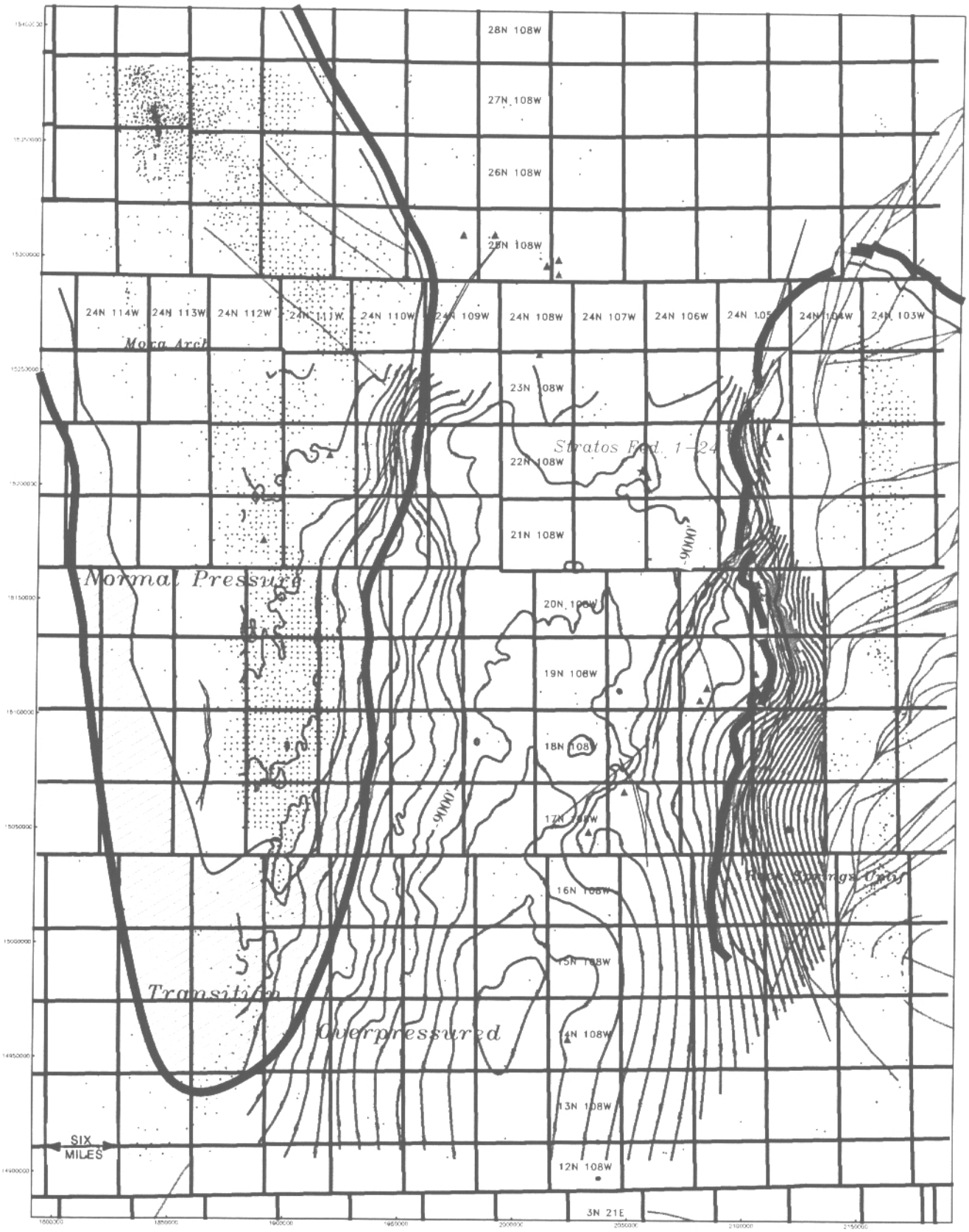

Figure 1-2. Structure map on top of Frontier Formation, Green River Basin, Wyoming. Contour interval = 500 ft.

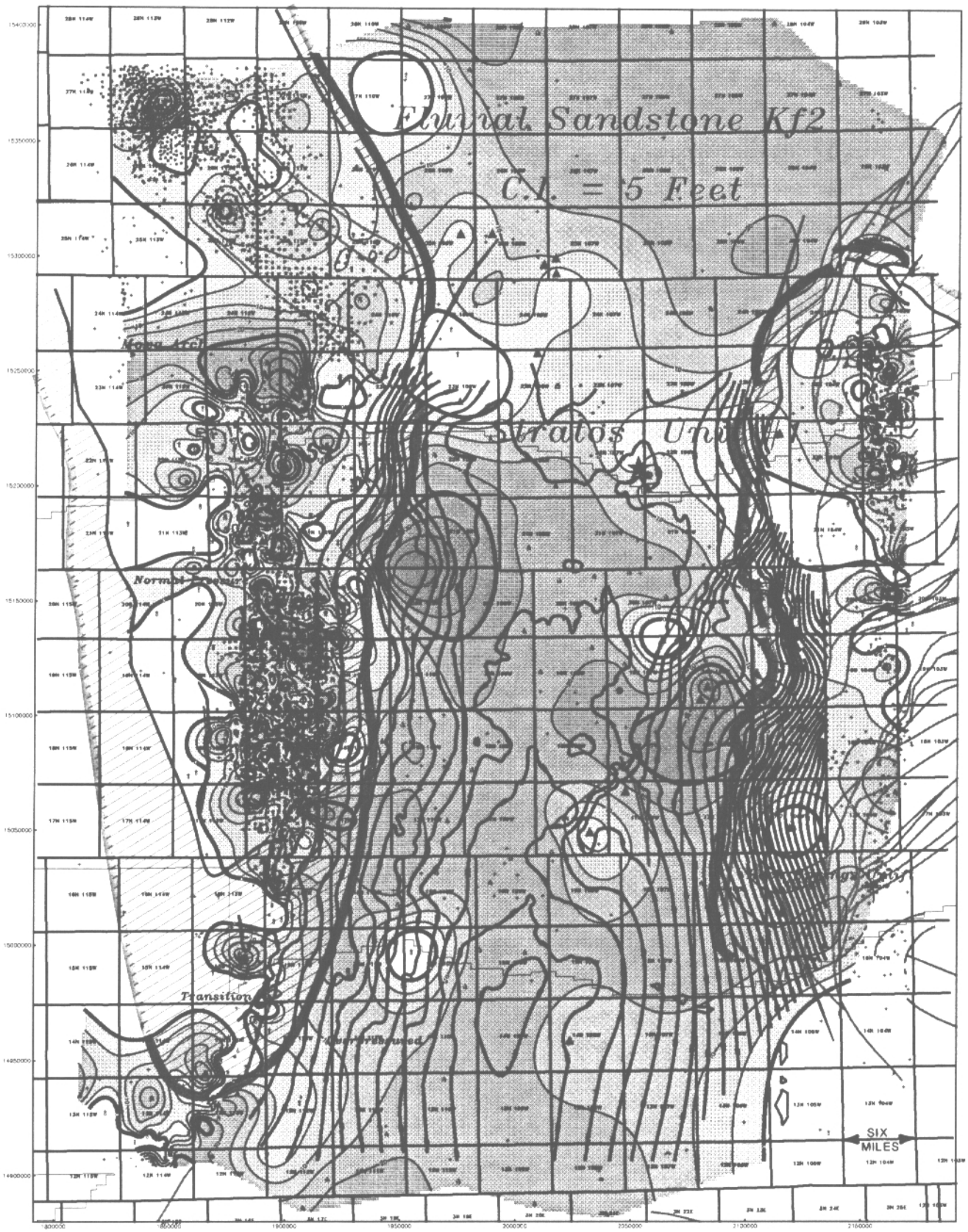

Figure 1-3. Regional isopach map of net feet of pay in the Second Frontier fluvial interval at the Stratos location (shown as star). Contour interval = 5 ft.

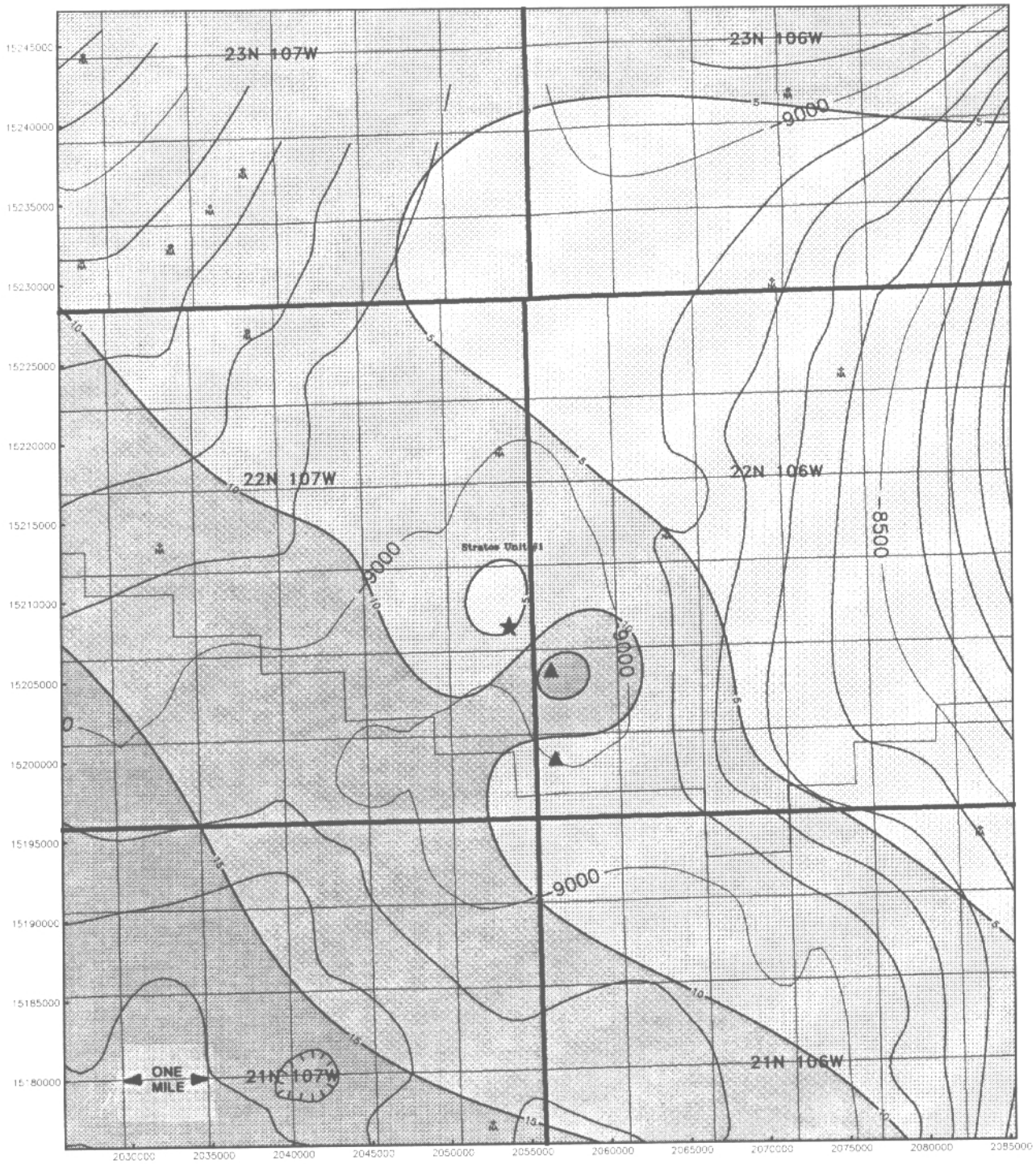

Figure 1-4. Local isopach map of net feet of pay in the Second Frontier fluvial interval at the Stratos location (shown as star). Contour interval = 5 ft.

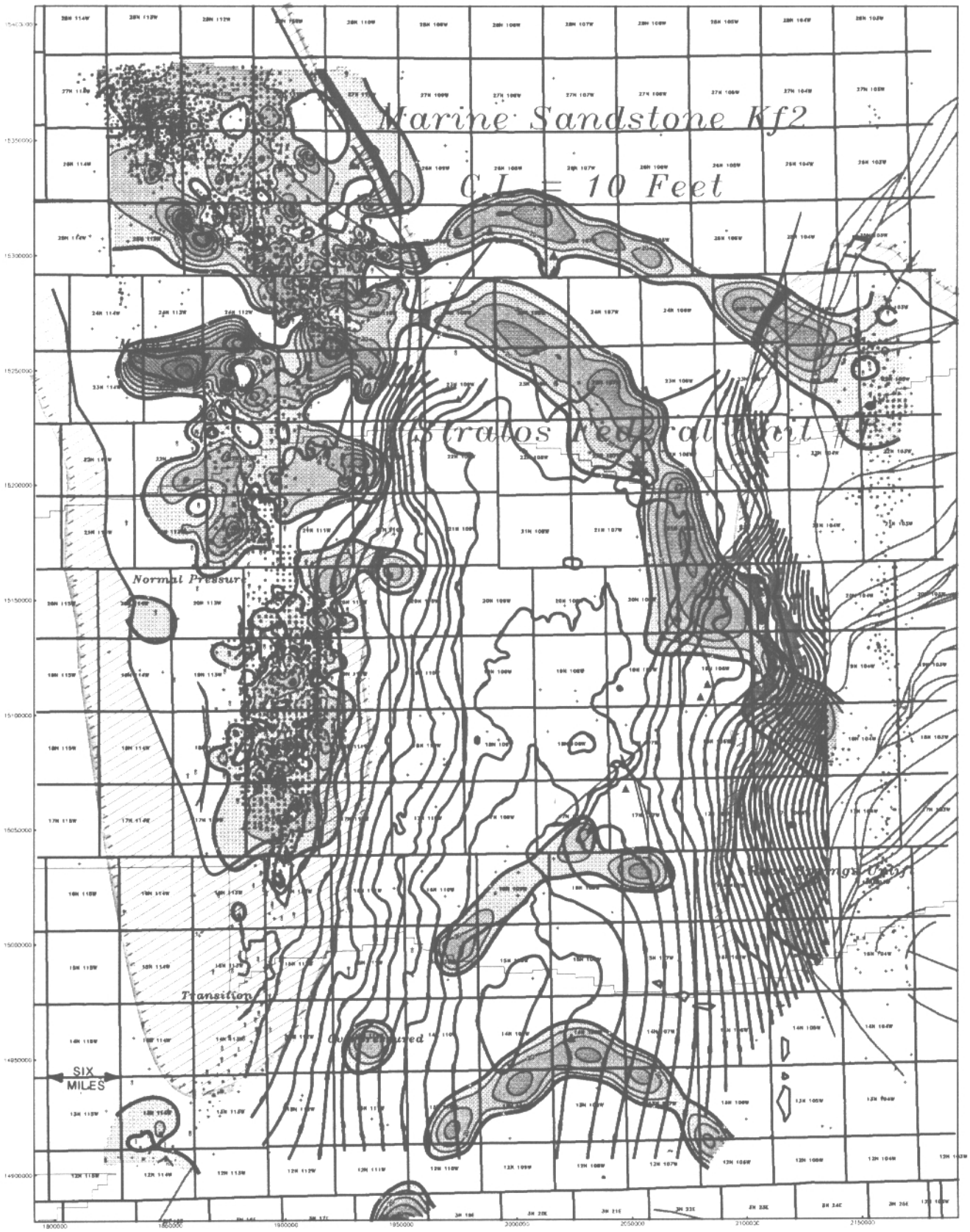

Figure 1-5. Regional isopach map of net feet of pay in the Second Frontier marine interval at the Stratos location (shown as star). Contour interval =10 ft.

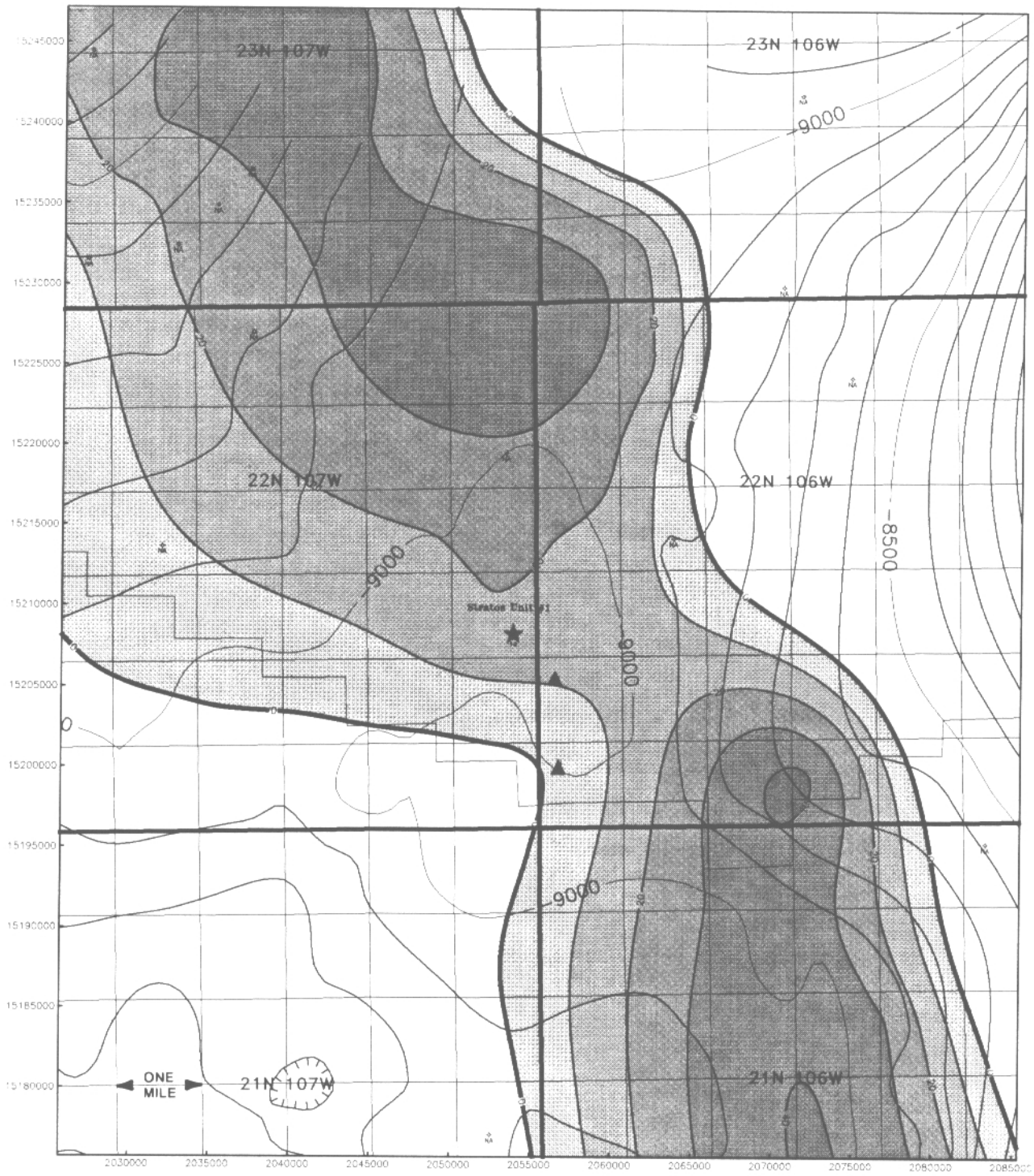

Figure 1-6. Local isopach map of net feet of pay in the Second Frontier marine interval at the Stratos location (shown as star). Contour interval =10 ft.

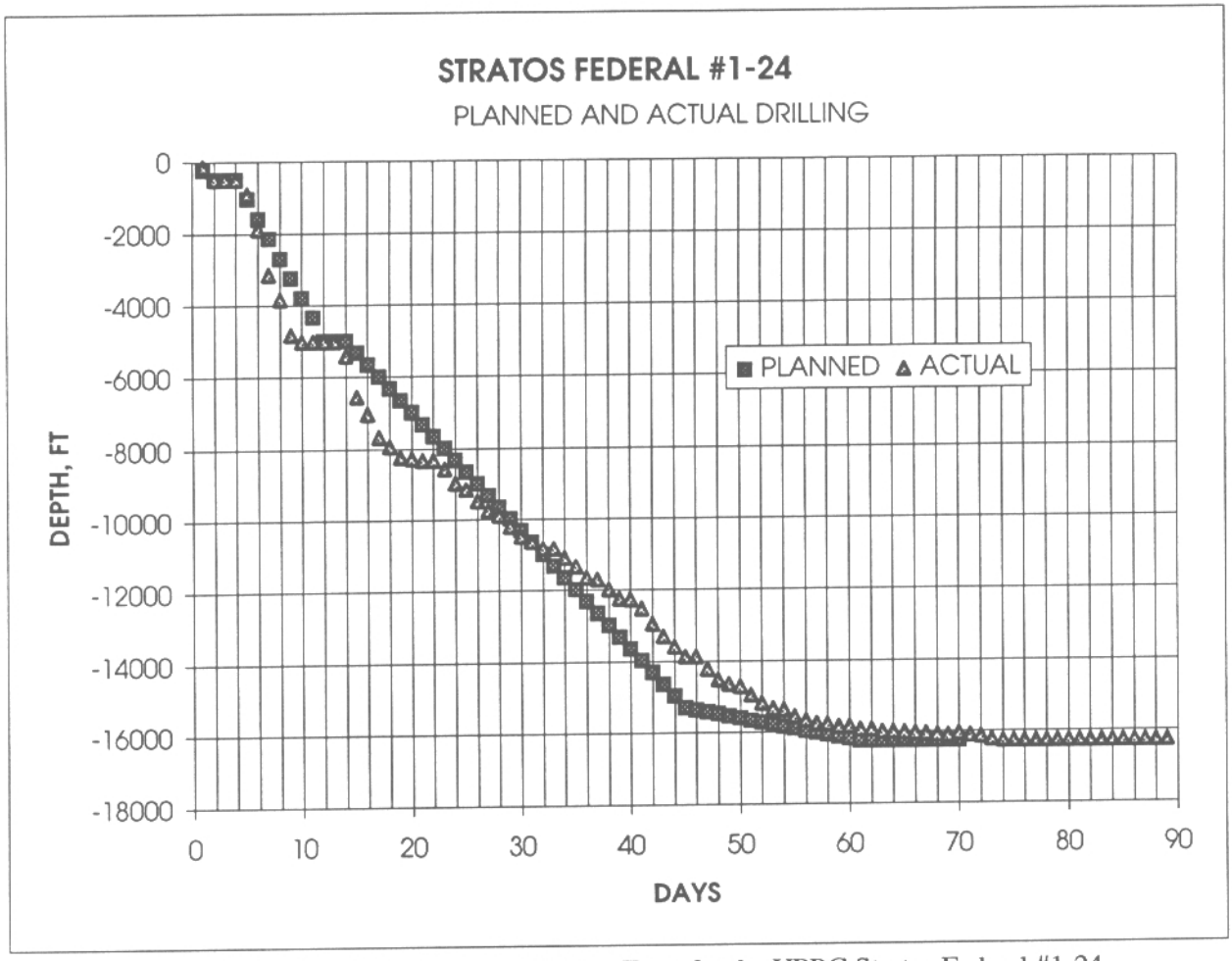

Figure 2-1. Plot of Depth versus Drilling Time for the UPRC Stratos Federal #1-24

APPENDIX 2 - FIGURE 2.2

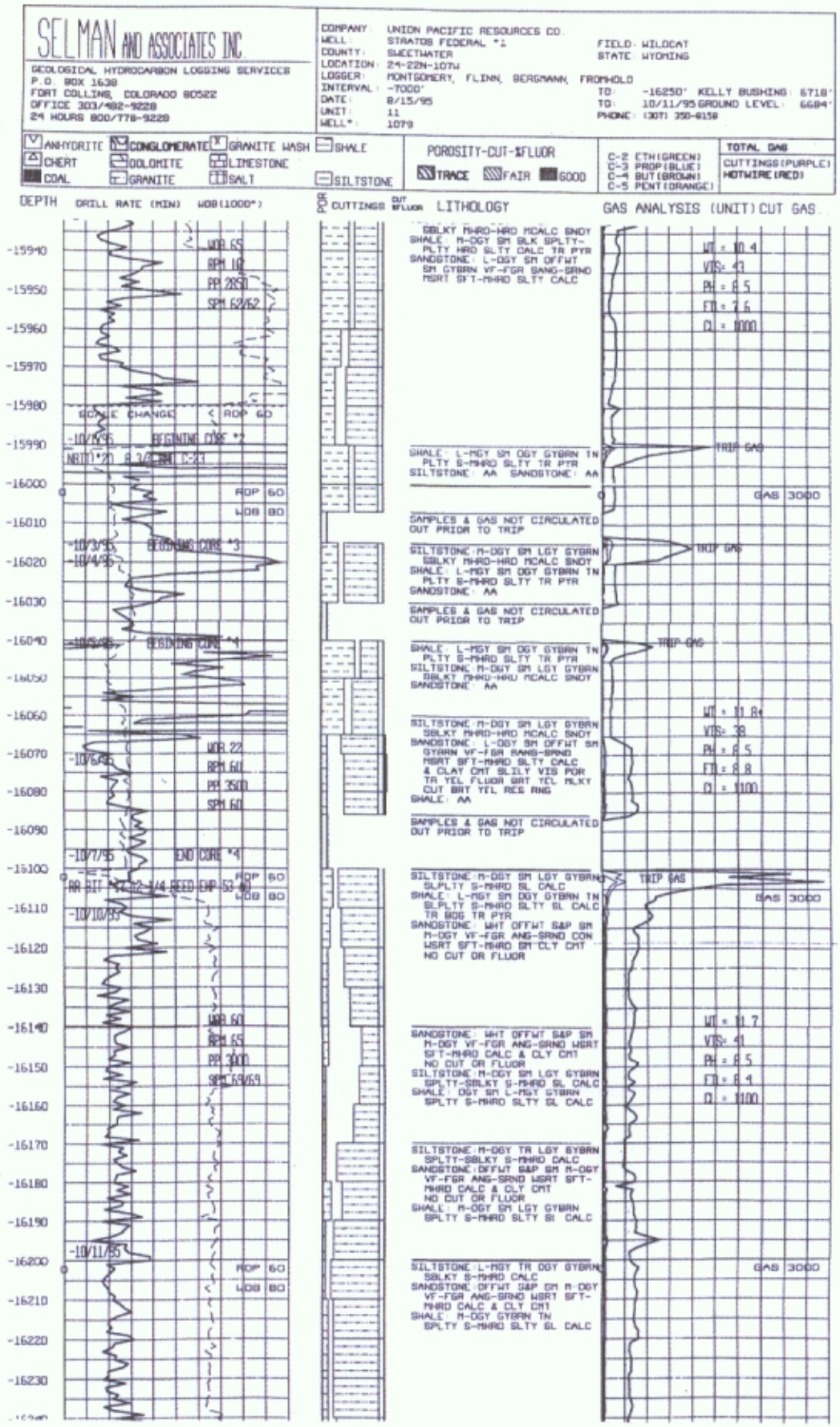

Figure 2-2. Mudlogger's Report.

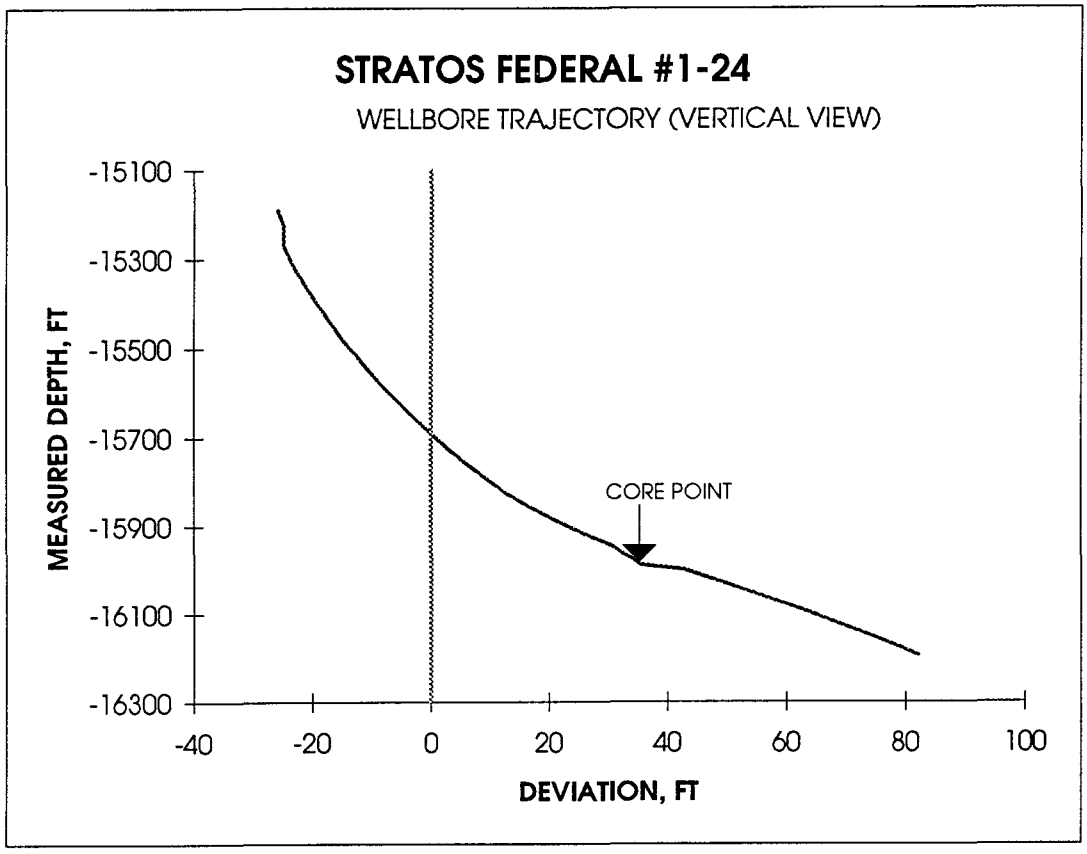

Figure 2-3 Wellbore Trajectory Diagram - Vertical View

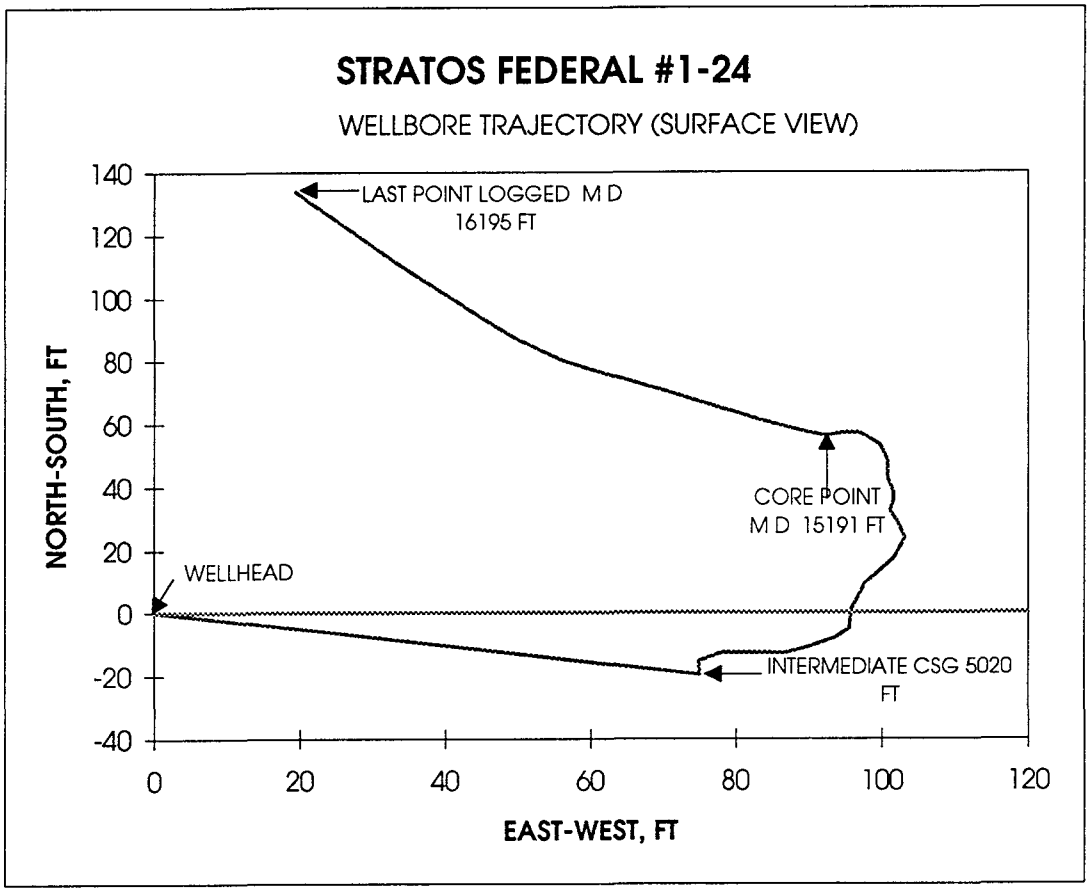

Figure 2-4 Wellbore Trajectory Diagram - Surface View

WELL NAME: UPR STRATOS FEDERAL UNIT No. 1
SL: SE/4 SEC. 24, T. 22 N., R. 107 W., 6TH PM
B-HL: 1412' FSL, 1273' FEL SEC. 24, T. 22 N., R. 107 W., 6TH PM
SWEETWATER COUNTY, WYOMING

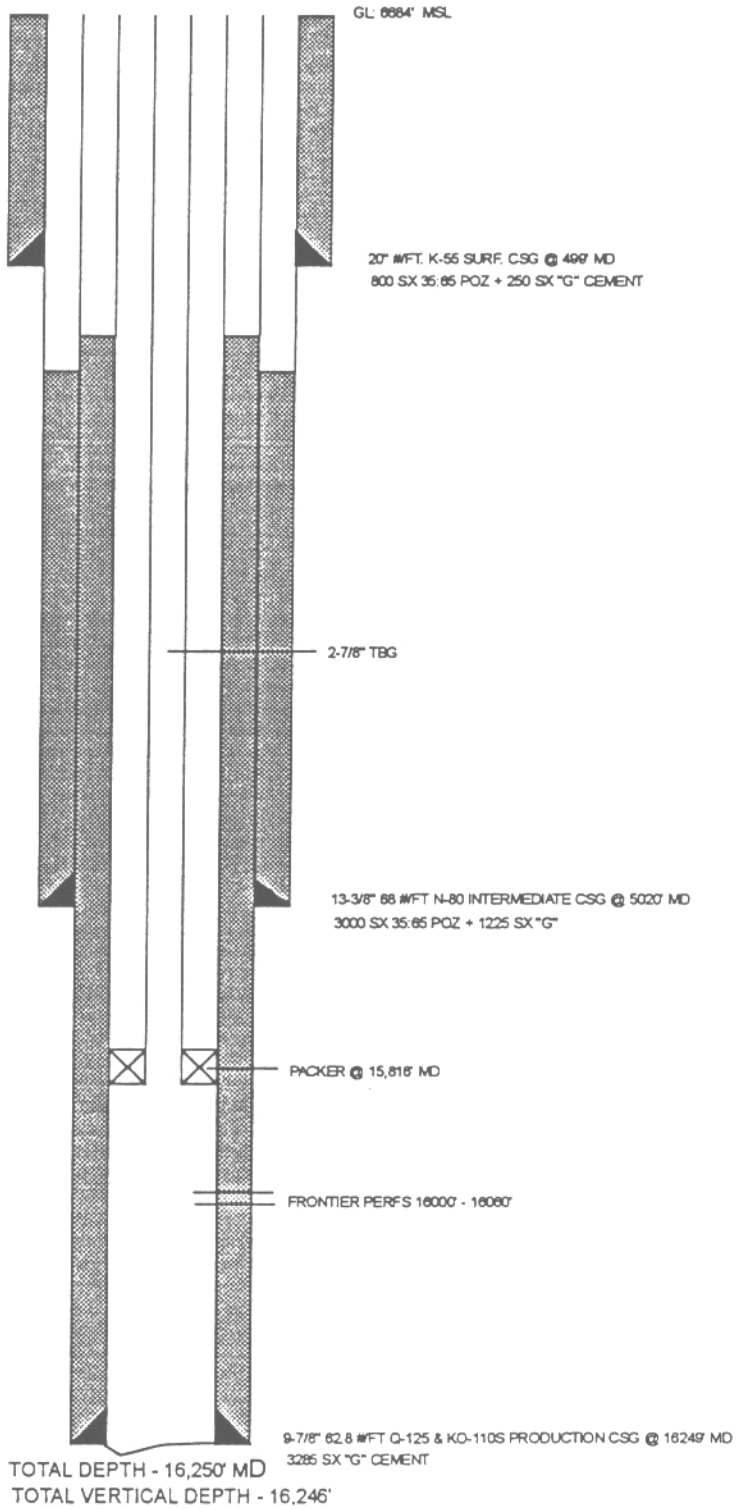

Figure 2-5. Wellbore Diagram.

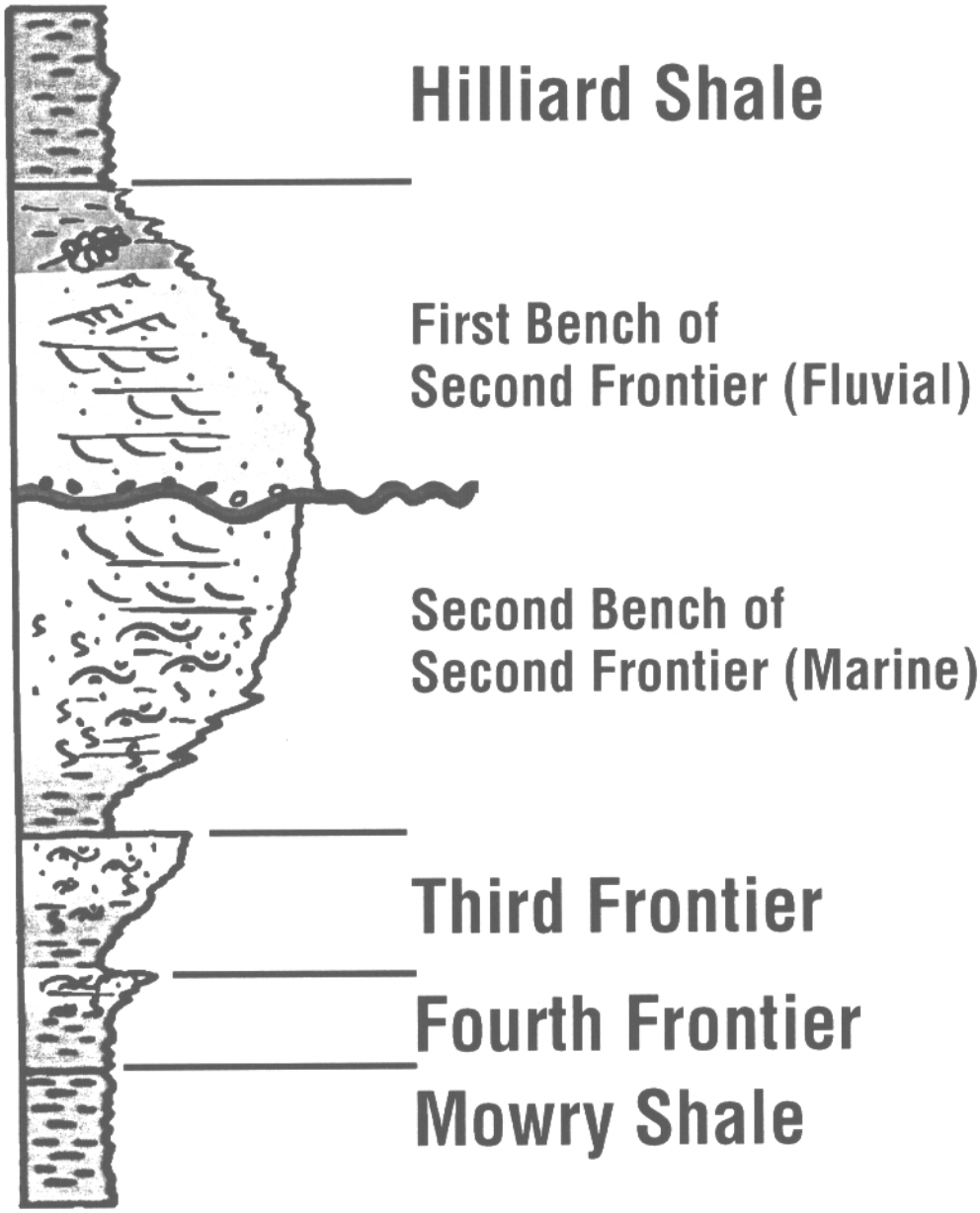

Figure 3-1. Schematic vertical profile of the Second Frontier Formation, Green River Basin, Wyoming.

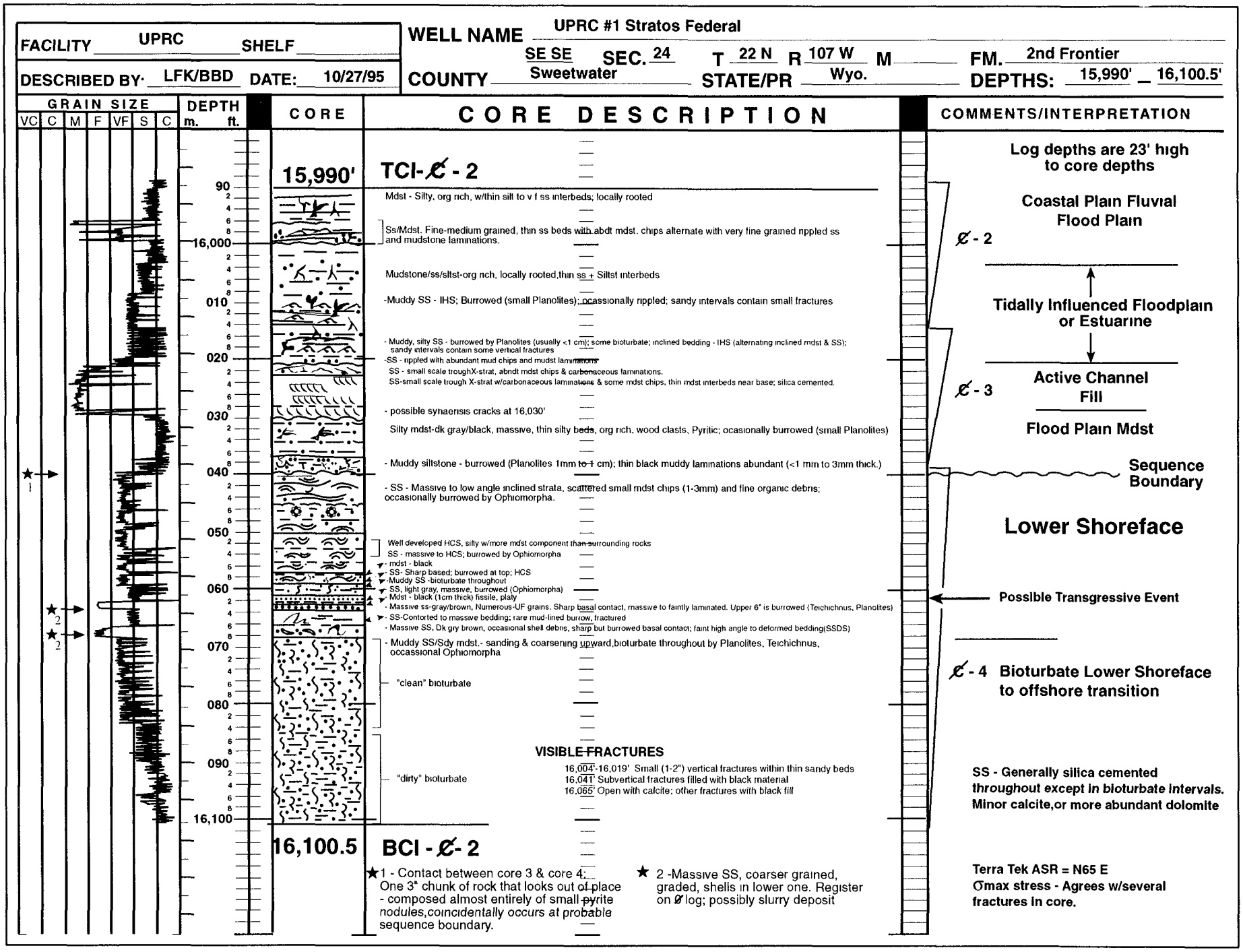

Figure 3-2. Core Description.

FACILITY USGS SHELF

DESCRIBED BY: Blakeney DATE: 9/18/89

WELL NAME ENERGY RESERVES GP 1-30 BLUE RIM FED.

LOCATION SEC. 30 T 22 N R 106 W M FM. FRONTIER

COUNTY Sweetwater STATE/PR Wyo. DEPTHS: 16,053' – 16,134'

GRAIN SIZE: VC C M F VF S C

DEPTH m. ft.

CORE

CORE DESCRIPTION

Top of Cored Interval
16053'

60

SS - Trough x-strat at base, massive at top; Shale clasts at top; sharp-based
MS burrowed - Synsedimentary faulting
SS, abundt. mdst, clasts, burrowed Planolites
MS black burrowed
SS - Massive with occ. shale clasts up to 1 cm in dia.; SSDS

SS trough x-strat; abundant shale clasts up to 1 cm.; SSDS (Slumping; oversteepened x-beds); no burrows

Internal scours w/abundant shale chips

abundant mdst. clasts

SS contains layers w/fairly abundant shale clasts; flat to wavy laminated near top with abund. mdst. laminae; Possible diffuse cross-bedding at base.

80

"clean" bioturbate ss/mdst.

SS/MS - Bioturbated; amount of SS increases upward & the SS coarsens upward from lower very fine to lower fine grained ; primarily Ophiomorpha, also Planolites

Isolated shale clasts

16100

MS/SS; very dark grey to black
- some vertical hairline cracks (probable dehydration cracks) - not calcite - filled.

SS/MS - bioturbated thoroughly; dark grey
- Inoceramid fragments at 16,112.2' - transgressive lag; flooding surface

120

Sandy sltst./MS - Alternating sltst./MS layers - sltst. are rippled to burrowed; some vertical hairline fractures that may be dehydration cracks (cont'd)
SS: flat laminated, rippled & burrowed at top (1 inch thick); a few vertical hairline calcite-filled fractures; ss is calc.
SS/MS - Alternating SS/MS layers; SS rippled; (low ampl. - some comb. flow with washed-over tops); burrowed Planolites-1/2 cm in dia., occ. Ophiomorpha; scattered pyrite(<1mm crystals); Helminthopsis at 16,124.2'

MS/SS w/ v.thin SS stringers
SS/MS Bioturbated; dark grey, Ophiomorpha, Terebellina

Bottom of Cored Interval
16134'

not calcite filled; some are continuous from vertical to a horizontal crack; these occur predominantly in the thin (<2 cm) mdst layers; some cut through mdst and SS layers; some are visible as cracks on bedding plane surfaces.

COMMENTS/INTERPRETATION

Marine-influenced fluvial overbank & small channel

Active fluvial channel fill

Fluvial

Marine

Coarsening-upward, shallow shelf sequence from offshore transition zone into shoreface (all bioturbated)

Flooding surface

Figure 3-2b. Core description for the ERG Blue Rim Federal # 1-30, Sec. 30-T22N - R106W.

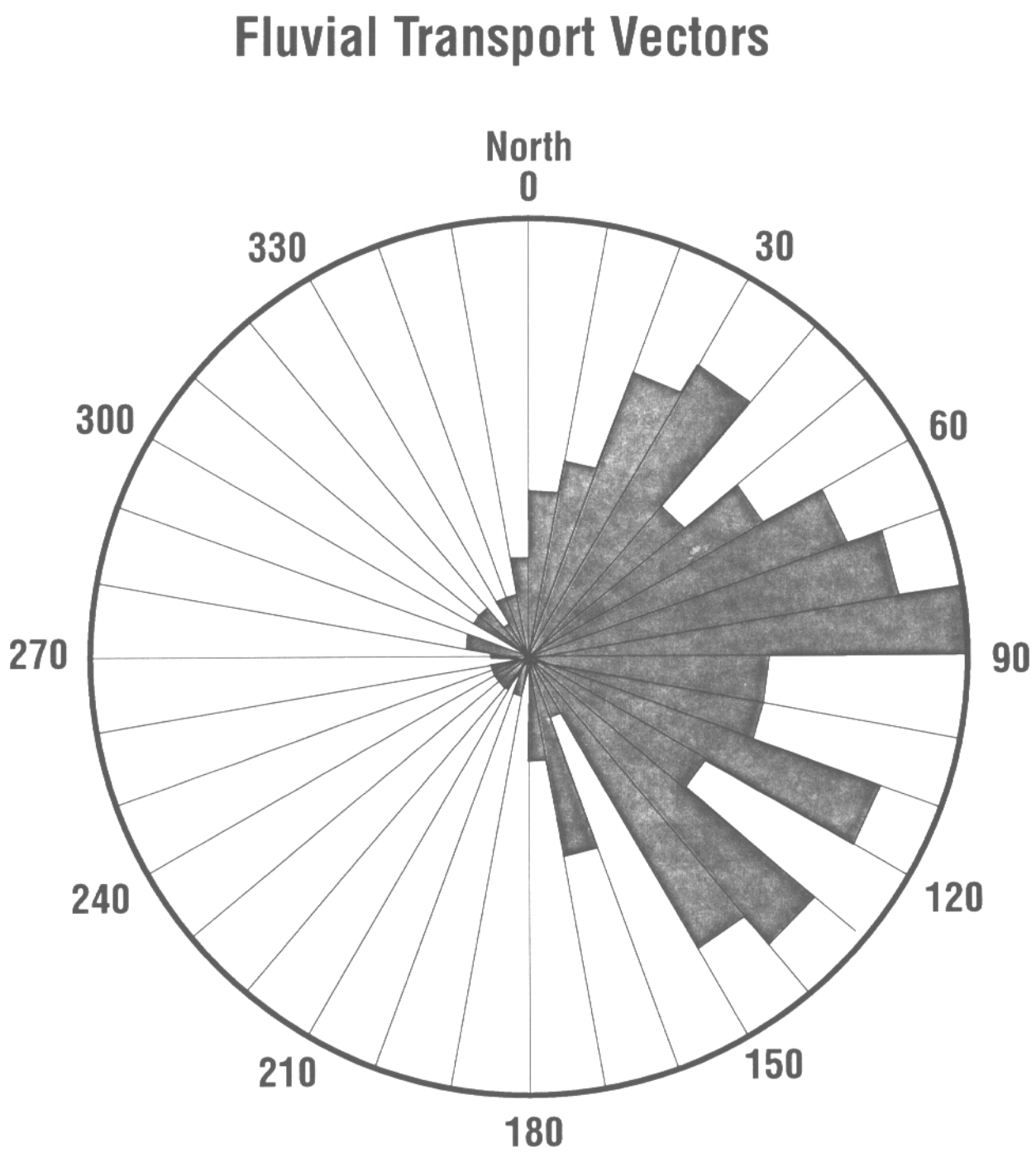

Figure 3-3. Dip azimuth plot for fluvial bedding planes.

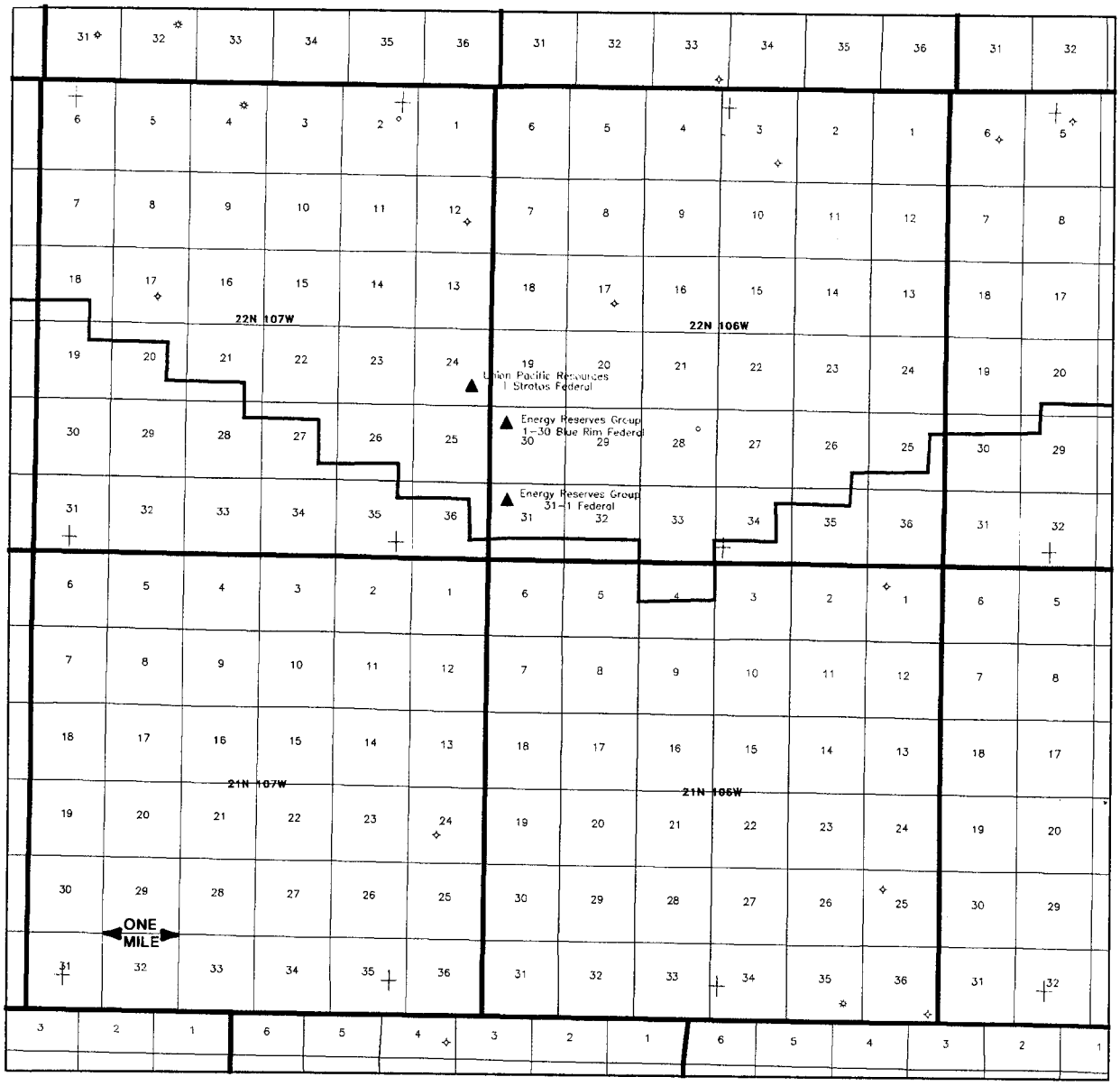

Figure 3-4. Location map for the UPRC Stratos #1-24.

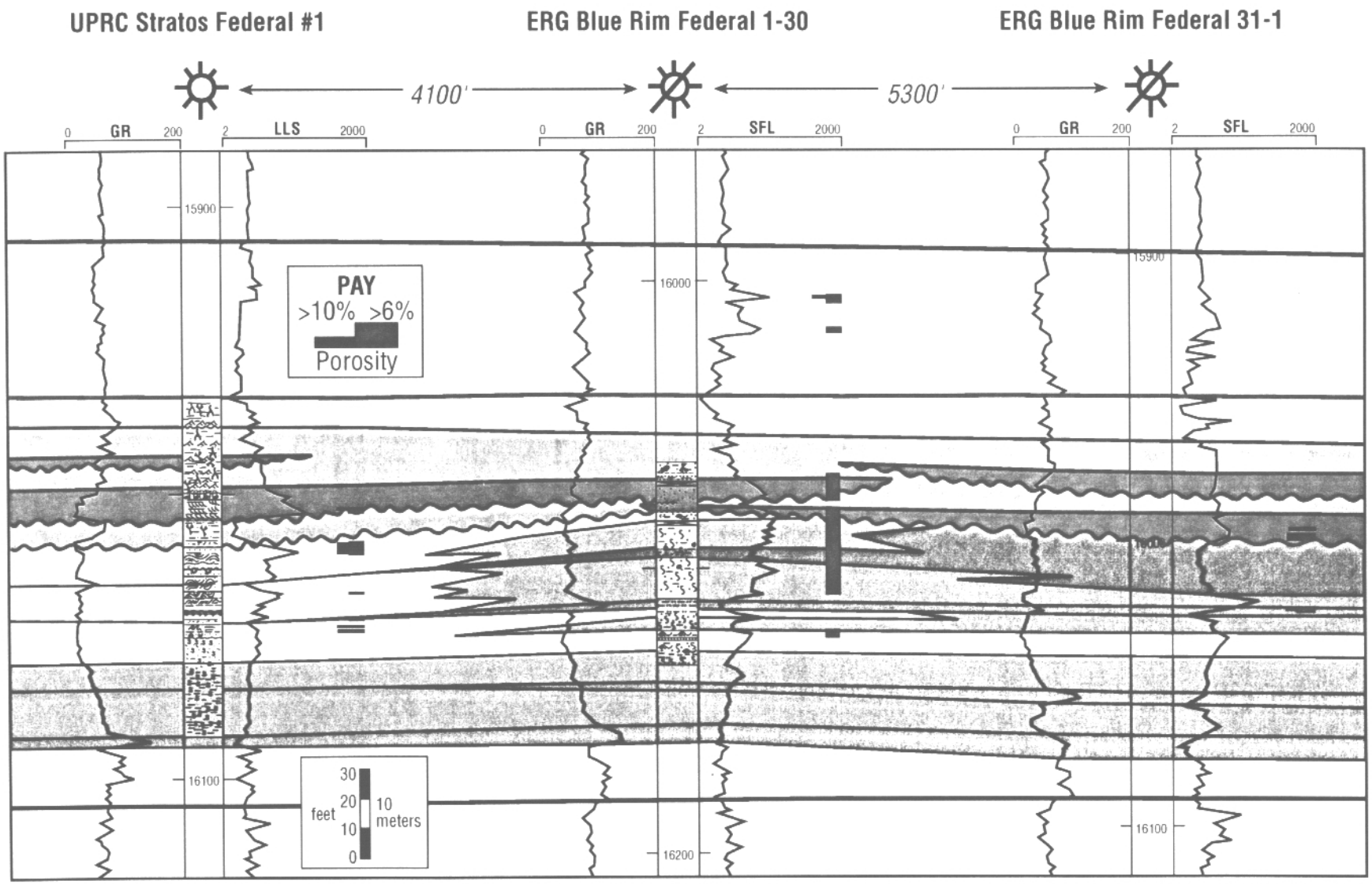

Figure 3-5. Stratigraphic cross section for the Stratos #1-24 and the two Blue Rim wells.

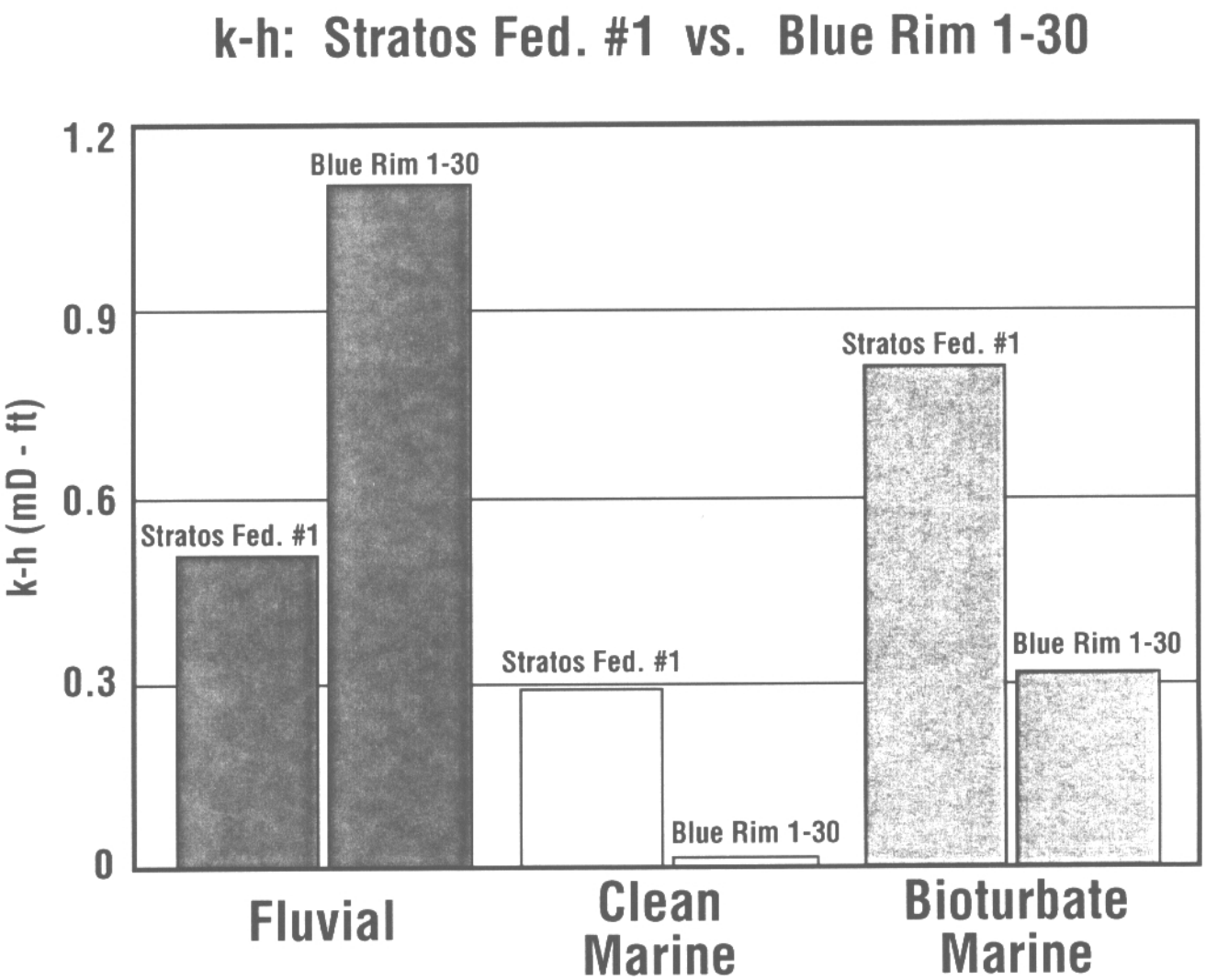

Figure 3-6. Comparison of total permeability-feet between the Stratos #1-24 and the Blue Rim #1-30 (Second Frontier sandstone only).

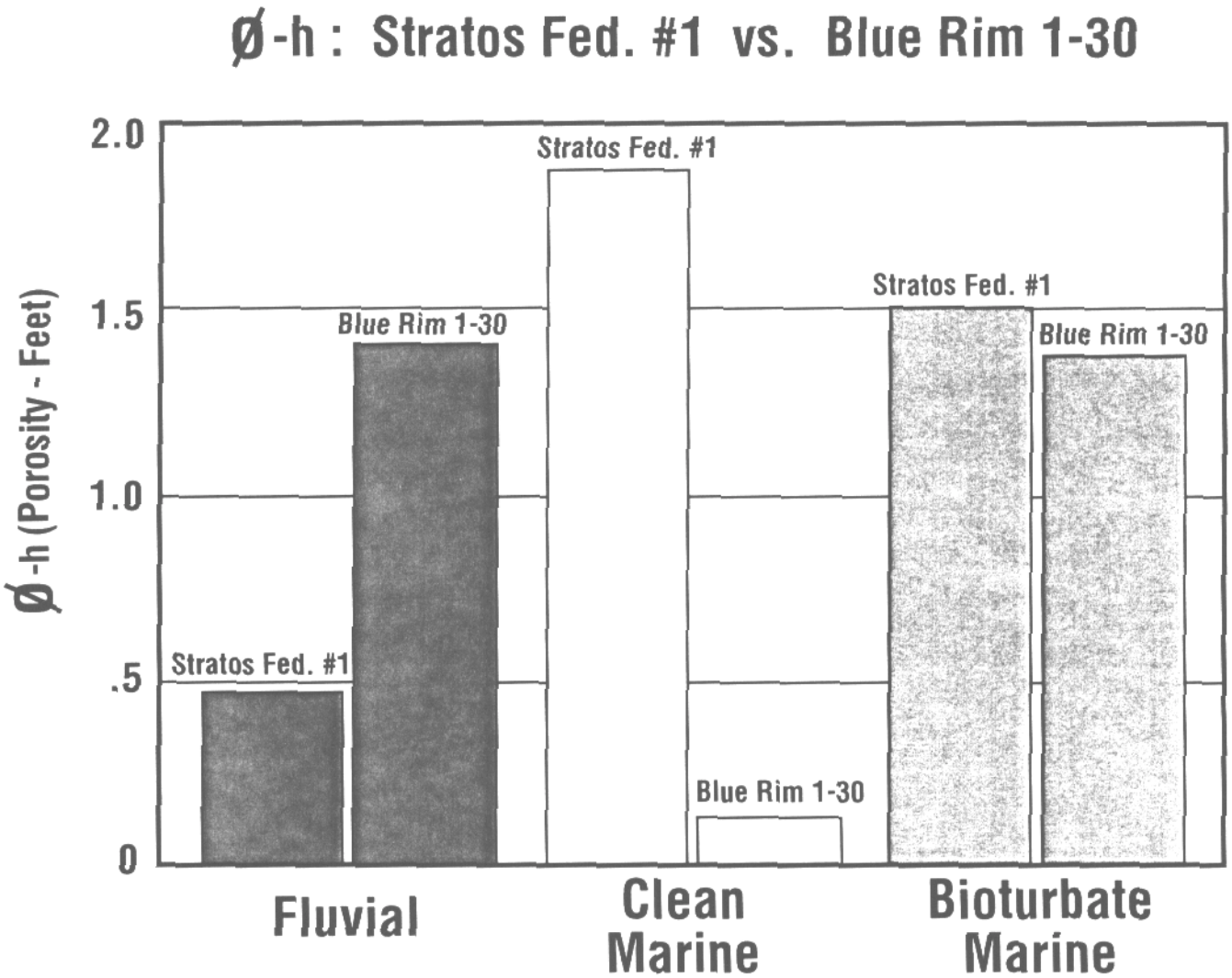

Figure 3-7. Comparison of total porosity-feet between the Stratos #1-24 and the Blue Rim #1-30 (Second Frontier sandstone only).

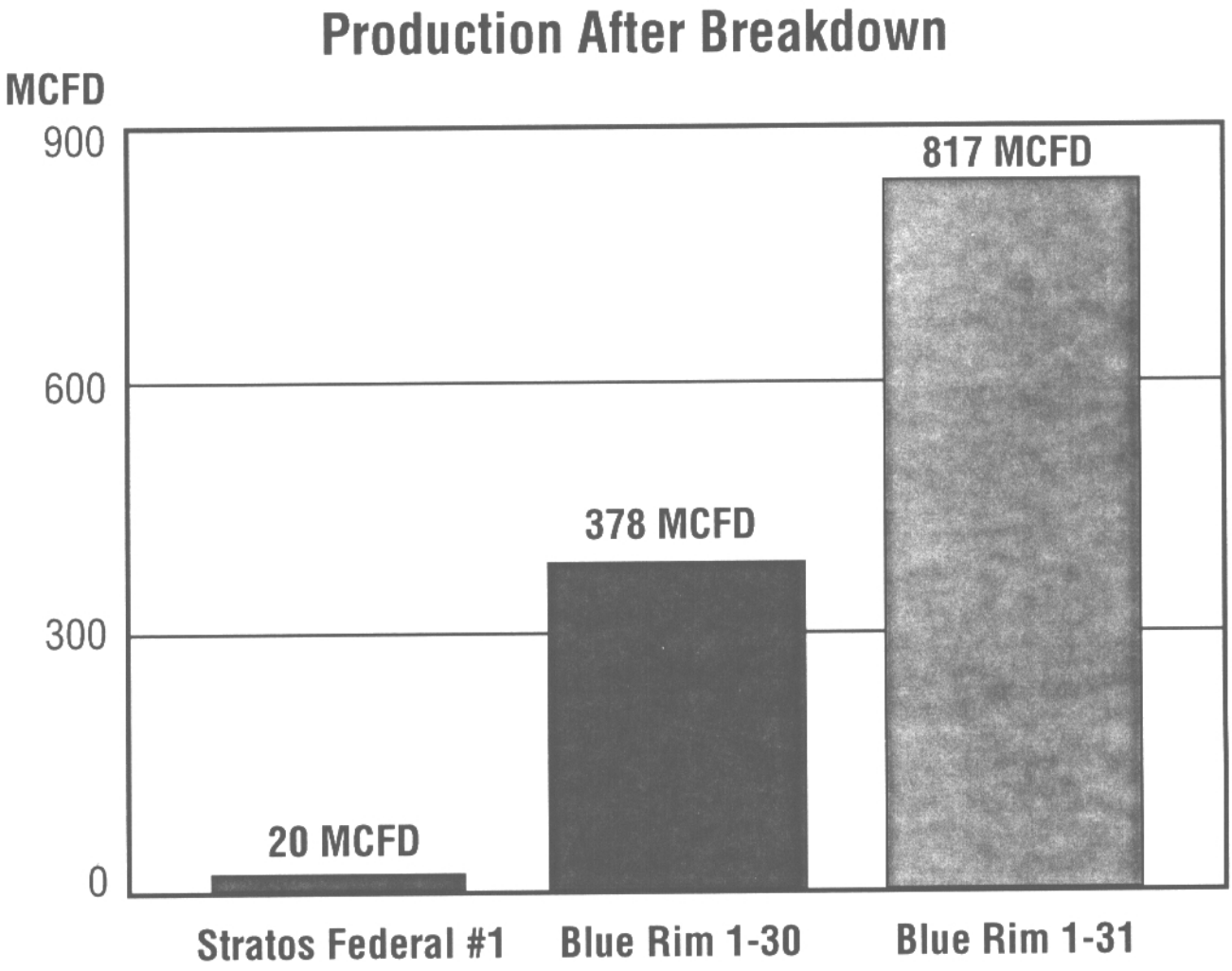

Figure 3-8. Comparison of post-breakdown flow rates between the Stratos and two Blue Rim wells.

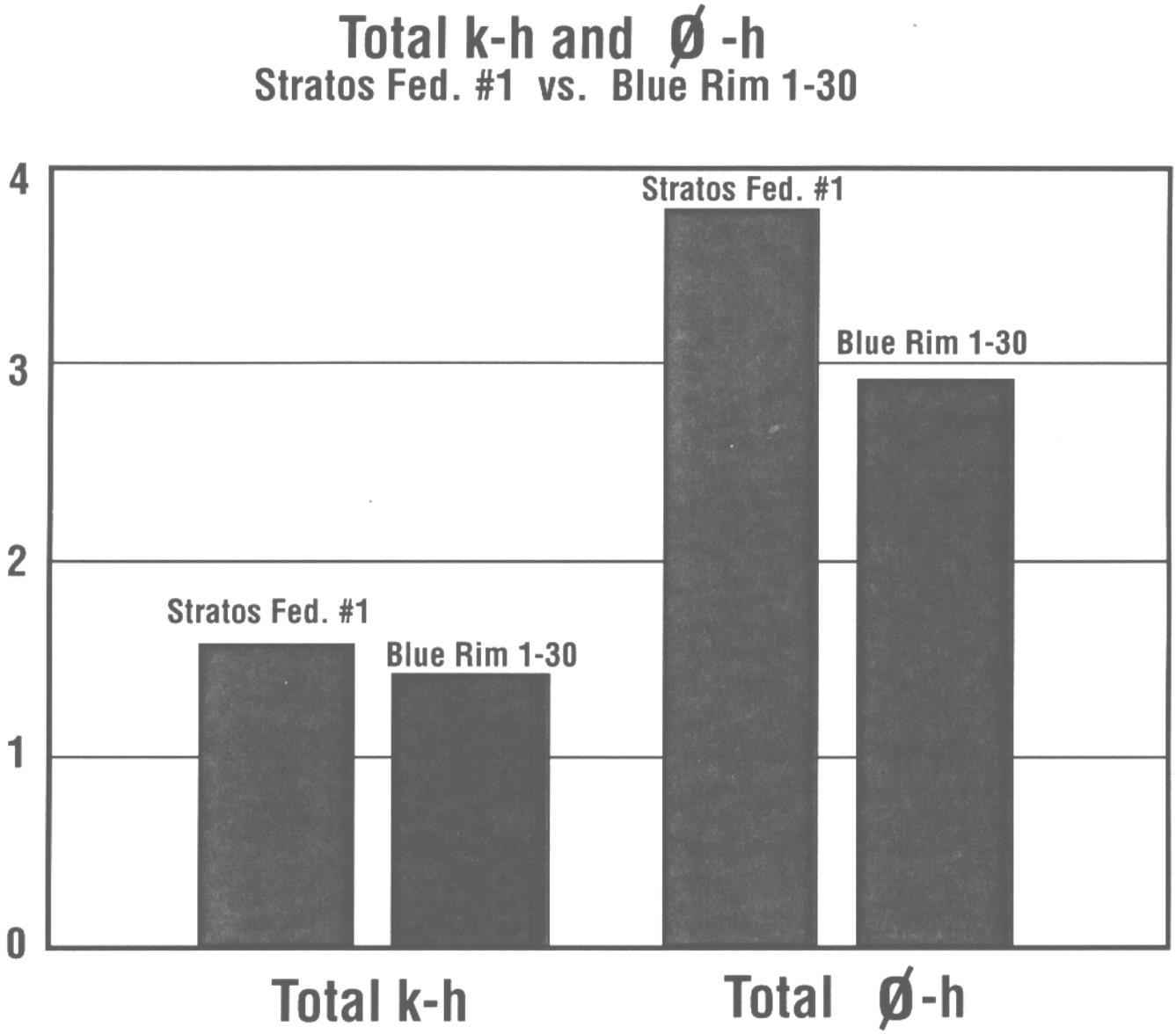

Figure 3-9. Summary plot of the comparison of total permeability-feet and porosity-feet between the Stratos #1-24 and the Blue Rim #1-30 (Second Frontier sandstone only).

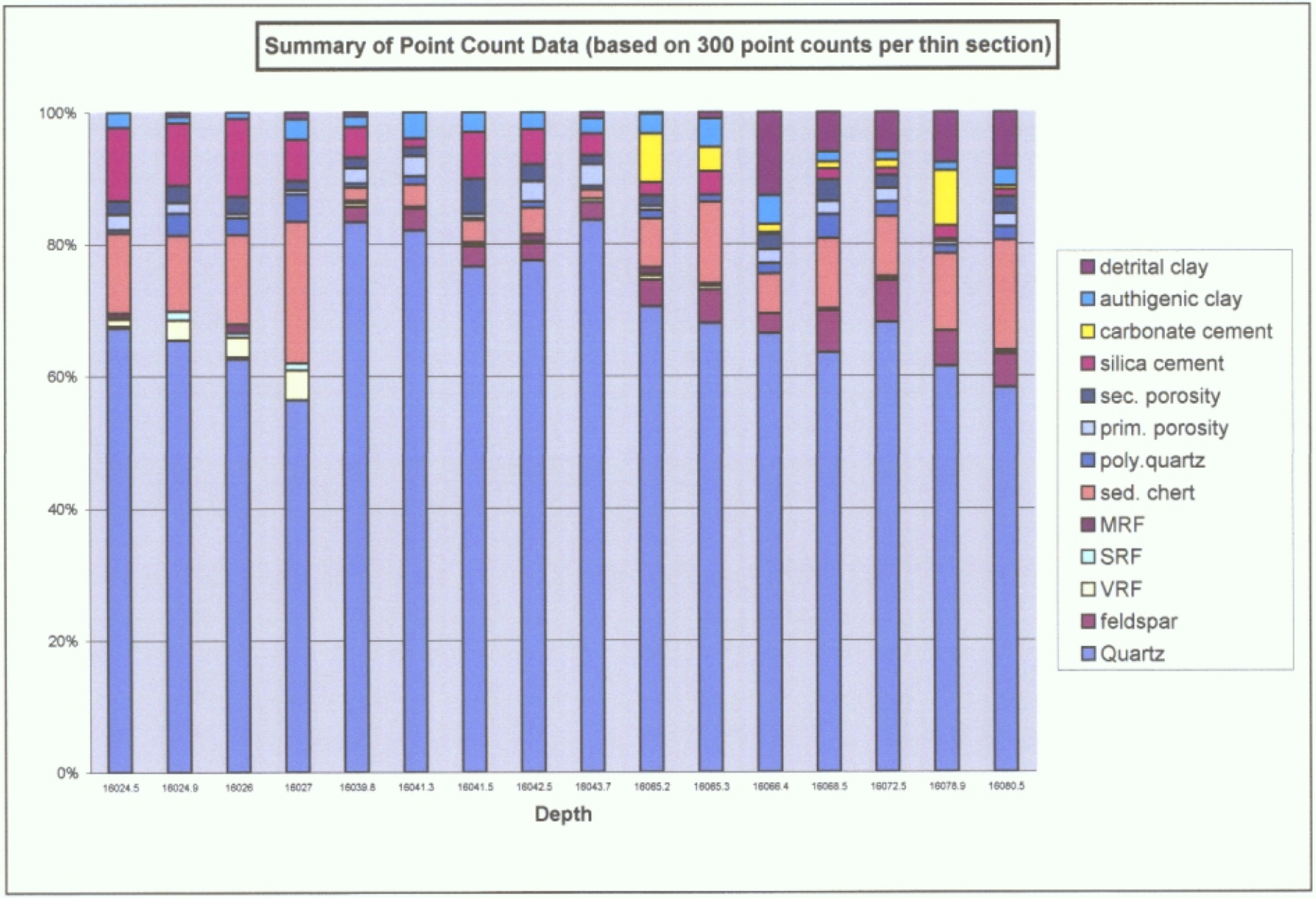

Figure 3–10. Summary of point count analysis for 2nd Frontier sandstones, Stratos #1.

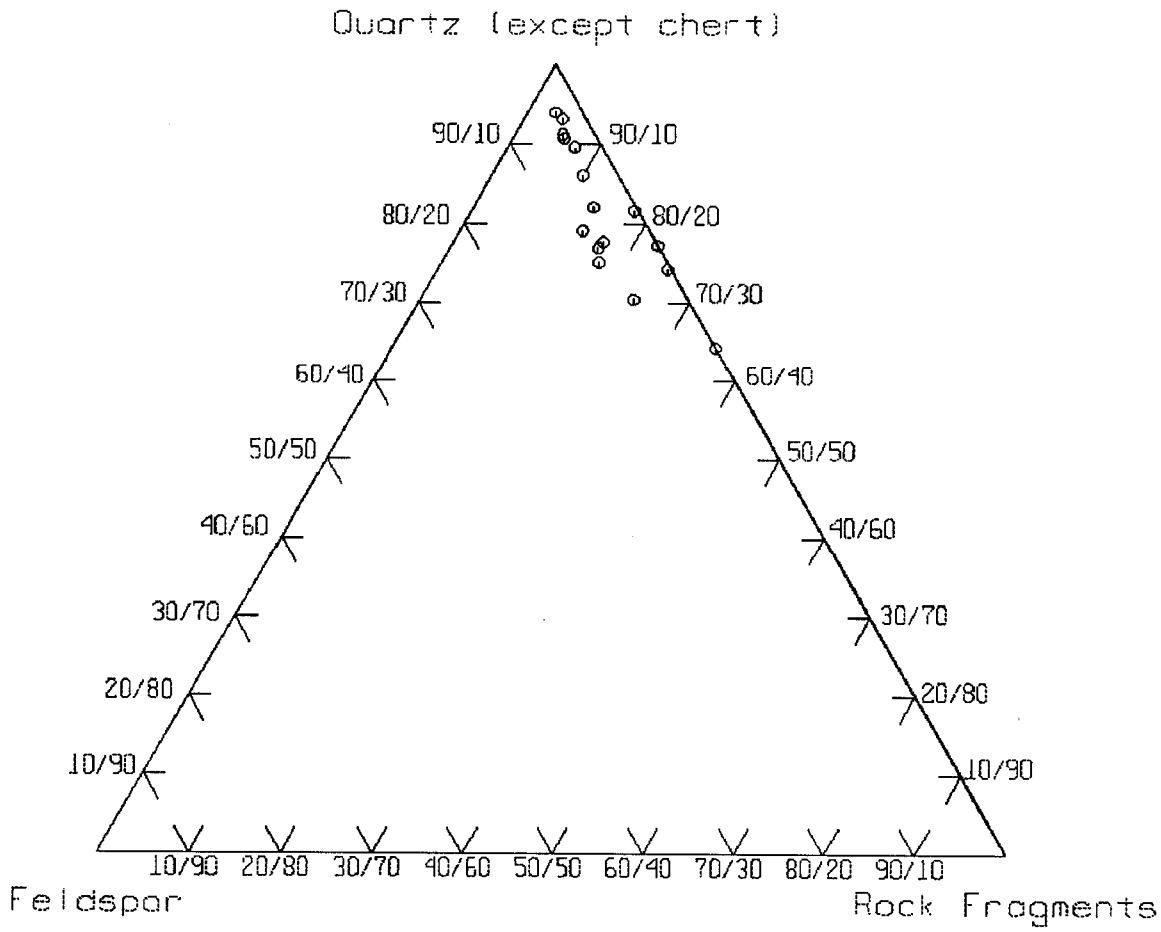

Figure 3-11. Ternary diagram for the petrographic classification of the Second Frontier sandstones.

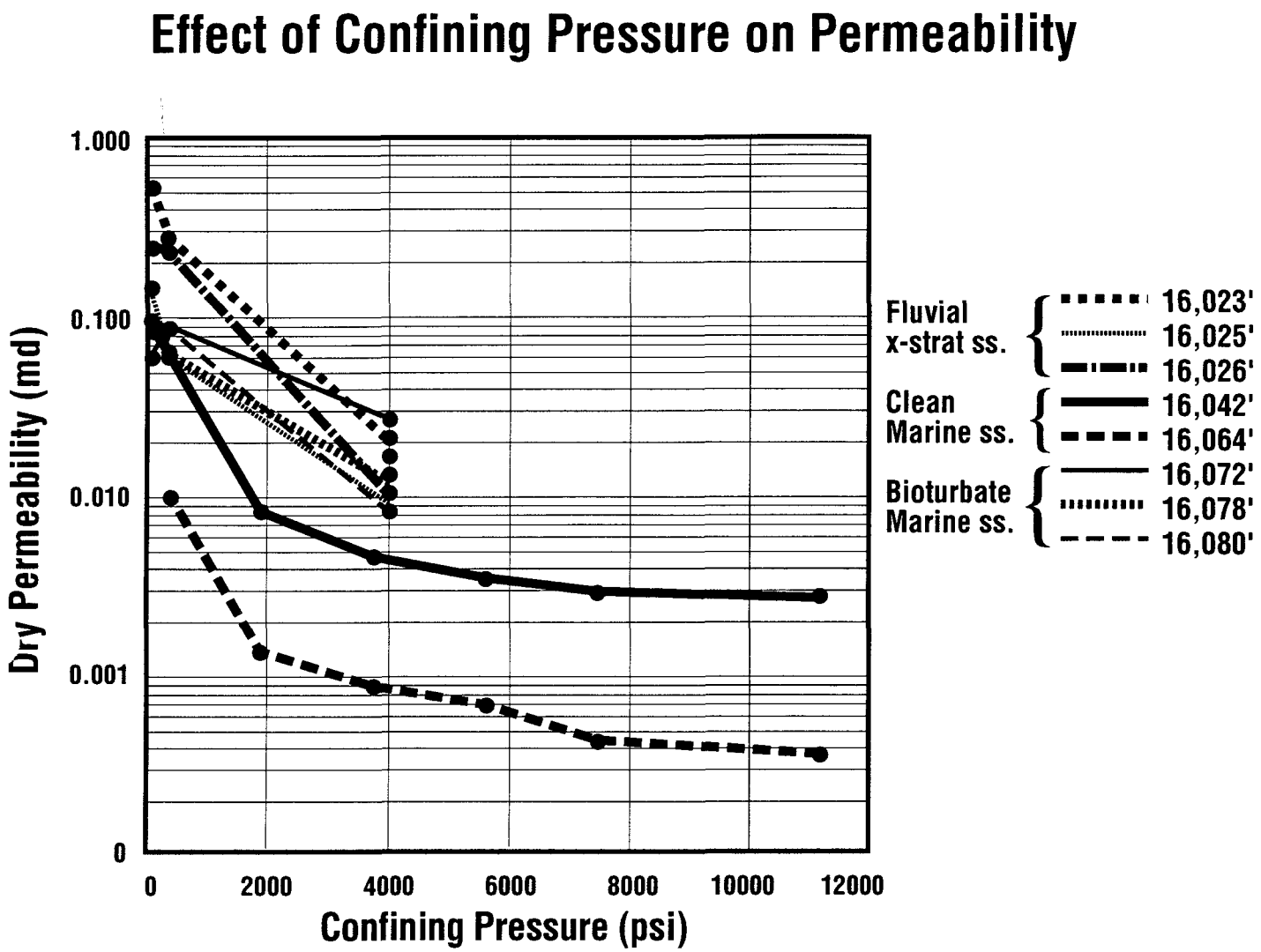

Figure 3-12 Effect of confining pressure on permeability of the Frontier sandstones

Representative scanned CL images

For all images: North is the top, west is on right hand side. Bar scale equals 100 microns.

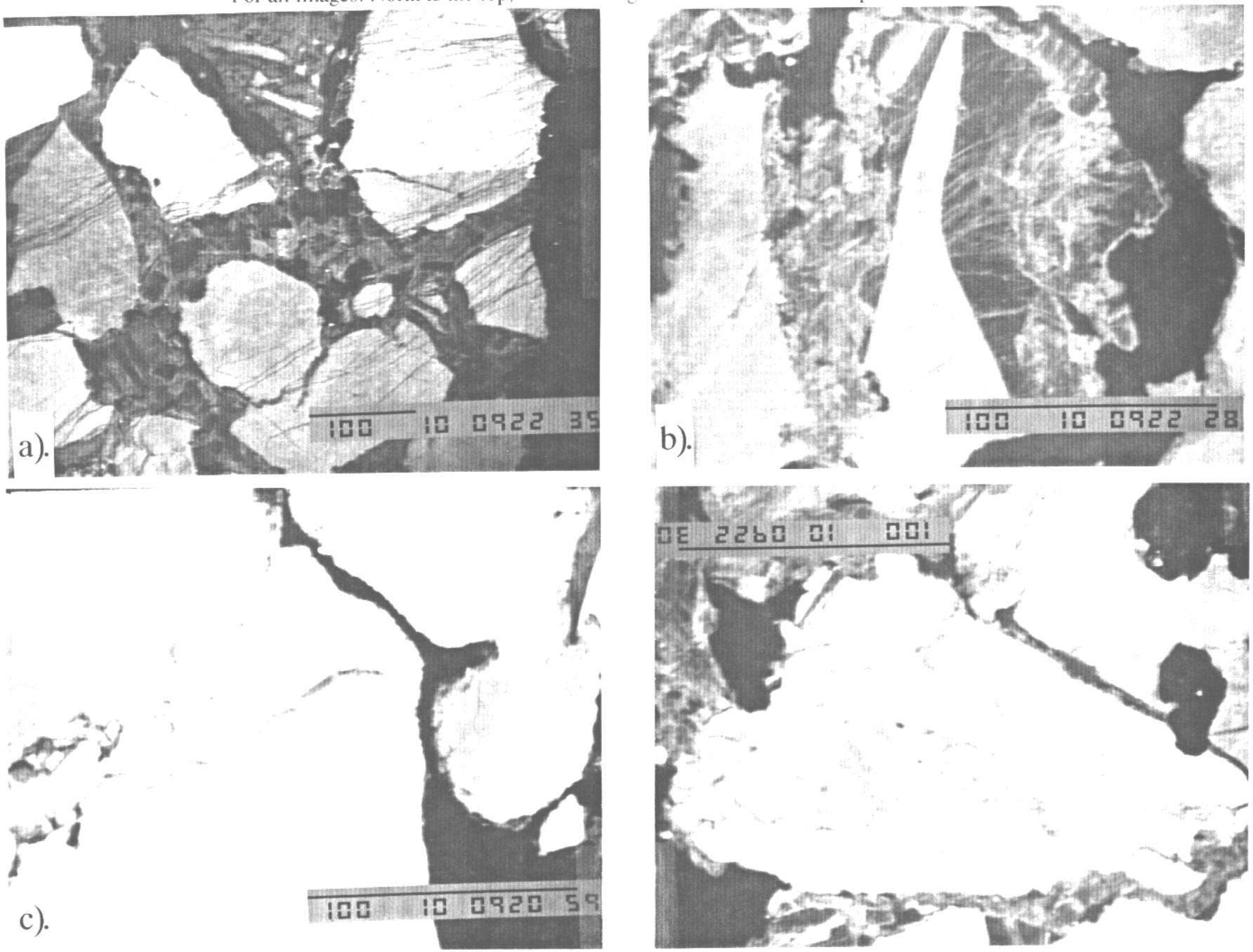

Figure 3-13. Representative scanned CL images.

Representative scanned CL images

a). Numerous northwest-trending traces of quartz-lined microfractures (category I, type a and b). Note strong preferred orientation.

b). High magnification shot of Ia fractured cutting across grain (light) and quartz cement (dark). Note northwest trend.

c). Detail of forked and branching microfractures near grain margin. Note northwest strike. Also note sutured grain contact to left (and parallel to) fracture traces.

d). Detail of a crushed grain cemented with quartz cement having more intense CL signature than is typical. Petrographically, this grain shows undulose extinction, but fractures are not visible. Dark east-west trending feature near top of grain in tentatively interpreted to be zone where quartz cement is fractured and/or partly dissolved (stylolite seam). Fracturing in this grain may be inherited from source rock, or could represent an early phase of quartz cement.

(from Laubach, 1996)

Figure 3-13. Representative scanned CL images.

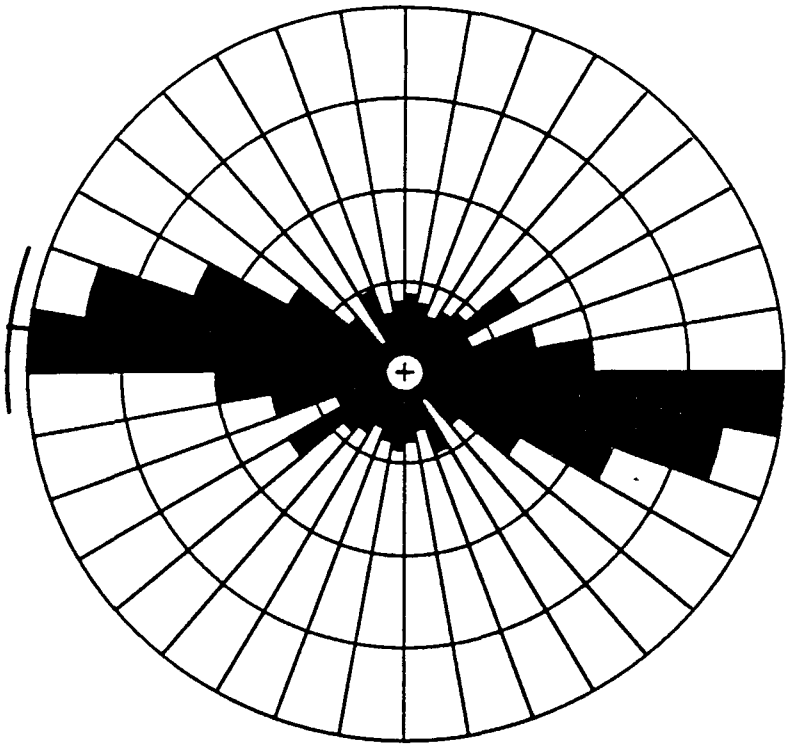

ST16027C-- all fracs, both areas 7/10	Statistics
N = 255	Vector Mean = 277.0
Class Interval = 10 degrees	Conf. Angle = 12.65
Maximum Percentage = 16.5	R Magnitude = 0.376
Mean Percentage = 5.56 Standard Deviation = 4.07	Rayleigh = 0.0000

Figure 3-14 Rose diagram showing the strike of measured microfractures from 16027 feet (Note that the area of thin section studied is less than 1% of total thin section)

Diagram of Stress and Fracture Directions

FHL (10/4/96)

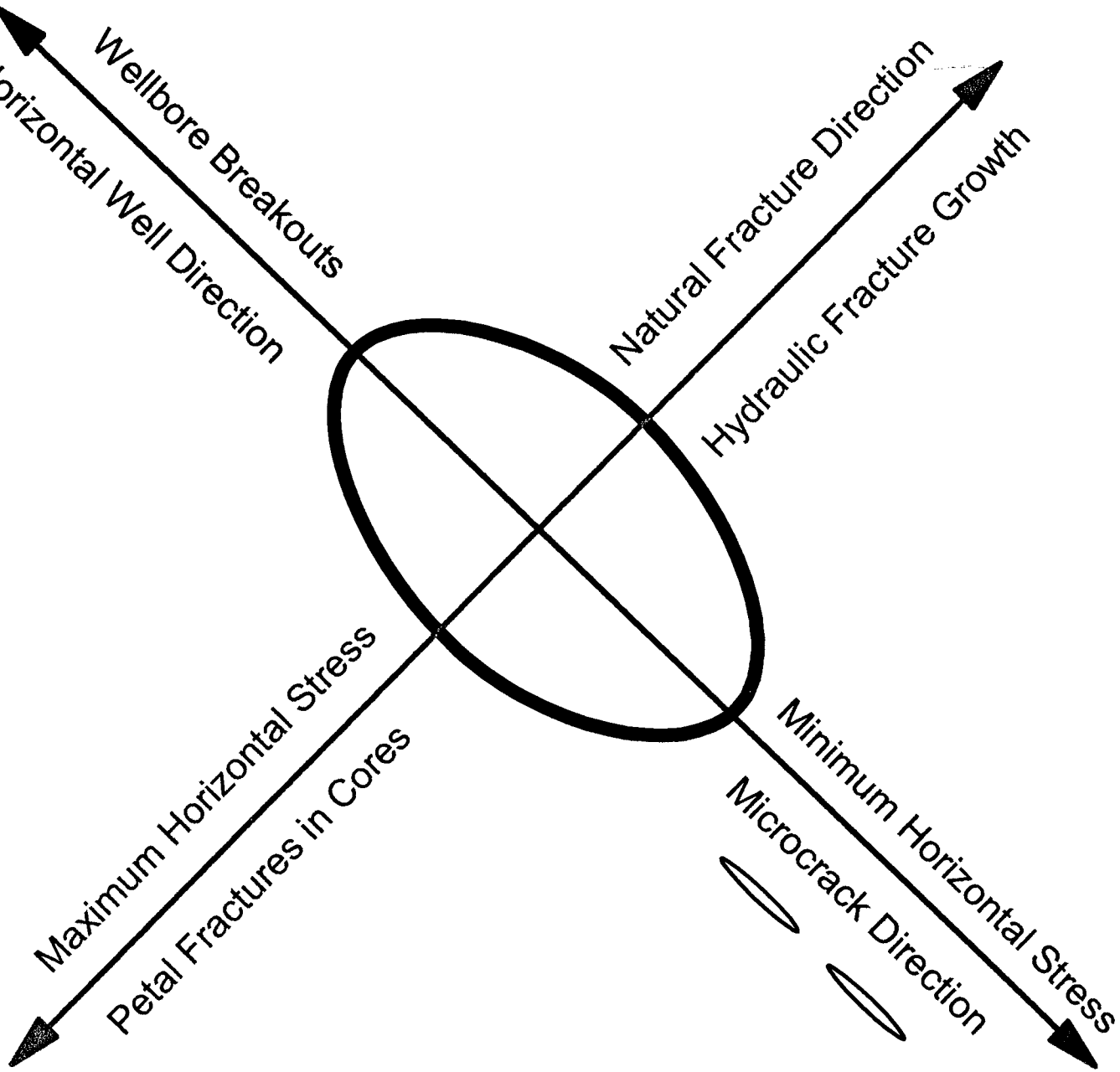

Figure 3-15. Relationship of wellbore breakout orientation, maximum horizontal stress, natural fracture orientation, and other features.

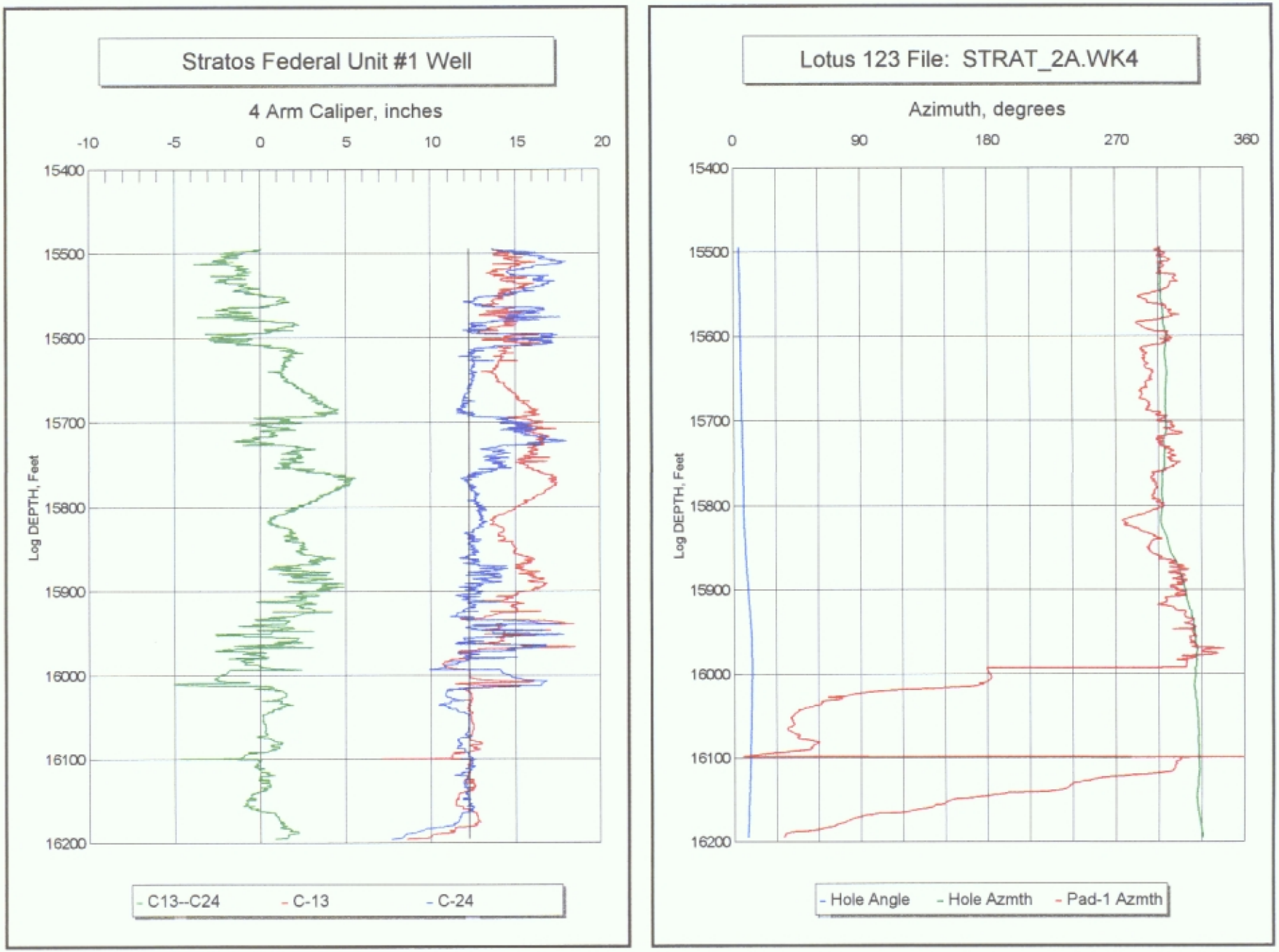

Figure 3-16. Plot of four-arm caliper data for the Frontier Formation (and part of the Baxter Shale) in the Stratos Federal #1-24

TABLE 2-1. LOG INVENTORY

STRATOS FEDERAL UNIT #1 12-1/4" Hole with 11 7 lb/gal Water based Mud			
OPEN HOLE LOGS	RUN 1 10/13/95	DSI (Dipole Shear Sonic Imager)	16231-15700'
		DSI (Dipole Shear Sonic Imager)	11281-7900'
		LLD (Laterolog Deep)	16141-5020'
		LLS (Laterolog Shallow)	16141-5020'
		SP (Spontaneous Potential)	16141-5020'
		GR (Gamma Ray)	16141-5020'
		Caliper	16141-5020'
		ARI (Azimuthal Resistivity Imager)	16141-5020'
	RUN 2 10/14/95	LDS (Litho-Density Sonde)	16141-5015'
		APS (Accelerated Porosity Sonde)	16141-5015'
		HNGS (Natural Gamma Ray Spectroscopy)	16141-5015'
	RUN 3 10/14-15/95	CMR (Combination Magnetic Resisitivity Tool)	16141-5020'
		CMR (Combination Magnetic Resisitivity Tool)	11150-7950'
		CNL (Compensated Neutron Log)	16141-5015'
		GR (Gamma Ray)	16141-5015'
	RUN 4 10/17/95	FMI (Formation MicroScanner Imager)	16150-15500'
		FMI (Formation MicroScanner Imager)	11100-7950'
		GR (Gamma Ray)	16150-15500'
		GR (Gamma Ray)	11100-7950'
CASED HOLE LOGS		CBL (Cement Bond Log)	16189-12000'
		Velocity Shots (every 50')	16150-500'
OTHER LOGS		MWD (Measurement While Drilling) Caliper	13870-16250'
		MWD (Measurement While Drilling) GR	13870-16250'
		Mud Log	7000-16250'

Table 3-1. Plug and Full Diameter Sample Routine Core Analysis Results

Sample Number	Depth (feet)	Permeability			Porosity (%)	Saturation		Grain Density (gm/cm^3)	Lithology
		Kh 65° (md)	Kh 155° (md)	Kv (md)		Oil (%)	H_2O (%)		
Frontier Formation									
Core 2	**15,990.0' - 16,015.0'**								
26@	15,999.5	<0.01	NA	NA	2.9	0.0	99.8	2.71	Sltst,dkgy,sil,sl/dol,sdy,clst
27@	16,003.9	<0.01	NA	NA	1.6	0.0	98.6	2.69	Sltst,dkgy,sil
28@	16,009.9	<0.01	NA	NA	0.6	0.0	93.1	2.67	Sltst,dkgy,sil,pof
Core 3	**16,015.0' - 16,039.6'**								
1	16,020.0 - 21.0	+0.85	+0.43	<0.01	3.3	0.0	75.2	2.66	Ss,gy,vf-fgr,sil,lam,carb,pof
2	16,021.0 - 22.0	<0.01	<0.01	<0.01	5.3	0.0	75.3	2.67	Ss,gy,vf-fgr,sil,cly,mdy clst
3	16,022.0 - 23.0	0.05	0.06	0.01	5.7	0.0	66.8	2.66	Ss,gy,f-mgr,sil,cly,xbdd,styl,clst
4	16,023.0 - 24.0	+0.17	+0.20	0.01	6.4	0.0	61.8	2.67	Ss,gy,fgr,sil,cly,bdd,clst,pof
5	16,024.0 - 25.0	0.04	0.04	0.02	7.3	0.0	58.1	2.66	Ss,gy,fgr,sil,cly,xbdd
6	16,025.0 - 26.0	0.15	0.13	0.04	6.5	0.0	48.0	2.65	Ss,gy,fgr,sil,cly,xbdd
7	16,026.0 - 27.0	0.25	0.23	0.04	6.5	0.0	60.0	2.66	Ss,gy,f-mgr,sil,cly,xbdd
8	16,027.0 - 28.0	+0.54	+0.74	0.03	4.4	0.0	62.5	2.65	Ss,gy,f-mgr,sil,cly,xbdd,pof
9	16,028.0 - 29.0	+0.45	0.09	0.02	4.1	0.0	66.0	2.66	Ss,gy,f-mgr,sil,cly,xbdd,carb clst
Core 4	**16,040.0' - 16,100.0'**								
10	16,040.0 - 41.0	<0.01	0.02	<0.01	7 4	0.0	42.7	2.66	Ss,gy,silt-vfgr,sil,v/slty,xbdd,clst
11	16,041.0 - 42.0	<0.01	<0.01	0.01	7 4	0.0	42.4	2.65	Ss,gy,vfgr,sil,bdd,clst
12	16,042.0 - 43.0	0.03	0.03	0.06	7.9	0.0	40.2	2.65	Ss,gy,vfgr,sil,pof,bur
13	16,043.0 - 44.0	0.02	0.01	0.02	9.5	0.0	40.5	2.67	Ss,gy,vfgr,sil,bur

Table 3-1. Core-derived, routine unstressed porosity and permeability for the UPRC Stratos Federal #1-24.

Table 3-1. continued

14	16,044.0 - 45.0	<0.01	<0.01	<0.01	8.2	0.0	49.1	2.68	Ss,gy,vfgr,sil,bdd
15	16,045.0 - 46.0	<0.01	<0.01	<0.01	8.4	0.0	47 4	2.68	Ss,gy,vfgr,sil,bdd
16	16,046.0 - 47.0	0.03	0.01	<0.01	7.5	0.0	53.3	2.66	Ss,gy,vfgr,sil,bdd,bur
17	16,047.0 - 48.0	<0.01	<0.01	<0.01	7.5	0.0	46.2	2.67	Ss,gy,vfgr,sil,xbdd,clst
18	16,048.0 - 49.0	<0.01	<0.01	<0.01	7 6	0.0	59.8	2.66	Ss,gy,vfgr,sil,xbdd,bur
19	16,049.0 - 50.0	<0.01	<0.01	<0.01	8.1	0.0	45.7	2.67	Ss,gy,vfgr,sil,xbdd,bur,clst
20	16,050.0 - 51.0	<0.01	<0.01	<0.01	8.1	0.0	48.2	2.66	Ss,gy,vfgr,sil
21	16,051.0 - 52.0	0.02	<0.01	<0.01	6.4	0.0	51.6	2.67	Ss,gy,vfgr,sil
22	16,052.0 - 53.0	+0.14	<0.01	<0.01	6.7	0.0	62.1	2.67	Ss,gy,vfgr,sil,xbdd,bur,pof
23	16,055.0 - 56.0	<0.01	<0.01	<0.01	4.2	0.0	65.4	2.66	Ss,gy,vfgr,sil,calc/dol,xbdd
24	16,056.0 - 57.0	<0.01	<0.01	<0.01	6.7	0.0	53.4	2.66	Ss,gy,vfgr,sil,calc/dol,xbdd,bur
25	16,057.0 - 58.0	<0.01	<0.01	<0.01	3.5	0.0	60.6	2.65	Ss,gy,vfgr,sil,calc/dol,xbdd,bur
26	16,058.0 - 59.0	<0.01	<0.01	<0.01	3.9	0.0	64.3	2.66	Ss,gy,vfgr,sil,calc/dol,xbdd,bur
27	16,059.0 - 60.0	0.01	<0.01	<0.01	5.8	0.0	81.2	2.67	Ss,gy,vf-fgr,sil,calc/dol,cly,v/bur
28	16,060.0 - 61.0	<0.01	<0.01	<0.01	6.0	0.0	70.5	2.67	Ss,gy,vf-fgr,sil,calc,dol,cly,v/bur
29	16,061.0 - 62.0	<0.01	<0.01	<0.01	5.2	0.0	75.8	2.67	Ss,gy,vfgr,sil,calc/dol,cly,v/bur
30	16,062.0 - 63.0	0.04	0.01	0.03	8.1	0.0	71.0	2.68	Ss,gy,f-mgr,cly,sil,calc/dol,xbdd,bur
31	16,063.0 - 64.0	0.03	0.03	0.03	7.9	0.0	73.0	2.67	Ss,gy,f-mgr,cly,sil,calc/dol,xbdd,bur
32	16,064.0 - 65.0	<0.01	<0.01	<0.01	5.9	0.0	43.3	2.66	Ss,gy,vfgr,sil,calc/dol,xbdd,bur
33@	16,065.0 - 66.0	<0.01	NA	NA	7.0	0.0	50.4	2.65	Ss,gy,vfgr,sil,calc,bdd,cff
34	16,066.0 - 67.0	0.05	0.05	0.03	9 4	0.0	69.1	2.66	Ss,gy,f-mgr,cly,sil,calc/dol,bur
35	16,067.0 - 68.0	0.05	0.05	0.05	9.1	0.0	67.9	2.66	Ss,gy,f-mgr,cly,sil,calc/dol,bur
36	16,068.0 - 69.0	0.06	0.06	0.04	11.1	0.0	57.8	2.66	Ss,gy,vf-mgr,sil,calc/dol,cly,v/bur
37	16,069.0 - 70.0	0.05	0.05	0.04	11.4	0.0	55.6	2.66	Ss,gy,vf-fgr,sil,calc/dol,cly,v/bur
38	16,070.0 - 71.0	0.05	0.05	0.05	11.1	0.0	52.2	2.66	Ss,gy,vf-fgr,sil,calc/dol,cly,v/bur

Table 3-1 Continued.

Table 3-1. continued

39	16,071.0 - 72.0	0.05	0.05	0.04	10.6	0.0	57.0	2.66	Ss,gy,vf-fgr,sil,calc/dol,cly,v/bur
40	16,072.0 - 73.0	0.09	0.69	0.04	10.0	0.0	62.6	2.66	Ss,gy,vf-fgr,sil,calc,cly,v/bur,fos
41	16,073.0 - 74.0	0.05	0.05	0.03	10.3	0.0	55.5	2.66	Ss,gy,vf-fgr,sil,calc,cly,v/bur,fos
42	16,074.0 - 75.0	0.04	0.05	0.04	9.5	0.0	61.5	2.66	Ss,gy,vf-fgr,sil,calc,cly,v/bur,fos
43	16,075.0 - 76.0	0.04	0.04	0.04	9 7	0.0	62.1	2.67	Ss,gy,vf-fgr,sil,calc,v/bur,clst
44	16,076.0 - 77.0	0.05	0.05	0.03	9 4	0.0	65.5	2.67	Ss,gy,vf-fgr,sil,calc,cly,v/bur
45	16,077.0 - 78.0	0.04	0.04	0.03	8.9	0.0	65.5	2.67	Ss,gy,vf-fgr,sil,calc,cly,v/bur
46	16,078.0 - 79.0	0.10	0.12	0.03	8.2	0.0	68.9	2.66	Ss,gy,vf-fgr,sil,calc,cly,v/bur
47	16,079.0 - 80.0	0.03	0.01	0.03	8.4	0.0	67.0	2.67	Ss,gy,vf-fgr,sil,calc,cly,v/bur
48	16,080.0 - 81.0	0.06	0.25	0.02	8.2	0.0	71.4	2.66	Ss,gy,vf-fgr,sil,calc,cly,v/bur
49	16,081.0 - 82.0	0.02	0.02	0.02	8.8	0.0	72.0	2.67	Ss,gy,vf-fgr,sil,calc,cly,v/bur
50	16,082.0 - 83.0	0.07	0.07	<0.01	8.4	0.0	72.1	2.68	Ss,gy,vf-fgr,sil,calc,cly,v/bur
51	16,084.0 - 85.0	<0.01	<0.01	<0.01	6.4	0.0	82.8	2.68	Ss,gy,vf-fgr,sil,calc,cly,v/bur

+ - Fracture affecting permeability
@ - Plug Dean-Stark Analysis - Not suitable for full diameter sampling

Table 3-1 Continued.

Description Scheme for Clastic Sedimentary Rocks

Rock Type, Color, Grain Size, Cement, Structures and Accessories

Key to Abbreviations

aff	- anhydrite filled fracture
alt	- altered
anhy	- anhydrite(ic)
arg	- argillaceous
bdd	- bedded
bent	- bentonite
bf	- buff
biot	- bioturbated
bit	- bitumen
bl	- blue(ish)
blk	- black
bnd	- banded
brec	- breccia(ted)
brn	- brown
bur	- burrowed
c	- coarse
calc	- calcite(areous)
carb	- carbonaceous
cff	- calcite filled fracture
cgl	- conglomerate
chky	- chalky
chlor	- chlorite
cht	- chert
chty	- cherty
clst	- clast
cly	- clay(ey)
clyst	- claystone
cob	- cobble
dism	- disseminated
dk	- dark
dff	- dolomite filled fracture
dol	- dolomite(ic)
f	- fine
fen	- fenestral
fis	- fissile
fos	- fossil(iferous)
frac	- fracture
fri	- friable
gff	- gouge filled fracture
glauc	- glauconitic
gn	- green
gr	- grain(ed)
grnl	- granule
gy	- gray
gyp	- gypsum(iferous)
hem	- hematite(ic)
if	- incipient fracture
incl	- inclusion

intprt	- interparticle
intrprt	- intraparticle
intxl	- intercrystalline
lam	- laminated
lav	- lavender
lig	- lignite(ic)
ls	- limestone
lt	- light
m	- medium
mar	- maroon
mas	- massive
mdy	- muddy
mic	- micro
mica	- micaceous
mol	- moldic
ms	- mudstone
mtx	- matrix
nod	- nodule(s)
o	- oil
of	- open fracture
ool	- oolitic
org	- organic
orng	- orange
pbl	- pebble
pel	- peloids
pff	- pyrite filled fracture
pis	- pisolitic
pk	- pink
pof	- partially open fracture
ppvgs	- pinpoint vugs
ptg	- parting(s)
purp	- purple
pyr	- pyrite(ic)
qff	- quartz filled fracture
qtz	- quartz
red	- red
sa	- salty
sdy	- sandy
sh	- shale
shy	- shaley
sid	- siderite
sil	- silica(eous)
sl/	- slightly
sltst	- siltstone
slty	- silty
ss	- sandstone
stn	- stain(ed)(ing)
str	- streak
styl	- stylolite
suc	- sucrosic
tan	- tan

Table 3-2. Overburden Permeability Results

Sample Number	Depth (feet)	Permeability (millidarcys)					
		Vertical		Horizontal 65°		Horizontal 155°	
		300 psi NES	4000 psi NES	300 psi NES	4000 psi NES	300 psi NES	4000 psi NES
6	16025.0 - 26.0	0.0312	0.0082	0.0604	0.0092	0.0602	0.0095
7	16026.0 - 27.0	0.0281	0.0057	0.2383	0.0102	0.1440	0.0123
40	16072.0 - 73.0	0.0331	0.0181	0.0885	0.0275	0.1658	0.0326
46	16078.0 - 79.0	0.0261	0.0119	0.0624	0.0116	0.0811	0.0128
48	16080.0 - 81.0	0.0198	0.0107	0.0895	0.0082	0.0413	0.0088
ASR #4	16027.0 - 28.0	0.0588	0.0263	0.1187	0.0212	0.1072	0.0229

NES - Net Effective Stress
Flowing Medium - Nitrogen Gas
Temperature - Ambient (approx. 23°C)

Table 3-2 Core-derived stressed permeabilities for the UPRC Stratos Federal #1-24.

Terra Tek Core Services

University Research Park 360 Wakara Way Salt Lake City Utah 84108 (801) 584-2480 TWX 910-925-5284

ENERGY RESERVES GROUP, INC.

Well:	Blue Rim Federal 1-30	State:	Wyoming	Date:	24 Jun 1982
Field:	Wildcat	County:	Sweetwater	TTCS File #:	180
Drilling Fluid:	Water base mud	Location:	Sec 30-T22N-R106W	Elevation:	6710.0

RETORT ANALYSIS - BOYLES LAW POROSITY

Sample Number	Depth (feet)	Permeability Horz (md)	Permeability Vert (md)	Porosity (%)	Saturation Oil (%)	Saturation H2O (%)	Grain Density (gm/cc)	Lithology
SECOND FRONTIER FORMATION								
1	16053.0-54.0	0.06	0.05	9.0	0.0	32.0	2.66	Sd,fg-vfg
2	16054.0-55.0	0.05	0.06	9.3	0.0	37.1	2.66	Sd,fg-vfg,shly incl
3	16055.0-56.0	0.06	0.05	5.7	0.0	30.0	2.65	Sd,fg-vfg,lig incl
	16056.0 - 16058.0							SH,SD STKS
4	16058.0-59.0	<0.01	<0.01	2.5	0.0	34.3	2.67	Sd,vfg,shly
5	16059.0-60.0	0.02	0.02	6.5	0.0	36.5	2.66	Sd,fg-vfg,shly incl
6	16060.0-61.0	0.03	0.03	7.4	0.0	34.6	2.66	Sd,fg-vfg
7	16061.0-62.0	0.05	0.05	9.7	0.0	41.8	2.66	Sd,fg-vfg
8	16062.0-63.0	0.09	0.05	10.4	0.0	42.7	2.66	Sd,fg-vfg
9	16063.0-64.0	0.18	0.08	9.7	0.0	41.1	2.65	Sd,fg-vfg
10	16064.0-65.0	0.10	0.08	8.2	0.0	39.8	2.65	Sd,fg-vfg,lam
11	16065.0-66.0	0.09	0.06	7.3	0.0	39.8	2.65	Sd,fg-vfg,lig lams
12	16066.0-67.0	0.16	0.06	6.8	0.0	35.0	2.65	Sd,fg-vfg,lig lams
13	16067.0-68.0	0.05	0.02	7.3	0.0	25.7	2.67	Sd,fg-vfg,lig lams
14	16068.0-69.0	0.02	0.01	7.5	0.0	39.1	2.65	Sd,fg-vfg,lig incl
15	16069.0-70.0	0.08	0.03	7.7	0.0	38.1	2.65	Sd,fg-vfg
16	16070.0-71.0	0.03	0.02	6.7	0.0	47.8	2.65	Sd,fg-vfg,lig lams
17	16071.0-72.0	0.02	<0.01	5.8	0.0	48.8	2.65	Sd,fg-vfg,sl/shly

Table 3-3. Core-derived, routine unstressed porosity and permeability for the ERG Blue Rim #1-30.

Terra Tek Core Services

University Research Park 360 Wakara Way Salt Lake City Utah 84108 (801) 584 2480 TWX 910-925-5284

ENERGY RESERVES GROUP, INC. Date: 24 Jun 1982 TTCS File #: 180

Well: Blue Rim Federal 1-30

Sample Number	Depth (feet)	Permeability Horz (md)	Permeability Vert (md)	Porosity (%)	Saturation Oil (%)	Saturation H2O (%)	Grain Density (gm/cc)	Lithology
18	16072.0-73.0	<0.01	<0.01	4.8	0.0	39.1	2.66	Sd,vfg,shly
19	16073.0-74.0	0.02	<0.01	6.3	0.0	71.4	2.68	Sd,vfg,sl/shly
20	16074.0-75.0	<0.01	<0.01	5.0	0.0	56.0	2.67	Sd,vfg,shly
21	16075.0-76.0	<0.01	<0.01	10.1	0.0	41.7	2.66	Sd,vfg,shly
22	16076.0-77.0	<0.01	<0.01	5.9	0.0	65.2	2.67	Sd,vfg,shly
	16077.0 - 16078.0							DRILLED INTERVAL
23	16078.0-79.0	0.04	0.03	6.7	0.0	29.3	2.65	Sd,vfg,sl/shly
24	16079.0-80.0	0.03	0.04	6.7	0.0	33.8	2.66	Sd,vfg,calc,sl/shly
25	16080.0-81.0	0.02	0.02	9.8	0.0	43.2	2.66	Sd,vfg,sl/shly
26	16081.0-82.0	0.04	0.04	10.4	0.0	39.4	2.66	Sd,vfg,sl/shly
27	16082.0-83.0	0.06	0.03	9.9	0.0	41.9	2.66	Sd,vfg,sl/shly
28	16083.0-84.0	0.02	0.02	9.6	0.0	49.5	2.67	Sd,vfg,sl/shly
29	16084.0-85.0	0.02	0.02	9.5	0.0	53.8	2.67	Sd,vfg,sl/shly
30	16085.0-86.0	0.02	0.02	8.7	0.0	63.4	2.67	Sd,vfg,shly
31	16086.0-87.0	0.01	0.01	7.5	0.0	70.0	2.68	Sd,vfg,shly
32	16087.0-88.0	<0.01	<0.01	6.3	0.0	79.1	2.68	Sd,vfg,shly
33	16088.0-89.0	<0.01	<0.01	2.5	0.0	69.6	2.69	Sd,vfg,calc,shly
34	16089.0-90.0	<0.01	<0.01	2.2	0.0	76.2	2.69	Sd,vfg,calc,shly
35	16090.0-91.0	<0.01	<0.01	2.2	0.0	69.6	2.69	Sd,vfg,calc,shly
36	16091.0-92.0	<0.01	<0.01	2.3	0.0	72.7	2.69	Sd,vfg,calc,shly
37	16092.0-93.0	<0.01	<0.01	3.7	0.0	80.8	2.70	Sd,vfg,calc,shly
38	16093.0-94.0	<0.01	<0.01	5.4	0.0	80.5	2.69	Sd,vfg,shly
39	16094.0-95.0	0.02	<0.01	5.2	0.0	72.0	2.69	Sd,vfg,shly

Terra Tek Core Services

University Research Park 360 Wakara Way Salt Lake City Utah 84108 (801) 584 2480 TWX 910-925 5264

ENERGY RESERVES GROUP, INC. Date: 24 Jun 1982 TTCS File #: 180

Well: Blue Rim Federal 1-30

Sample Number	Depth (feet)	Permeability Horz (md)	Permeability Vert (md)	Porosity (%)	Saturation Oil (%)	Saturation H2O (%)	Grain Density (gm/cc)	Lithology
40	16095.0-96.0	<0.01	<0.01	4.4	0.0	62.0	2.69	Sd,vfg,shly
41	16096.0-97.0	<0.01	<0.01	4.5	0.0	72.3	2.69	Sd,vfg,shly
42	16097.0-98.0	<0.01	<0.01	4.2	0.0	83.3	2.68	Sd,vfg,shly
43	16098.0-99.0	<0.01	<0.01	3.8	0.0	78.4	2.68	Sd,vfg,shly
44	16099.0-00.0	<0.01	<0.01	3.8	0.0	70.8	2.69	Sd,vfg,shly
45	16100.0-01.0	0.03	<0.01	3.7	0.0	83.8	2.69	Sd,vfg,shly
46	16101.0-02.0	0.10+	<0.01	4.0	0.0	82.9	2.69	Sd,vfg,shly
47	16102.0-03.0	<0.01	<0.01	3.9	0.0	87.2	2.69	Sd,vfg,shly
	16103.0 - 16122.0							SH,SL/SDY
48	16122.0-23.0	0.31+	<0.01	2.7	0.0	76.9	2.70	Sd,vfg,slty,sh stks
49	16123.0-24.0	<0.01	<0.01	2.7	0.0	79.3	2.69	Sd,vfg,slty,sh stks
	16124.0 - 16125.0							SH,SD STKS
50	16125.0-26.0	<0.01	<0.01	1.9	0.0	67.9	2.68	Sd,vfg,slty,sh stks
	16126.0 - 16127.0							SH,SD STKS
51	16127.0-28.0	<0.01	<0.01	2.2	0.0	75.5	2.68	Sd,vfg,slty,sh stks
52	16128.0-29.0	<0.01	<0.01	3.2	0.0	74.4	2.69	Sd,vfg,slty,sh stks
53	16129.0-30.0	<0.01	<0.01	2.8	0.0	75.1	2.68	Sd,vfg,slty,sh stks
	16130.0 - 16131.0							SH,SD STKS
54	16131.0-32.0	<0.01	<0.01	1.8	0.0	85.7	2.67	Sd,vfg,slty,sh stks
	16132.0 - 16135.0							SH,SL/SDY
	16135.0 - 16681.0							DRILLED INTERVAL
	16681.0 - 16689.0							SHALE

+ Horizontal dehydration crack

Composition of 2nd Frontier Sandstones - Stratos #1

	Depth															
	16024.5	16024.9	16026	16027	16039.8	16041.3	16041.5	16042.5	16043.7	16065.2	16065.3	16066.4	16068.5	16072.5	16078.9	16080.5
Quartz	66.6	64.3	61.6	54	82.3	81.3	75.6	77	83.3	70	67.3	66	63.3	68	61	58
feldspar	0.3	0	0.3	0	2.3	3.3	3	2.6	2.6	4	5	3	6.3	6.3	5.3	5
VRF	1	3	3	4.3	0.6	0	0.3	0.3	0.6	0.6	0.6	0	0.3	0.3	0	0.3
SRF	0.3	1.3	0.6	1	0.3	0.3	0.3	0	0	0.3	0	0	0	0.3	0	0.3
MRF	0.6	0	1.3	0	0	0	0	1	0	1	0.3	0	0	0	0	0
sed. chert	12	11.3	13.3	20.6	2	3.3	3.3	4	1.3	7.3	12.3	6	10.6	9	11.6	16.6
poly.quartz	0.6	3.3	2.6	4	0.6	1.3	0.3	1	0.6	1.3	1	1.6	3.6	2.3	1.3	2
prim. porosity	2.3	1.6	0.6	0.6	2.3	3	0.6	3	3.3	0.6	0	2	2	2	0.6	2
sec. porosity	2	2.6	2.6	1.3	1.6	1.3	5.3	2.6	1.3	1.6	0	2.3	3.3	2	0.3	2.6
silica cement	11	9.3	11.6	6	4.6	1.3	7	5.3	3.3	2	3.6	0.3	1.6	1	2	1
carbonate cement	0	0	0	0	0	0	0	0	0	7.3	3.6	1.3	1	1.3	8.3	0.6
authigenic clay	2.3	1	1	3	1.6	4	3	2.6	2.3	3	4.3	4.3	1.6	1.3	1.3	2.6
detrital clay	0	0.6	0	1	0.6	0	0	0	1	0.3	1	12.6	6	6	7.6	8.6
other	0.6	1.3	1	4	0.6	0.6	1	0.3	0	0.3	0.6	0.3	0	0	0.3	0

Table 3-4. Results of point count analysis for the Second Frontier sandstones in the UPRC Stratos #1-24.

TS#	Total Por %	MODAL ANALYSIS (%) - INCLUDES POROSITY																																	
		SILICICLASTIN FRAMEWORK GRAINS																CARBONATE FRAMEWORK GRAINS				CLAY and Matrix							CEMENTS						POROSITY	
												OTHER		OTHER		OTHER					OTHER						OTHER			CARBONATE		OTHER		INT	MOL
		MQ	PQ	FD	CT	SRF	IRF	MRF	RFU	OT	HM	PHO	GL	PY	MI	OT	HC	DO	CA	SID	OT	MA	DM	KA	ILL	CHL	%	AQ	CA	DO	SID	PY	SUL	%	%
	1	2	3	4	5	6	7	8	9	10	11			12		13	14	15	16	17		18	19	20	21	22	23	24	25	26	27		28	29
6a	tr	44.7	1.7	tr	14.0	2.3	2.7	3.0	0.7	-	tr	-	-	-	0.3	-	-	-	-	-	-	tr	-	-	5.3	-	-	-	25.3	-	-	tr	-	-	tr
31a	1.0	65.0	tr	1.3	5.3	0.7	4.0	1.0	1.0	1.3	tr	-	-	tr	tr	-	-	-	-	-	-	17.0	-	-	0.3	-	-	-	1.7	1.3	tr	-	0.3	-	0.3	0.7
37	2.0	47.3	tr	6.0	6.0	1.7	8.0	1.0	1.0	0.7	tr	-	0.3	tr	0.3	-	-	-	-	-	-	5.7	-	-	9.3	-	-	-	9.3	2.0	tr	-	0.3	-	1.3	0.7

MO - MONOCRYSTALLINE QUARTZ
PQ - POLYCRYSTALLINE QUARTZ
CT - CHERT
FD - FELDSPAR
SRF - SEDIMENTARY ROCK FRAGMENT
F - METAMORPHIC ROCK FRAGMENT

IRF - IGNEOUS ROCK FRAGMENT
RFu - UNDIFFERENTIATED FRAGMENT
PY - PYRITE
MI - MICA
HC - HYDROCARBON
BIO - BIOCLASTS

PR - PLANT REMAINS
PHO - PHOSPHATES
CAR - CARBONACEOUS
KA - KAOLINITE
IL - ILLITE
CHL - CHLORITE
DO - DOLOMITE

AQ - AUTHIGENIC SILICA
SM - SILICA MATRIX
HM - HEAVY MINERALS
SI D- SIDERITE
LEU - LEUCOXENE
CA - CALCITE

ANH - ANHYDRITE
GL - GLAUCONITE
MA - MATRIX
INT - INTERGRANULAR POROSITY
MOL - GRAIN MOLDIC POROSITY

Table 3-5. GR Petrology Consultants, Inc.'s petrographic analysis of three samples from the Second Frontier.

Summary of XRD Bulk Analysis
Stratos Fed #1 Sandstone

Sample.	Depth (ft)	Qtz	K-Feld	Na-Feld	Cal	Dol	Sid	Hal	Pyr	Kaol	Ill	Chl	Ml	Sm
Hy-6a	16025.25	93.0	tr	3.0	-	-	-	-	tr	1.0	4.0	tr	1.0	
Hy-31a	16063.20	75.0	tr	8.7	1.7	tr	1.3	-	1.3	3.3	7.0	tr	1.0	-
Hy-37	16069.20	78.0	tr	6.0	5.0	1.0	-	-	1.0	1.0	6.0	tr	1.0	-

Qtz - Quartz (SiO_2)	Hal - Halite (NaCl)	Ml *- Mixed-Layer Clay
K-Feld* - Potassic Feldspar	Pyr - Pyrite (FeS_2)	Chl *- Chorite
Na-Feld*- Sodic Feldspar	Mack - Mackinawite (Fe_9S_8)	Ot - Other
Cal - Calcite ($CaCO_3$)	Kaol *- Kaolinite	Sm* - Smectite
Dol - Dolomite ($(Ca,Mg)CO_3$)	Ill* - Illite (inlcudes mica and clasts)	* - Complex Silicates
Sid - Siderite ($FeCO_3$)		P - Present

Table 3-6a. X-Ray difraction analyses.

Summary of XRD Glycolated Clay Analysis
Stratos Fed #1 Sandstone

Sample No.	Tot Clay	Kaol	Ill	Ml	Chl	Sm
Hy-6a	6.0	40.0	46.0	22.0	4.0	-
Hy-31a	11.3	42.0	55.0	8.0	5.0	-
Hy-37	8.0	17.0	69.0	8.0	6.0	-

Ot - Other non clay grains or cements
Kaol - Kaolinte
Ill- Illite
Chl - Chlorite
Ml- Mixled Layer Clay
Sm - Smectite
Tot Clay - Total clay in bulk sample

Table 3-6b. X-Ray diffraction analyses.

FULL DIAMETER FRACTURE PERMEABILITY MEASUREMENTS			
Sw_i (%)	Overburden Pressure (psi)	Gas Permeability (mD)	% Change in Permeability
Fluvial Facies - FD #12 - 16042 ft			
0	375	0.06000	0.00 (baseline)
0	1880	0.00823	-86.3
0	3750	0.00455	-92.4
0	5640	0.00346	-94.2
0	7500	0.00290	-95.2
0	11200	0.00265	-95.6
100	3750	0.00032	-99.5
Sw_{irr}	3750	0.00031	-99.5
Marine Facies - FD #32 - 16064 ft			
0	375	0.010000	0.00
0	1880	0.001350	-86.5
0	3750	0.000850	-91.5
0	5640	0.000670	-93.3
0	7500	0.000420	-95.8
0	11200	0.000350	-96.5
100	3750	0.000044	-99.6
Sw_{irr}	3750	<0.000010	-99.9

Table 3-7. Full diameter fracture permeability measurements - Hycal Laboratories.

INCREMENTAL PHASE TRAP EVALUATION TESTS					
Fluvial - Sample 6A 16025.25 ft.			Marine - Sample 37 16069.20 ft.		
Sw_i	Gas Permeability (mD)	% Change	Sw_i	Gas Permeability (mD)	% Change
0.00 (unstressed)	0 2000	0 0	0 00 (unstressed)	0 1300	0 0
0.30	0 0116	-94 2	0 30	0.0104	-92.0
0 40	0 0091	-95.4	0 40	0 0054	-95 8
0 50	0 0052	-97.4	0 50	0 0022	-98 3
0 60	0 0023	-98 8	0 60	0 0007	-99 4
0 70	0.0017	-99 2	0 70	0 0005	-99 6

Table 3-8. Incremental phase trap evaluation tests - Hycal Laboratories.

Sample ID	Depth (feet)	θ (Master Scribe)	Source
UB256	16025 6	231	UPRC Stratos
UB262	16026 2	232	UPRC Stratos
UB384	16038 4	293	UPRC Stratos
UB501	16050 1	146	UPRC Stratos
UB513	16051 3	145	UPRC Stratos
UB519	16051 9	145	UPRC Stratos

Note that the orientations are relative to true north

Table 3-9. Samples used in Sandia's core-based in situ stress tests.

Category	Habit	Length (range)	Shape	Distribution	Interpretation (application[4])
I Straight[1]	Isolated, locally parallel sets	µm to mm, gradational to macroscopic	Lens, aspect ratios 10^{-3}, 10^{-4}	All formations & depths	Equivalent to macrofractures (regional)
II Web[1,2]	Curved, intersecting, crisscrossing & radiating arrays	= grain size & smaller	Lens to irregular & angular	All formations & depths	Primarily due to grain-grain interaction (local)
III Truncated[1,3]	Isolated within grains; end within grains or at grain margins	= grain size & smaller	Simple tabular	All formations	Inherited (none[5])

[1]All categories consist mainly of opening-mode fractures
[2]Intersecting arrays of contemporaneous fractures
[3]May end within grains and have crisscrossing patterns that resemble category II
[4]Appropriate scale for use as a postdepositional structural indicator
[5]Inherited fractures may have application as provenance indicators

Table 3-10 Microfracture categories and their interpreted origen

From Laubach, S.E., in press, Method to detect natural fractures in sandstones. American Association of Petroleum Geologists, v.81, no.3.

Microfracture Category			Microfracture Type: Decreasing size and/or resolution of relation to cement[1] →				
			Large trans-granular	Trans-cement, intra-cement	Probable trans-cement	Ambiguous relation to cement	Indistinct relation to cement
Reliability based on style	Reliable	I Fractures having straight traces	a+ Highly reliable	a Reliable	b Marginally reliable	c Marginally unreliable	d Unreliable
	Unreliable	II Fractures in crisscrossing arrays	n.a.	Present (rare)[2]	Present[2]	Present[2]	Present
		III Inherited fractures	n.a	n.a.	n a.	Possibly inherited[3]	Probably Inherited[4]

[1]Based on crosscutting and abutting relation of vein fill to cement
[2]Unreliable based on fracture style
[3]Category III fractures may be mistaken for category I or II, type c
[4]Many type d fractures are also category III

Table 3-11 Microfracture data quality index for assessing reliability of macrofracture strike determination

From Laubach, S.E., in press, Method to detect natural fractures in sandstones. American Association of Petroleum Geologists, v.81, no.3.

(Well Drilled with 12-1/4" Bit, Cored from 15,990' to 16,100' with 8-3/4" Core Bit and Reamed Out to 12-1/4")

Log Depth Range, Feet	Interval	Four-Arm Caliper Results	Inferred maximum horizontal stress direction	Formation	C13, inches	C24, inches	GR, API
15,495 to 15,498	3 ft	Round Borehole	None	Upper Frontier	13.9	14.2	74.4
15,498 to 15,514	16 ft	33.2 deg. Breakout Direction	North 56.8 West, Max.Horz.Stress	Upper Frontier U-1	14.7	16.7	70.4
15,514 to 15,526	12 ft	Nearly Round Borehole	None	Upper Frontier	14.2	15.3	69.8
15,526 to 15,536	10 ft	40.8 deg. Breakout Direction	North 49.2 West, Max.Horz.Stress	Upper Frontier U-2	14.7	16.6	75.4
15,536 to 15,564	28 ft	Round Borehole	None	Upper Frontier	14.3	14.2	83.2
15,564 to 15,579	15 ft	37.5 deg. Breakout Direction	North 52.5 West, Max.Horz.Stress	Upper Frontier U-3	14.3	15.7	78.8
15,579 to 15,581	2 ft	Round Borehole	None	Upper Frontier	14.5	14.2	74.5
15,581 to 15,591	10 ft	288.8 deg. Breakout Direction	North 18.8 East, Max.Horz.Stress	Upper Frontier U-4	14.2	12.6	82.3
15,591 to 15,595	4 ft	Round Borehole	None	Upper Frontier	13.1	12.8	90.2
15,595 to 15,608	13 ft	36.5 deg. Breakout Direction	North 53.5 West, Max.Horz.Stress	Upper Frontier U-5	14.8	16.7	71 1
15,608 to 15,612	4 ft	Round Borehole	None	Upper Frontier	14.7	14.3	77.0
15,612 to 15,647	35 ft	291.6 deg. Breakout Direction	North 21.6 East, Max.Horz.Stress	Upper Frontier U-6	14.0	12.5	89.5
15,647 to 15,694	47 ft	292.1 deg. Breakout Direction	North 22.1 East, Max.Horz.Stress	Upper Frontier U-7	15.1	12.2	90.1
15,694 to 15,727	33 ft	Round Borehole	None	Upper Frontier	16.2	15.6	80.0
15,727 to 15,809	82 ft	302.0 deg. Breakout Direction	North 32.0 East, Max.Horz.Stress	Upper Frontier U-8	16.1	13.1	73.0
15,809 to 15,824	15 ft	Round Borehole	None	Upper Frontier	13.8	13.0	71.1
15,824 to 15,931	107 ft	305.7 deg. Breakout Direction	North 35.7 East, Max.Horz.Stress	Upper Frontier U-9	15.1	12.6	75.4
15,931 to 15,993	62 ft	Round Borehole	None	Upper Frontier	13.5	13.2	80.6
15,993 to 16,006	13 ft	88.7 deg. Breakout Direction	North 1.3 West, Max.Horz.Stress	Fluvial	12.4	14.6	53.5
16,006 to 16,017	11 ft	275.4 deg. Breakout Direction	North 5.4 East, Max.Horz.Stress	Shale (Fluvial/Marine)	13.5	15.0	83.0
16,017 to 16,045	28 ft	Nearly Round Borehole	None	Clean Marine Zone	12.3	11 1	40.0
16,045 to 16,057	12 ft	Round Borehole	None	Clean Bioturbate Zone	12.4	12.2	35.4
16,057 to 16,077	20 ft	Round Borehole	None	Dirty Bioturbate Zone	12.4	12.1	76.7
16,077 to 16,170	93 ft	Round Borehole	None	Lower Shale Zone	12.2	12.1	101.7

Table 3-12. Summary of four-arm caliper data for the Frontier Formation, Stratos Federal #1-24